SOME NEW COSMOLOGICAL APPLICATIONS OF THE ENERGY-MOMENTUM SQUARED GRAVITY

by

Nebiye Merve Uzun

B.S., Physics, Boğaziçi University, 2010

M.S., Physics, Boğaziçi University, 2013

Submitted to the Institute for Graduate Studies in
Science and Engineering in partial fulfillment of
the requirements for the degree of
Doctor of Philosophy

Graduate Program in Physics

Boğaziçi University

2021

Dedicated to the memory of Professor John David Barrow

ACKNOWLEDGEMENTS

I would like to express my sincere gratitude to my supervisor Prof. O. Teoman Turgut for his support, guidance, and kindness throughout my PhD study.

I thank to my co-supervisor Assoc. Prof. Özgür Akarsu for providing me with the opportunity to become his student and suggesting me the research subject. I am very grateful for his scientific guidance, patience, and encouragement throughout my research. This thesis would not have been possible without his knowledge and intuition.

I am indebted to Prof. John D. Barrow, who passed away on September 26, 2020, for his valuable contributions and suggestions regarding both works constituting this thesis.

Special thanks to Assoc. Prof. J. Alberto Vazquez and Dr. Charles V. R. Board, whom I have collaborated with during my research, as well as, Assoc. Prof. Nihan Katırcı, Prof. Suresh Kumar, Assoc. Prof. Jorge Noreña for their valuable comments added a lot to the works.

I would like to express my thanks to all my friends, colleagues, and members of Boğaziçi University Physics Department. Very special thanks to my dear friends Dr. Merve Tarman Algan, Dr. Emine Ertuğrul, and Dr. Emine Şeyma Kutluk.

Finally, I am grateful to my parents for their unconditional love and support.

ABSTRACT

SOME NEW COSMOLOGICAL APPLICATIONS OF THE ENERGY-MOMENTUM SQUARED GRAVITY

We investigate two specific forms of a new-type of modified gravity called Energy-Momentum Squared Gravity (EMSG) constructed by the addition of the term $f(T_{\mu\nu}T^{\mu\nu})$ to the Einstein-Hilbert action with a cosmological constant (Λ). First, we propose a new model of EMSG, called Energy-Momentum Log Gravity (EMLG) described by $f(T_{\mu\nu}T^{\mu\nu}) = \alpha \ln(\lambda T_{\mu\nu}T^{\mu\nu})$. This choice is made as a specific way of including new terms in the right-hand side of the Einstein field equations, resulting in constant effective inertial mass density and leading to an explicit exact solution of the dust energy density in terms of redshift. We look for viable cosmologies, in particular, an extension of standard ΛCDM model. The EMLG provides an effective dynamical dark energy passing below zero at large redshifts, accommodating a mechanism for screening Λ, in line with suggestions for alleviating some of the tensions between observational data sets prevailing within the ΛCDM model. We present a theoretical investigation and then constrain the free parameters of the model using the latest observational data, and discuss the results. Second, we simultaneously replace the spatially flat Robertson-Walker metric with its simplest anisotropic extension, and couple the CDM to the gravity via the EMSG of the form $f(T_{\mu\nu}T^{\mu\nu}) \propto T_{\mu\nu}T^{\mu\nu}$. These two modifications can mutually cancel out, namely, the shear scalar can be screened completely, and reproduce mathematically the same Friedmann equation of the ΛCDM model. This evades the BBN limits on the anisotropy, and thereby provides an opportunity to manipulate the CMB quadrupole temperature fluctuation at the desired amount. We also discuss the consequences of the model on the very early times and far future of the Universe.

ÖZET

ENERJİ-MOMENTUM KARELİ GENELÇEKİMİN BAZI YENİ KOZMOLOJİK UYGULAMALARI

Kozmolojik sabit (Λ) içeren Einstein-Hilbert eylemine $f(T_{\mu\nu}T^{\mu\nu})$ teriminin eklenmesiyle kurulmuş, Enerji-Momentum Kareli Genelçekim (EMSG) olarak bilinen yeni bir tür değiştirilmiş genelçekim kuramının iki özel biçimi araştırılmıştır. İlk olarak, $f(T_{\mu\nu}T^{\mu\nu}) = \alpha \ln(\lambda T_{\mu\nu}T^{\mu\nu})$ ile tanımlanan Enerji-Momentum Loglu Genelçekim (EMLG) adı verilen yeni bir EMSG modeli ileri sürülmüştür. Bu, Einstein alan denklemlerinin sağ tarafına etkin olarak sabit eylemsizlik kütle yoğunluğu veren yeni terimler eklemesi ve toz için enerji yoğunluğunun kırmızıya kayma cinsinden açık ve tam çözümünün bulunmasına olanak sağlaması bakımından özel bir seçimdir. Özellikle standart ΛCDM modelinin bir uzantısı niteliği gösteren, gerçek evreni betimleyebilecek kozmolojik çözümler aranmıştır. EMLG, ΛCDM modelinde farklı gözlemsel veri kümeleri arasında ortaya çıkan bazı gerilimlerin azaltılması için önerilen çözümler doğrultusunda, yüksek kırmızıya kayma değerlerinde (kozmolojik sabitin perdelenmesiyle uyumlu olarak) enerji yoğunluğu sıfırın altına inebilen etkin bir karanlık enerji sağlayabilmektedir. Bu modelin serbest parametreleri, kuramsal bir incelemesi sunulduktan sonra, en güncel gözlemsel veriler kullanılarak sınırlanmış ve sonuçlar tartışılmıştır. İkinci olarak, CDM genelçekime $f(T_{\mu\nu}T^{\mu\nu}) \propto T_{\mu\nu}T^{\mu\nu}$ biçimindeki EMSG ile bağlanmış ve beraberinde düz Robertson-Walker uzayzaman metriği en basit yönbağımlı uzantısıyla değiştirilmiştir. Bu iki değişiklik birbirini yok edebilmektedir, şöyle ki, makaslama skalerinin tamamen perdelenmesiyle ΛCDM modelindekiyle matematiksel olarak aynı Friedmann denklemi türetilebilmektedir. Bu, yönbağımlılığı BBN sınırlamalarından kurtarması dolayısıyla CMB kuadrupol sıcaklık dalgalanmasını istenilen miktarda değiştirmeye olanak sağlamıştır. Bu modelin Evrenin en erken zamanları ve uzak geleceği açısından sonuçları da tartışılmıştır.

TABLE OF CONTENTS

LIST OF FIGURES

LIST OF TABLES

LIST OF SYMBOLS

a	Scale factor
c	Speed of light
f	Function
g	Determinant of the metric tensor
$g_{\mu\nu}$	Metric tensor
g_*	Effective number of degrees of freedom
G	Gravitational constant
$G_{\mu\nu}$	Einstein tensor
$\mathcal{G}$	Gauss-Bonnet scalar
h	Reduced Hubble parameter
$h_{\mu\nu}$	Projection tensor
$\hbar$	Reduced Planck constant
H	Hubble parameter
j	Jerk parameter
k	Spatial curvature parameter
k_{B}	Boltzmann constant
K	Number of parameters
ℓ	Multipole moment
L	Likelihood
$\mathcal{L}$	Lagrangian density
N	Dimension
p	Pressure
q	Deceleration parameter
r	Distance
R	Ricci scalar
$R_{\mu\nu}$	Ricci curvature tensor
s	Average expansion scale factor
S	Action

t	Time
T	Temperature
$T_{\mu\nu}$	Energy-momentum tensor
$\mathcal{T}$	Trace of energy-momentum tensor
$\mathbf{T^2}$	Self-contraction of energy-momentum tensor
u^μ	Four velocity
v_r	Recessional velocity
V	Potential of scalar field
w	Equation of state parameter
z	Redshift
α	Model parameter
α'	Normalized model parameter
Γ	Scattering rate
ζ	Bulk viscosity coefficient
θ	Angle
Θ	Volume expansion rate
κ	Newton's constant
λ	Wavelength of light ray
Λ	Cosmological constant
ρ	Energy density
$\sigma_{\alpha\beta}$	Shear tensor
σ^2	Shear scalar
τ	Torsion scalar
ϕ	Scalar field in Jordan frame
ψ	Scalar field in Einstein frame
ω	Coupling parameter
Ω	Density parameter

LIST OF ACRONYMS/ABBREVIATIONS

1D	One Dimensional
2D	Two Dimensional
2dF	Two Degree Field Galaxy Redshift Survey
3D	Three Dimensional
AIC	Akaike Information Criterion
BAO	Baryon Acoustic Oscillations
BBN	Big Bang Nucleosynthesis
BD	Brans-Dicke
BOSS	Baryon Oscillation Spectroscopic Survey
CC	Cosmic Chronometers
CDM	Cold Dark Matter
CL	Confidence Level
CMASS	Constant Mass
CMB	Cosmic Microwave Background
DE	Dark Energy
DM	Dark Matter
DR	Data Release
EF	Einstein Frame
EFE	Einstein Field Equations
EH	Einstein-Hilbert
EMLG	Energy-Momentum Log Gravity
EMPG	Energy-Momentum Powered Gravity
EMSG	Energy-Momentum Squared Gravity
EMT	Energy-Momentum Tensor
EoS	Equation of State
GB	Gauss-Bonnet
GR	General Relativity
JF	Jordan Frame

ΛCDM	Lambda Cold Dark Matter
LQC	Loop Quantum Cosmology
LRS	Locally Rotationally Symmetric
MCMC	Markov Chain Monte Carlo
NGC	New General Catalogue
PLK	Planck Satellite
RW	Robertson-Walker
SDSS	Sloan Digital Sky Survey
SN	Supernovae
VSL	Varying Speed of Light
WIMPs	Weakly Interacting Massive Particles
WMAP	Wilkinson Microwave Anisotropy Probe

1. INTRODUCTION

Cosmology is the branch of physics studying the largest-scale structures and dynamics of the Universe as a whole. It aims at drawing the self-consistent picture of the origin, evolution and the fate of the Universe relying on a unique model that is testable with observations. A cosmological model is characterized by specifying the spacetime geometry of the Universe, the physical behavior of the material filling the Universe and the interaction between this geometry and this material.

It can be said that cosmology as a formal science in its current sense has begun with the establishment of Einstein's gravitational theory, the General Relativity (GR) at the beginning of the previous century. Nevertheless, the ground-breaking discovery was that the Universe has been expanding. The solid evidence of the cosmic expansion has led to the idea that if we rewind this expansion, the Universe should have once been started from an extremely hot and dense state. This Big Bang model, which is now seen as the valid description of the cosmic history with a broad consensus, rests on four observational pillars: (i) the Hubble diagram as a measure of the expansion, (ii) abundances of light elements produced by Big Bang Nucleosynthesis (BBN), (iii) the Cosmic Microwave Background (CMB) and (iv) large-scale structure formation [1]. However, the model owes this success to the introduction of two mysterious components: dark matter (DM) and dark energy (DE).

Resulting from the cumulative efforts of astronomers such as Vesto Slipher and Georges Lemaître, in 1929, Edwin Hubble discovered that characteristic spectral lines of galaxies are redshifted by an amount proportional to their distances and, correspondingly, these galaxies are receding away from us according to a linear relation between their nonrelativistic recessional velocities v_r and distances r as [2]

$$v_r = H_0\, r \tag{1.1}$$

where H_0 is named Hubble "constant". Equation (1.1) is called as the Hubble-Lemaître law. The value of H_0 is determined by calculating the slope of the line in the Hubble diagram which depicts the recession velocities of distant galaxies with respect to their distances. The amount of aforementioned redshift of spectral lines are defined by the fractional change in their observed wavelength as follows

$$z = \frac{\lambda_{\text{obs}} - \lambda_{\text{em}}}{\lambda_{\text{em}}}. \tag{1.2}$$

Here λ_{em} is the wavelength of the light ray emitted from the galaxy and λ_{obs} is the wavelength observed by us. As a result, these observations reveal the fact that the Universe is expanding. If the expansion of space is at a factor of a during the transit of the light ray, the wavelength of the light is stretched out by this expansion which leads to the relation

$$\frac{\lambda_{\text{obs}}}{\lambda_{\text{em}}} = \frac{a(t_{\text{obs}})}{a(t_{\text{em}})} = 1 + z \tag{1.3}$$

where t_{em} is the time of the emission of light from the galaxy and t_{obs} is the time of observation. The present value of scale factor is conventionally set to one, i.e. $a(t_{\text{obs}}) = 1$. During the expansion, the comoving distance that is the difference between coordinates of two points remains constant. What grows with time is the physical distance which equals to the comoving distance times the scale factor. The rate of expansion is expressed by the Hubble parameter H as

$$H = \frac{\dot{a}}{a} \tag{1.4}$$

which is a quantity varying with time and H_0 denotes its present-day value whose precise measurement is a problematic issue in the current cosmology (see, e.g., [3] for a comprehensive list of references regarding the issues in measuring the value of H_0). For now, it can be said that on average $H_0 \approx 70\,\text{km}\,\text{s}^{-1}\text{Mpc}^{-1}$, but we will refer to this point later in Section 1.2.

The time elapsed from Big Bang to the present day is about 13.8 Gyr (assuming the standard cosmological model). At very early times when the Universe had a much higher density and temperature (at energy scale of $\sim 1\,\mathrm{MeV}$ which corresponds to the typical nuclear binding energy), protons and neutrons were in thermal equilibrium, namely continuously interacting with other particles around, and there were no bound nuclei. As the Universe had expanded and cooled, the energy scale decreased to values at which photons (constitutes radiation along with neutrinos) could not destroy bound nuclei any more. At energy scale of $\sim 0.1\,\mathrm{MeV}$ (time scale of $\sim 100\,\mathrm{s}$), the formation of light elements consisting of largely helium-4 along with smaller amounts of deuterium, helium-3 and lithium-7 occured in a process named as *Big Bang Nucleosynthesis* (BBN). The abundance of these light elements, in particular that of deuterium, depend on the total baryon (protons and neutrons along with electrons which are technically leptons but have negligible mass compared to nuclei) density in the Universe and well constrains its value to merely 5% of the total cosmic density today. On the other hand, through a wide variety of probes, we know that the total pressureless matter density constitutes 30% of the present-day cosmic density, thus, BBN strongly supports the argument that the vast majority (more than 80%) of matter in the Universe is in the nonbaryonic form.

When photons were sufficiently energetic to ionize the neutral atoms but incapable of dissociating bound nuclei, the Universe was filled with "baryon-photon fluid" which is a plasma of free nuclei, electrons and photons in equilibrium. As the Universe continued to expand and cool with evolving time, energy of photons fell below the amount needed to ionize the hydrogen atom, which has the minimum ionization energy with the value of 13.6 eV. In order to form neutral hydrogen, free electrons and protons joined in a process called *recombination* occurring at an energy scale of 0.25 eV. Even though the very early Universe was radiation-dominated, the cosmic energy density started to be dominated by matter at this epoch (matter-radiation equality time scale corresponds to 10^4yr). Following recombination, photons propagated freely without scattering which rendered the Universe transparent. This process, which is named *decoupling*, took place at the energy scale of about 0.1 eV (time scale of 10^5yr).

Namely, decoupling occurred when the temperature of the Universe was about 3000 K. However, as a result of redshift, these decoupled photons today have wavelengths in the microwave region and comprise the so-called *Cosmic Microwave Background* (CMB). The CMB can be interpreted as a snapshot of the Universe at the time of decoupling. The spectrum of CMB fits to that of black-body with a temperature precisely measured as $T_0 = 2.7255 \pm 0.0006\,\mathrm{K}$ today [4]. It should be noted here that the epoch of decoupling can be more formally expressed as the period when the scattering rate of photons equal to the expansion rate of the Universe. In fact, this is not specific to photons, same process occurs for other species of particles in the early Universe. If a particle has a scattering rate Γ much grater than the expansion rate H of the Universe, that is $\Gamma \gg H$, it stays in equilibrium and interacts continuously with other particles. When the scattering rate starts to fall behind the expansion rate ($\Gamma \approx H$), the particle decouples from the rest of the cosmic plasma and this process is known as *freeze-out*. Since the interaction rates, which are proportional to density squared, were typically high, the early Universe was in a relatively simpler state consisting of particles in equilibrium beside being smooth.

In 1992, the satellite mission COBE detected anisotropies, fluctuations in different directions, in CMB which implies that the early Universe was not perfectly smooth [5]. Nevertheless, these are very tiny fractional temperature fluctuations in the order of one in 100,000. The power spectrum of CMB anisotropies was currently measured with high precision and mapped over a large range of angular scales [6]. This spectrum exhibits a characteristic pattern of peaks and troughs which are imprints of *acoustic oscillations* that the baryon-photon fluid had experienced before the decoupling occurred. Similar to the production of sound waves in air, the cosmic plasma was compressed (hot regions) and rarefied (cold regions) under counteracting influences of high pressure exerted by photons and gravitational potential wells produced by pressureless matter, hence photons produced acoustic waves that can be seen in CMB spectrum. As these compressions and rarefactions take place in the baryon-photon fluid, their reflection on baryons is also observed as *baryon acoustic oscillations* (BAO). Detailed analysis of acoustic peaks in CMB spectrum revealed that the gravitational effect stemming from

the baryons alone is inadequate to generate the temperature fluctuations beyond the first peak (fundamental wave). From the ratios of amplitudes of adjacent peaks, CMB anisotropies determines that there exists roughly five times more nonbaryonic matter than baryonic one which agrees well with the constraint from BBN. It is also crucial that the position of the first peak is the strongest evidence for the spatial flatness of the Universe.

Contrary to the smoothness of the early Universe, we know that the present Universe contains a wide range of structures from stars and planets to galaxies and clusters of galaxies. The distribution of galaxies has been mapped out by various sky surveys, especially the Sloan Digital Sky Survey (SDSS) and the Two Degree Field Galaxy Redshift Survey (2dF). These maps exhibit that galaxies are not distributed homogeneously, moreover, their distribution is not random. There exists almost no galaxies in some regions surrounded by a large amount of galaxies at their nearest neighborhood. Both temperature variations mapped out by CMB observations and galaxy distributions mapped by sky surveys manifest that the Universe transitioned from a state of smoothness to a state of extreme inhomogeneity as it expanded and cooled. *Gravitational instability* is so far the best explanation for this transition. Since the density perturbations were adiabatic in the early Universe, namely perturbations in all species of particles were on the same scale being proportional to each other, we can extract from the CMB anisotropies that irregularities in the distribution of matter were also initially small. During the matter-dominated era, slightly overdense regions drew matter from their neighbouring regions and rendered themselves denser than before which enhanced the accumulation of matter from underdense to overdense regions as time evolved. This instability due to the attractive nature of gravity has made the initially tiny irregularities grow into the large-scale bound structures we observe in the present Universe. Note that although this process was led mainly by gravity, the growth of structure was slowed down by the expansion of the background Universe and the pressure of baryon-photon fluid existing until decoupling. Independent from BBN and CMB, observations related to the structure in the Universe necessitates the existence of nonluminous form of matter in addition to baryons. Strong evidence is

based on mass estimates deduced from galaxy rotation curves and galaxy velocities within clusters. The discrepancy between the mass values inferred through gravity and detected by electromagnetic radiation reveals that more than 80% of the total matter present in the Universe is invisible. The structure formation also supports the nonbaryonic nature of this additional component which decoupled from photons and started to form sufficiently deep gravitational potential wells much before the recombination era.

What we know about the mysterious component which contribute to almost 85% of the total matter density present in the Universe is that it moves very slowly compared to the speed of light (cold) and interacts extremely weakly with ordinary matter and electromagnetic field (dark). Accordingly, this nonrelativistic and invisible component is named as *cold dark matter* (CDM). As CDM does not take part in BBN which requires a small amount of baryonic matter corresponding to a few percent of the cosmic energy density, it is expected to be nonbaryonic in origin. Also, nonbaryonic CDM is consistent with the explanation of the structure formation through gravitational instability. Among many other candidates, the most favoured candidate for CDM is some new and as-yet-undiscovered species of particles, particularly Weakly Interacting Massive Particles (WIMPs). They interact through not only gravity but also weak nuclear force or any unknown weaker force, and have large mass ($10-1000$ GeV) compared to particles in Standard Model. We would like to add that in spite of its popularity, several investigations for alternatives to WIMPs are also being carried out. While the nature of CDM keeps its mystery, the picture of Big Bang model is not yet complete for us since 70% of the present-day cosmic energy budget is still missing.

Following the discovery of the expanding Universe, for almost 70 years, cosmologists had tried to measure the deceleration of this expansion due to the gravitational nature of conventional matter. Contrary to this common expectation, two independent teams, the Supernova Cosmology Project [7] and the High-z Supernova Search Team [8] announced in 1998 that the expansion of the Universe has been accelerating for the past 5 Gyr. This breakthrough has changed the direction of studies in

cosmology. Today a wide variety of probes has confirmed the acceleration and this phenomenon motivates the vast majority of the researches. Since the expansion of the late Universe is at an accelerating epoch, this requires a new component producing a repulsive effect in the field equation of GR. Different than the conventional forms of matter, it has a negative pressure and does not participate in gravitational collapse. Due to our limited knowledge about its nature, this component is named as *dark energy* (DE) which accounts for roughly 70% of the total energy budget of the Universe today. The most straightforward candidate for DE is the cosmological constant Λ that was originally introduced by Einstein in order to achieve a static universe solution in his field equation. The joint observational evidences supporting the cosmological constant Λ and cold dark matter build the standard model of cosmology entitled Lambda Cold Dark Matter (ΛCDM). In the following sections, we shall present the theoretical framework of the ΛCDM model. Then, we shall mention problematic issues relating to the cosmological constant and the model itself. We shall also discuss in detail some of the possible alternative cosmological models having a DE which is not constant.

Units and Convention. In this thesis, we make use of Planck units such that $c = \hbar = k_{\rm B} = 1$ where c is the speed of light, $\hbar$ is the reduced Planck constant, and $k_{\rm B}$ is the Boltzmann constant. We find convenient to define $\kappa = 8\pi G$ scaling the Newton's constant G by a factor of 8π and then set $\kappa = 1$ for brevity throughout the thesis. We use metric signature $(-,+,+,+)$.

1.1. Standard Model of Cosmology: Standard ΛCDM Model

The standard ΛCDM model is based on two main assumptions. First, the expanding Universe is spatially homogeneous and isotropic described by the Robertson-Walker (RW) metric (in line with Cosmological Principle)

$$\mathrm{d}s^2 = -\mathrm{d}t^2 + a^2 \left[\frac{\mathrm{d}r^2}{1-kr^2} + r^2(\mathrm{d}\theta^2 + \sin^2\theta \mathrm{d}\phi^2)\right], \tag{1.5}$$

where $a = a(t)$ is the scale factor as a function of cosmic (proper) time t and k represents the spatial curvature taking values $\{-1, 0, 1\}$ for open, flat and closed 3-spaces respectively. Second, the theory of gravity valid on cosmological scales is General Relativity expressed by the Einstein-Hilbert (EH) action which includes the positive cosmological constant Λ

$$S = \int \mathrm{d}^4x\sqrt{-g}\,\left[\frac{1}{2}(R - 2\Lambda) + \mathcal{L}_\mathrm{m}\right] \tag{1.6}$$

where $g = \det(g_{\mu\nu})$ is the determinant of the metric $g_{\mu\nu}$, $R = g^{\mu\nu}R_{\mu\nu}$ is the Ricci scalar calculated from the Ricci curvature tensor $R_{\mu\nu}$ and $\mathcal{L}_\mathrm{m}$ is the Lagrangian density corresponding to the material content of the Universe. By taking the variation of (1.6) with respect to the inverse metric $g^{\mu\nu}$, the corresponding Einstein Field Equations (EFE) read

$$G_{\mu\nu} + \Lambda g_{\mu\nu} = T_{\mu\nu}. \tag{1.7}$$

Here the Einstein tensor $G_{\mu\nu}$ describes the spacetime geometry and is defined as

$$G_{\mu\nu} = R_{\mu\nu} - \frac{1}{2}Rg_{\mu\nu}, \tag{1.8}$$

and the energy-momentum tensor (EMT) $T_{\mu\nu}$ represents the material content and is defined by $\mathcal{L}_\mathrm{m}$ as

$$T_{\mu\nu} = -\frac{2}{\sqrt{-g}}\frac{\delta(\sqrt{-g}\mathcal{L}_\mathrm{m})}{\delta g^{\mu\nu}} = g_{\mu\nu}\mathcal{L}_\mathrm{m} - 2\frac{\partial\mathcal{L}_\mathrm{m}}{\partial g^{\mu\nu}}. \tag{1.9}$$

From (1.7), the contracted Bianchi identity, i.e., $\nabla^\mu G_{\mu\nu} = 0$, directly implies

$$\nabla^\mu T_{\mu\nu} = 0 \tag{1.10}$$

which means that EMT is covariantly conserved. One further assumption of the standard ΛCDM model is that the material content of the Universe is represented by the

EMT of perfect fluid as

$$T_{\mu\nu} = (\rho + p)u_\mu u_\nu + p g_{\mu\nu} \tag{1.11}$$

together with the barotropic equation of state (EoS)

$$p = w\rho, \tag{1.12}$$

where w = constant, $u^\mu = (1, 0, 0, 0)$ is the four velocity of the fluid in comoving coordinates, ρ is the energy density and p is the pressure of the fluid. Substituting (1.5), (1.11) and (1.12) into (1.7), one eventually reaches Friedmann equations, the field equations governing the ΛCDM universe, as follows

$$3H^2 + \frac{3k}{a^2} - \Lambda = \rho, \tag{1.13}$$

$$-2\dot{H} - 3H^2 - \frac{k}{a^2} + \Lambda = w\rho \tag{1.14}$$

which are the energy density (1.13) and pressure (1.14) equations respectively. Calculating directly $\nu = 0$ component of Equation (1.10) or manipulating Equations (1.13) and (1.14) gives the following continuity equation

$$\dot{\rho} + 3H(1 + w)\rho = 0. \tag{1.15}$$

The solution to the Equation (1.15) dictates that for any constant EoS parameter w,

$$\rho \propto a^{-3(1+w)}. \tag{1.16}$$

For matter $w = 0$ and the evolution equation of pressureless matter (dust) energy density is

$$\rho_{\mathrm{m}} = \rho_{\mathrm{m0}}\, a^{-3} \tag{1.17}$$

and $w = 1/3$ for radiation (relativistic species) leads to the energy density evolution as

$$\rho_{\rm r} = \rho_{\rm r0}\, a^{-4}, \tag{1.18}$$

where $\rho_{\rm m0}$ and $\rho_{\rm r0}$ are the present-day values of the energy densities of matter and radiation respectively. At this point, we note that the radiation density $\rho_{\rm r}$ is composed of conventional sources such as photons and three species of massless neutrinos while the matter density $\rho_{\rm m}$ is composed of conventional baryonic matter and the nonbaryonic component CDM. Additionally, the bare cosmological constant Λ on the left-hand side of the Equation (1.13) can be moved to the right-hand side and treated as the constant vacuum energy density with EoS parameter $w = -1$ (i.e. $p_\Lambda = -\rho_\Lambda$). Eventually, the Friedmann equations (1.13) and (1.14) of the multi-fluid ΛCDM universe can be rewritten as

$$3H^2 + \frac{3k}{a^2} = \frac{\rho_{\rm m0}}{a^3} + \frac{\rho_{\rm r0}}{a^4} + \Lambda, \tag{1.19}$$

$$-2\dot{H} - 3H^2 - \frac{k}{a^2} = \frac{1}{3}\frac{\rho_{\rm r0}}{a^4} - \Lambda. \tag{1.20}$$

We note that the spatial curvature k evolving with a^{-2} might be interpreted as a source with EoS parameter $w = -1/3$. However, relying on the inflationary paradigm [9–12], the standard ΛCDM model assumes the Universe is spatially flat ($k = 0$). For a spatially flat universe, i.e. $k = 0$, (1.19) and (1.20) reduces to

$$3H^2 = \frac{\rho_{\rm m0}}{a^3} + \frac{\rho_{\rm r0}}{a^4} + \Lambda, \tag{1.21}$$

$$-2\dot{H} - 3H^2 = \frac{1}{3}\frac{\rho_{\rm r0}}{a^4} - \Lambda. \tag{1.22}$$

Here we see that there is a direct connection between geometry and energy. For the Universe to be able to have flat geometry, the total cosmic density must be equal to a special value which is the *critical density* defined as

$$\rho_{\rm crit} = 3H^2. \tag{1.23}$$

If the total cosmic energy density is higher than this critical density ($\rho_{\rm total} > \rho_{\rm crit}$), the Universe is spatially closed. The cosmic energy density lower than the critical value ($\rho_{\rm total} < \rho_{\rm crit}$) implies that the Universe is spatially open. Also, it is important to emphasize that (1.21) exhibits that the radiation density ($\rho_{\rm r} \propto \frac{1}{a^4}$) dilutes faster than the matter density ($\rho_{\rm m} \propto \frac{1}{a^3}$) while Λ remains constant. As we discussed before, at very early times Universe was radiation-dominated whereas it was matter-dominated for most of the history of Universe since $z \approx 3400$ and the cosmological constant is indeed significant relatively recently. Domination of cosmological constant over all sources leads to the so-called de Sitter universe with constant Hubble parameter, namely $H = \sqrt{\frac{\Lambda}{3}}$. Going one step further, one might express the Hubble parameter (1.21) of the standard ΛCDM model as follows

$$\frac{H^2}{H_0^2} = \Omega_{\rm m0}(1+z)^3 + \Omega_{\rm r0}(1+z)^4 + \Omega_{\Lambda 0}, \tag{1.24}$$

where $\Omega_{\rm m0} = \frac{\rho_{\rm m0}}{3H_0^2}$, $\Omega_{\rm r0} = \frac{\rho_{\rm r0}}{3H_0^2}$, and $\Omega_{\Lambda 0} = \frac{\Lambda}{3H_0^2}$ are the present-day density parameters of matter, radiation and the cosmological constant respectively. Here we have used the fact that $a = (1+z)^{-1}$. Evaluated at $z = 0$ (today), (1.24) implies that $\Omega_{\rm m0} + \Omega_{\rm r0} + \Omega_{\Lambda 0} = 1$. In the light of our discussion before, we can reach that $\Omega_{\rm m0} \sim 0.3$, $\Omega_{\Lambda 0} \sim 0.7$ and the radiation density is today negligible with $\Omega_{\rm r0} \sim 10^{-4}$.

The standard ΛCDM model is the most economical cosmological model that successfully explains the late-time accelerated cosmic expansion and it is in fairly good agreement with the currently available high-precision data [6,8,13–16]. Nevertheless, it suffers from profound theoretical issues relating to the cosmological constant Λ [17–19]. The presence of Λ term in the EH action by alone induces the "cosmological constant problem", viz., the huge discrepancy, which is 10^{123} orders of magnitude, between its observed value $\sim 10^{-47}\,{\rm GeV}^4$ explaining the accelerated expansion of the Universe and its theoretical value $\sim 10^{76}\,{\rm GeV}^4$ predicted by the quantum field theory [20]. On the other hand, as we have indicated before, the late-time accelerated expansion of the Universe is relatively recent phenomenon which causes the "cosmic coincidence problem" implying that the present-day is a special epoch with nearly equal energy densities

of cosmological constant and matter. This problem signals the extreme fine-tuning of initial conditions required to be able to satisfy $\rho_\Lambda/\rho_{\rm m} \sim 1$ at the present time for not only Λ but also other DE models [21]. Reasonable consistency of the standard ΛCDM model with most of the currently available data [6,8,13–16] implies that the deviations from the standard ΛCDM model should not be drastic from the phenomenological point of view whereas they can be conceptually very different. Certainly, the aforementioned notoriously challenging theoretical issues related to Λ [17–19] along with the recent theoretical (e.g., de Sitter Swampland conjecture [22–29]) and observational (e.g., persistent tensions among some existing datasets [30–49]) developments might require profound modifications giving rise to an evolving DE component that we shall discuss in the next section.

1.2. Dynamical Dark Energy

Despite being the simplest and most successful cosmological model that delineates the dynamics and the large-scale structure of the observable Universe and that is in good agreement with most of the currently available data [6,8,13–16], the standard ΛCDM model suffers from tensions of various degrees of significance between some existing data sets [30–49] besides the issues on the theoretical side. As a crucial example, the measured value of Hubble constant, $H_0(\Lambda{\rm CDM}) = 66.93 \pm 0.62\,{\rm km\,s^{-1}Mpc^{-1}}$, from the CMB data by the Planck Collaboration [16] in the standard ΛCDM model is 3.4σ lower than the model-independent local value, $H_0 = 73.24 \pm 1.74\,{\rm km\,s^{-1}Mpc^{-1}}$, obtained using Cepheid variables and supernovae (SN) by Riess et al. [50]. Moreover, the Lyman-α forest measurements of the BAO by the Baryon Oscillation Spectroscopic Survey (BOSS) prefer a smaller value of the pressureless matter density parameter than is preferred by the CMB data within the standard ΛCDM model [51]. Such tensions are of considerable importance since detection of even small deviations from the basic ΛCDM model could imply profound modifications to the fundamental theories underpinning this model. For instance, the BOSS collaboration reported a clear detection of DE in [36], consistent with positive Λ for $z < 1$, but with a preference for a DE yielding negative energy density values for $z > 1.6$. Figure 11 of [36] shows that BAO+Type

Ia SN+Planck data combinations prefer a DE density passing below zero in the redshift interval $1.6 < z < 3.0$. Likewise, the BOSS collaboration measurement [36] of $H(z = 2.34) = 222 \pm 7 \mathrm{km\,s^{-1}Mpc^{-1}}$ is in significant tension ($\sim 2{-}2.5\sigma$) with the higher value preferred by the standard ΛCDM model. They then argued that the Lyman-α data from $z \sim 2.3$ can be accommodated by a nonmonotonic evolution of $H(z)$, and thus of $\rho_{\mathrm{total}}(z)$ within GR, which is difficult to achieve in any model with nonnegative DE density. However, a "physical DE" having negative energy density would be physically problematic, hence DE might rather be an "effective source" arising from a modified theory of gravity. In line with this, [52] discusses that the Lyman-α data can be addressed by using a physically motivated modified gravity model which gives rise to the alteration of the Friedmann equation for $H(z)$ itself. They further construct a null diagnostic based on Hubble parameter measurements, also relevant to the Lyman-α data, used to determine whether DE is Λ or not and suggest that tension in this diagnostic can be alleviated in models in which Λ is dynamically screened, requiring an effective DE density crossing below zero and concurrently exhibiting a pole in its EoS parameter at large redshifts.

1.2.1. Extensions of Standard ΛCDM Model

Attempts to resolve the issues related to the standard ΛCDM model can be classified into two categories. First is the invocation of new kinds of exotic sources having a large negative pressure by remaining in the framework of GR. As is known, the cosmological constant Λ is the simplest of this type of sources and more complicated, namely dynamical, ones are introduced in the literature. One example is the generalization of the barotropic EoS of perfect fluid via the introduction of the nonlinear stresses, namely $p = -\rho - f(\rho)$ (where f is an arbitrary function) [53, 54]. A new form of fluid stress can also be obtained by extending the barotropic EoS with the addition of a bulk viscous stress which leads to $p = w\rho - 3H\zeta(\rho)$ (where ζ is the bulk viscosity coefficient) [55]. Also, DE was commonly tried to be explained by employing a scalar field (quintessence) with various forms of potentials in the material content of the Universe [56, 57]. Regarding all these proposals in the context of accelerated

cosmic expansion, it should be noted that the problem with the introduction of exotic fluid stresses to the EFE is that it suffers from the violation of strong energy condition which can be seen from the acceleration equation obtained from (1.13) and (1.14) as

$$\frac{\ddot{a}}{a} = -\frac{1}{6}(\rho + 3p) + \frac{\Lambda}{3}. \tag{1.25}$$

In the case of absence of Λ, the strong energy condition $\rho + 3p \geq 0$ leads to a decelerating universe ($\ddot{a} < 0$) so that a physical DE component responsible for the accelerated expansion should violate this condition by satisfying $\rho + 3p < 0$. Moreover, in line with the recent observations discussed before, the possibly required negative energy density for DE is a problematic issue for a physical source.

The second approach is the replacement of GR with a modified gravity theory relying on the idea that GR is invalid on cosmological scales. The basic principle is to change the form of coupling between the spacetime represented by the metric $g_{\mu\nu}$ and the material content represented by the EMT $T_{\mu\nu}$. While it is possible to apply this modification at the level of field equations, the more common and formal method is to start from the action functional. The action of a gravity theory is composed of curvature and matter sectors and can be generalized as

$$S = \int \mathrm{d}^4x\sqrt{-g}\ (\mathcal{L}_\mathrm{c} + \mathcal{L}_\mathrm{m}) \tag{1.26}$$

where $\mathcal{L}_\mathrm{c}$ is the curvature part of the Lagrangian density and $\mathcal{L}_\mathrm{m}$ is the matter part of the Lagrangian density. Note that $\mathcal{L}_\mathrm{c} = \frac{1}{2}R$ corresponds to EH action representing the standard GR. Any change in the curvature sector results in modification on the left-hand side of EFE and analogously, modifying the matter sector alters the appearance of the EMT on the right-hand side. The literature to date is usually concentrated on left-hand side/curvature-type modifications. Accordingly, the widely-known modifications to the curvature sector are $f(R)$ gravity in which the linear term R is replaced by an analytical function of it, scalar-tensor theories including the famous Brans-Dicke (BD) gravity, Gauss-Bonnet (GB) gravity $f(\mathcal{G})$ constructed from a Lovelock scalar

$\mathcal{G}$ and teleparallel gravity $f(\tau)$ where the torsion scalar τ is included in the action (see [58–64] for reviews on DE and modified theories of gravity). The main idea behind this type of modifications is to generalize the linear function of R either by coupling it to extra fields or by adding new scalars derived from higher order curvature related terms into the action. Conversely, the research related to the right-hand side/EMT-type modifications is very limited. The first example is $\Lambda(\mathcal{T})$ gravity [65] in which the cosmological term is considered as a function of the trace $\mathcal{T}$ of EMT instead of a constant value. $f(R,\mathcal{T})$ [66] and $f(R,\mathcal{T}^{\phi})$ [67] models add the trace of $T_{\mu\nu}$ to the matter Lagrangian density while generalizing the linear curvature term to an arbitrary function of R. A more generalized model $f(R,\mathcal{L}_{\rm m})$ [68] studies nonminimal curvature-matter coupling and, in the same manner, $f(R,\mathcal{T},R_{\mu\nu}T^{\mu\nu})$ gravity [69–71] includes the coupling between Ricci curvature and EMT. In the framework of teleparallel equivalent of GR, $f(\tau,\mathcal{T})$ [72] includes the nonminimal coupling of torsion and matter. At this point, one might think that likewise the interpretation of Λ either as a bare cosmological constant on the left-hand side or a vacuum energy density on the right-hand side in the GR, a similar correspondence might be found between the curvature-type and EMT-type modifications. Although there exists such cases, it is not always possible or at least trivial so that focusing on only curvature-type modifications may cause leaving out a rich class of modified gravity models stemming from matter-type modifications.

Regardless of the method concerning the alteration of the standard GR, the most general modification to the $H(z)$ of ΛCDM model can be expressed by

$$3H^2(z)=\rho_{\rm m0}(1+z)^3\big[1-u(z)\big]+\Lambda-v(z), \tag{1.27}$$

involving functions $u(z)$ and $v(z)$ that represent two principal modifications. The function $u(z)$ stems from the nonconservation of the matter stresses and $v(z)$ stands for the new extra terms resulting from the modification of EH action. Interpreting all the terms other than the matter density term $\rho_{\rm m0}(1+z)^3$ as arising from DE, i.e.

writing $3H^2(z) = \rho_{\rm m0}(1+z)^3 + \rho_{\rm DE}$, would lead to an effective DE of the form

$$\rho_{\rm DE} = \Lambda - \rho_{\rm m0} u(z)(1+z)^3 - v(z). \tag{1.28}$$

It can be seen that $u(z) > 0$ and $v(z) > 0$ would drive $\rho_{\rm DE}$ towards negative values. When we have $\rho_{\rm m0} u(z)(1+z)^3 + v(z) > \Lambda$, $\rho_{\rm DE}$ crosses below zero, thereby Λ could be screened. Dynamical $u(z)$ and $v(z)$ functions are familiar from scalar-tensor theories, as we mentioned before, most studied and well established models among the alternative theories describing gravity. In order to illustrate how these modification functions arise, we shall now particularly analyze the scalar-tensor theory in the context of isotropic cosmology. The action representing the scalar-tensor theory in the so-called Jordan frame (JF) is [60]

$$S^{\rm JF} = \int {\rm d}^4x\sqrt{-g}\,\left[\frac{1}{2}\left(\phi R - \frac{\omega(\phi)}{\phi}\nabla_\mu\phi\nabla^\mu\phi - 2\Lambda(\phi)\right) + \mathcal{L}_{\rm m}\right] \tag{1.29}$$

where $\omega(\phi)$ is the coupling parameter of the scalar field ϕ to matter and $\Lambda(\phi)$ is the dynamical cosmological term related to the potential of the scalar field. In the $\omega \to$ constant and $\Lambda \to 0$ limit, this model reduces to BD gravity [73] which is the well known first extension of GR. The corresponding field equation obtained with the metric variation reads

$$\phi G_{\mu\nu} + \left(\Box\phi + \frac{\omega}{2\phi}(\nabla\phi)^2 + \Lambda(\phi)\right)g_{\mu\nu} - \nabla_\mu\nabla_\nu\phi - \frac{\omega}{\phi}\nabla_\mu\phi\nabla_\nu\phi = T_{\mu\nu}. \tag{1.30}$$

We note that in JF the gravitational field is characterized by both the metric $g_{\mu\nu}$ and the scalar field ϕ which couples with the curvature term. The matter Lagrangian does not depend on ϕ explicitly and EMT is covariantly conserved. We can switch to the Einstein frame (EF) representation of the theory using the conformal transformation defined as $g_{\mu\nu} = \bar{g}_{\mu\nu}/\phi$ and write the action of the scalar-tensor theory in EF as

$$S^{\rm EF} = \int {\rm d}^4x\sqrt{-\bar{g}}\,\left[\frac{1}{2}\bar{R} - \left(\frac{1}{2}\bar{\nabla}_\mu\psi\bar{\nabla}^\mu\psi + V(\psi)\right) + \bar{\mathcal{L}}_{\rm m}\right] \tag{1.31}$$

where $V(\psi) = \Lambda/\phi^2$ and ψ is the corresponding scalar field in EF. Here quantities and operators with over-bars are defined by the metric $\bar{g}_{\mu\nu}$. The field equation of the theory in EF is

$$\bar{G}_{\mu\nu} = \bar{T}_{\mu\nu} + \bar{\nabla}_\mu\psi\bar{\nabla}_\nu\psi - \left(\frac{1}{2}\bar{\nabla}_\epsilon\psi\bar{\nabla}^\epsilon\psi + V(\psi)\right)\bar{g}_{\mu\nu}. \tag{1.32}$$

The advantage of EF is that the curvature and the scalar field are decoupled now and the field equation of this frame is equivalent to EFE with the contribution of canonical scalar field as a new type of matter. Consequently, EMT in this frame is not conserved because of the nonzero covariant derivative of $T_{\mu\nu}$ calculated as

$$\bar{\nabla}_\mu\bar{T}^{\mu\nu} = \sqrt{\frac{1}{2(3+2\omega)}}\bar{T}\,\bar{\nabla}^\nu\psi. \tag{1.33}$$

Assuming RW metric and perfect fluid EoS, the modified Friedmann equation in JF takes the following form

$$3H^2 = \frac{\rho}{\phi} - \frac{3k}{a^2} - 3H\frac{\dot{\phi}}{\phi} + \frac{\omega}{2}\frac{\dot{\phi}^2}{\phi^2} + \frac{\Lambda(\phi)}{\phi}, \tag{1.34}$$

and corresponding equation in EF is

$$3\bar{H}^2 = \bar{\rho} + \frac{\dot{\psi}^2}{2} + V(\psi). \tag{1.35}$$

Comparing (1.34) and (1.35) with the general form of ΛCDM extension (1.27), one can see that $u(z)$ stands for a varying effective gravitational coupling strength in the JF, namely $G_{\text{eff}} \sim \frac{1}{\phi}$. On the other hand, $u(z)$ is generated by the nonconservation of matter in the EF [74]. Concurrently, $v(z)$ stands for the new terms due to the scalar field ϕ associated with varying gravitational "constant", G in JF and those due to ψ associated with the nonconservation of EMT in EF. In such models, when the effective gravitational coupling strength gets weaker with increasing redshift, ρ_{DE} (as defined in (1.28)) becomes negative at large redshifts [74–77].

A set of other examples of $\rho_{\rm DE}$ crossing below zero exist in cosmological models based on GB gravity [78] which is constructed with the addition of the arbitrary function $f(\mathcal{G})$ of the GB invariant $\mathcal{G} = R^2 - 4R_{\mu\nu}R^{\mu\nu} + R_{\mu\nu\sigma\epsilon}R^{\mu\nu\sigma\epsilon}$ into the EH action. Linear contribution of GB scalar to the action functional (i.e. $f(\mathcal{G}) \propto \mathcal{G}$) does not induce any change on the dynamics of the GR since it is a topological invariant in four dimensions. However, nontrivial functions of $\mathcal{G}$ introduce new curvature-type terms to the field equations of GR. For spatially flat RW spacetime, the modified Friedmann equation of GB gravity reads

$$3H^2 = \rho_{\rm r} + \rho_{\rm m} - f + \mathcal{G}\frac{\partial f}{\partial \mathcal{G}} - 24\dot{\mathcal{G}}H^3\frac{\partial^2 f}{\partial \mathcal{G}^2} \tag{1.36}$$

where GB scalar takes the form of $\mathcal{G} = 24H^2(\dot{H} + H^2)$. In this model, matter and radiation component evolve as in the GR resulting in $u(z) = 0$. The new terms coming from the GB modification generates dynamical $v(z)$ and the corresponding effective DE has the energy density as $\rho_{\rm DE} = -f + \mathcal{G}\frac{\partial f}{\partial \mathcal{G}} - 24\dot{\mathcal{G}}H^3\frac{\partial^2 f}{\partial \mathcal{G}^2}$. We note that this model does not contain a true cosmological constant and naturally is free from its problematic issues. Unless we specify how the GB term will contribute to the action functional of the model, it is difficult to realize the zero-crossing behavior of $\rho_{\rm DE}$. However, depending on the choice of the function f, $\rho_{\rm DE}$ might vanish as it has been shown in [78] that effective EoS of DE in power-law model of $f(\mathcal{G})$ with noninteger powers exhibits a pole-like behavior in the matter-dominated epoch. Theories in which Λ relaxes from a large initial value via an adjustment mechanism [79, 80] might be classified in this category as well. The "Relaxed Universe" model was originally proposed as an extension of GR at the level of field equations in which an adjustment mechanism relaxes the initial large value of the cosmological constant and eventually leaves a tiny positive cosmological term. However, it is later understood that this adjustment mechanism can be formalized in the context of generalized GB gravity in which $f(\mathcal{G})$ is replaced by the general function $f(R, \mathcal{G})$ including arbitrary forms of R and $\mathcal{G}$.

In Loop Quantum Cosmology (LQC), corrections due to the effects of quantum geometry give rise to the possibility of exhibiting such a zero-crossing behavior [81,

82]. The effective Friedmann equation of LQC can be written as $3H^2 = \rho(1 - \lambda\rho)$ where λ is a positive constant. Here the total energy density ρ is conserved but its components are not separately. Comparing with (1.27), we see that $u(z)$ is generated by the nonconservation of fluid stresses and $v(z)$ stands for the extra term (i.e., $-\lambda\rho^2$) coming from the quantum geometry corrections. It is remarkable that the minus sign accompanying ρ^2 term plays a crucial role in rendering the zero-crossing behavior of the effective DE component possible.

Besides all these, braneworld models [83, 84] and higher dimensional cosmologies that accommodate dynamical reduction/contraction of the internal space [85–89] might be other possible candidates exhibiting such behavior. In these models, universe is described by (1+3+N) dimensional spacetime where three dimensional external space represents the expanding Universe we observe today while extra N dimensions describes internal space that we cannot observe directly and locally. The extra terms coming from this internal space can behave as an effective DE with negative energy density in the modified Friedmann equation.

In this thesis, as a new example of such zero-crossing models, we investigate a particular theory of modified gravity: Energy-Momentum Squared Gravity (EMSG) [90–96], which generalizes the form of the matter Lagrangian in a nonlinear way and generates dynamical $u(z)$ and $v(z)$ functions concurrently. We make a specific choice of model within the theory, in order to establish whether it is a good candidate for such behaviour. Before proceeding with our choice, we shall now give a brief discussion of EMSG theory and some models studied in the framework of EMSG.

2. ENERGY-MOMENTUM SQUARED GRAVITY

From the EH action of GR, it is possible to design a generalization involving nonlinear matter terms, by adding some analytic functions of a new scalar $\mathbf{T^2} = T_{\mu\nu}T^{\mu\nu}$ formed from the EMT, $T_{\mu\nu}$, of the matter stresses [90]. Such generalizations of GR result in new contributions by the usual material stresses to the right-hand side of the EFE, $v(z)$, without invoking new forms of matter and lead in general to nonconservation of the material stresses, $u(z)$. Moreover, this generalization differs from $f(\mathcal{T})$-type theories in the sense that modifications arising from EMSG can still survive even if EMT is traceless, i.e. $\mathcal{T} = 0$.

2.1. Field Equations

The action of EMSG model is constructed by the addition of the term $f(T_{\mu\nu}T^{\mu\nu})$ to the EH action with a bare cosmological constant, Λ, as follows

$$S = \int \mathrm{d}^4x\sqrt{-g}\,\left[\frac{1}{2}(R - 2\Lambda) + f(T_{\mu\nu}T^{\mu\nu}) + \mathcal{L}_{\mathrm{m}}\right] \tag{2.1}$$

where R is the scalar curvature, g is the determinant of the metric $g_{\mu\nu}$, $\mathcal{L}_{\mathrm{m}}$ is the Lagrangian density corresponding to the matter field described by the EMT $T_{\mu\nu}$. We retain the bare cosmological constant, Λ, in the model in accordance with the Lovelock's theorem [97, 98] which states that it arises as a constant of nature. According to the theorem, the only possible second-order Euler-Lagrange expression obtainable in a four-dimensional space from a scalar density of the form $\mathcal{L} = \mathcal{L}(g_{\mu\nu})$ is $E_{\mu\nu} = \sqrt{-g}\,(\lambda_1 G_{\mu\nu} + \lambda_2 g_{\mu\nu})$, where λ_1 and λ_2 are constants, leading to Newton's gravitational constant $G \equiv \kappa/8\pi$ and cosmological constant Λ in EFE $G_{\mu\nu} + \Lambda g_{\mu\nu} = \kappa T_{\mu\nu}$ (see [60, 99, 100] for further information).

We now take the variation of the action (2.1) with respect to the inverse metric $g^{\mu\nu}$ as follows

$$\delta S = \int \mathrm{d}^4x \Bigg[\frac{1}{2}\frac{\delta(\sqrt{-g}R)}{\delta g^{\mu\nu}} - \Lambda\,\frac{\delta(\sqrt{-g})}{\delta g^{\mu\nu}} + \frac{\delta(\sqrt{-g}\mathcal{L}_{\mathrm{m}})}{\delta g^{\mu\nu}} + f(T_{\sigma\epsilon}T^{\sigma\epsilon})\,\frac{\delta(\sqrt{-g})}{\delta g^{\mu\nu}} + \frac{\partial f}{\partial(T_{\alpha\beta}T^{\alpha\beta})}\frac{\delta(T_{\sigma\epsilon}T^{\sigma\epsilon})}{\delta g^{\mu\nu}}\sqrt{-g}\Bigg]\delta g^{\mu\nu} \tag{2.2}$$

and, as usual, define the EMT of the matter field in terms of the matter Lagrangian density $\mathcal{L}_{\mathrm{m}}$ as follows

$$T_{\mu\nu} = -\frac{2}{\sqrt{-g}}\frac{\delta(\sqrt{-g}\mathcal{L}_{\mathrm{m}})}{\delta g^{\mu\nu}} = g_{\mu\nu}\mathcal{L}_{\mathrm{m}} - 2\frac{\partial\mathcal{L}_{\mathrm{m}}}{\partial g^{\mu\nu}}. \tag{2.3}$$

Here, we notice that the terms in the first line of (2.2) leads to the standard field equation of GR (Equation (1.7)) so that new contributions will arise due to the terms in the second line. As we make use of the relation

$$\delta\left(\sqrt{-g}\right) = -\frac{1}{2}\sqrt{-g}\,g_{\mu\nu}\,\delta g^{\mu\nu}, \tag{2.4}$$

the only nontrivial term is the last one leading to a new tensor defined as

$$\theta_{\mu\nu} \equiv \frac{\delta(T_{\sigma\epsilon}T^{\sigma\epsilon})}{\delta g^{\mu\nu}}. \tag{2.5}$$

To calculate this tensor, we rewrite the self contraction of EMT as $T_{\sigma\epsilon}T^{\sigma\epsilon} = g^{\sigma\lambda}g^{\epsilon\gamma}T_{\lambda\gamma}T_{\sigma\epsilon}$ and substitute into Equation (2.5) which yields

$$\frac{\delta(T_{\sigma\epsilon}T^{\sigma\epsilon})}{\delta g^{\mu\nu}} = \left(g^{\epsilon\gamma}\frac{\delta g^{\sigma\lambda}}{\delta g^{\mu\nu}} + g^{\sigma\lambda}\frac{\delta g^{\epsilon\gamma}}{\delta g^{\mu\nu}}\right)T_{\lambda\gamma}T_{\sigma\epsilon} + g^{\sigma\lambda}g^{\epsilon\gamma}\left(T_{\sigma\epsilon}\frac{\delta T_{\lambda\gamma}}{\delta g^{\mu\nu}} + T_{\lambda\gamma}\frac{\delta T_{\sigma\epsilon}}{\delta g^{\mu\nu}}\right). \tag{2.6}$$

Now we write the variation of EMT using the definition in Equation (1.9) as follows

$$\frac{\delta T_{\sigma\epsilon}}{\delta g^{\mu\nu}} = -g_{\sigma\mu}g_{\epsilon\nu}\mathcal{L}_{\mathrm{m}} + g_{\sigma\epsilon}\frac{\delta\mathcal{L}_{\mathrm{m}}}{\delta g^{\mu\nu}} - 2\frac{\delta^2\mathcal{L}_{\mathrm{m}}}{\delta g^{\mu\nu}\delta g^{\sigma\epsilon}}, \tag{2.7}$$

where we have used the relation

$$\delta g_{\sigma\epsilon} = -g_{\sigma\mu} g_{\epsilon\nu} \delta g^{\mu\nu}. \tag{2.8}$$

Substituting (2.7) into (2.6) and using (2.8) gives

$$\frac{\delta(T_{\sigma\epsilon} T^{\sigma\epsilon})}{\delta g^{\mu\nu}} = 2T^{\gamma}_{\mu} T_{\nu\gamma} - 2T_{\mu\nu}\mathcal{L}_{\mathrm{m}} + 2\mathcal{T}\frac{\delta \mathcal{L}_{\mathrm{m}}}{\delta g^{\mu\nu}} - 4T^{\sigma\epsilon}\frac{\delta^2 \mathcal{L}_{\mathrm{m}}}{\delta g^{\mu\nu}\delta g^{\sigma\epsilon}} \tag{2.9}$$

with $\mathcal{T}$ being the trace of the EMT, $T_{\mu\nu}$. Finally, we replace the first variation of matter Lagrangian density with the expression derived from (1.9) and arrive at

$$\theta_{\mu\nu} = -2\mathcal{L}_{\mathrm{m}}\left(T_{\mu\nu} - \frac{1}{2}g_{\mu\nu}\mathcal{T}\right) - \mathcal{T}T_{\mu\nu} + 2T^{\gamma}_{\mu}T_{\nu\gamma} - 4T^{\sigma\epsilon}\frac{\partial^2 \mathcal{L}_{\mathrm{m}}}{\partial g^{\mu\nu}\partial g^{\sigma\epsilon}}. \tag{2.10}$$

Accordingly, the modified EFE read

$$G_{\mu\nu} + \Lambda g_{\mu\nu} = T_{\mu\nu} + f g_{\mu\nu} - 2\frac{\partial f}{\partial(T_{\mu\nu}T^{\mu\nu})}\theta_{\mu\nu}. \tag{2.11}$$

We note that the last term of (2.10) vanishes since the EMT given in (2.3) does not include the second variation of the matter Lagrangian density $\mathcal{L}_{\mathrm{m}}$. Also, the definition of $\mathcal{L}_{\mathrm{m}}$ that gives rise to the perfect-fluid EMT is not unique, and hence one could choose either $\mathcal{L}_{\mathrm{m}} = p$ or $\mathcal{L}_{\mathrm{m}} = -\rho$, which lead to the same EMT. In the present study, we assume $\mathcal{L}_{\mathrm{m}} = p$. It is noteworthy that interpreting Λ either as a bare cosmological constant or a vacuum energy density leads to two different field equations in EMSG in contrast to GR and we proceed with the bare cosmological constant interpretation in the rest of the study. It can be seen from (2.11) that in vacuum, GR and EMSG are equivalent, namely, all vacuum solutions of GR satisfy the field equations of EMSG provided that the function f is chosen in a way that $f(T_{\mu\nu}T^{\mu\nu}) = 0$ when $T_{\mu\nu} = 0$.

2.2. Cosmological Models based on EMSG

The EMSG model was first proposed in [90] where the specific functions $f(\mathbf{T^2}) = \alpha\sqrt{\mathbf{T^2}}$ and $f(\mathbf{T^2}) = \alpha(\mathbf{T^2})^{-1/4}$ are studied in the context of isotropic cosmology with the aim of explaining accelerated expansion without invoking any DE source including Λ. Next, a particular example $f(\mathbf{T^2}) = \alpha\mathbf{T^2}$ which is the simplest linear contribution of the new scalar, has been studied in various contexts in [91, 93–95, 101–105]. At this point, we should clarify that the term "EMSG" is used in the related literature for both the generalized theory which includes any arbitrary function of the self-contraction of EMT expressed as $f(\mathbf{T^2})$ in the EH action and the specific model of the form $f(\mathbf{T^2}) \propto \mathbf{T^2}$ which corresponds to the addition of the square of EMT alone into the action. EMSG of this form in the presence of dust satisfies the EMT conservation and yields

$$3H^2 = \Lambda + \rho_{\rm m} + \alpha\rho_{\rm m}^2. \tag{2.12}$$

Comparing to (1.27), it can be deduced that $u(z) = 0$ and $v(z) = -\alpha\rho_{\rm m}^2 = -\alpha\rho_{\rm m0}^2(1+z)^6$. Such an additional quadratic contribution of the matter energy density is reminiscent of the loop quantum gravity [82] for $\alpha < 0$, which would lead to negative DE in the past, while the case $\alpha > 0$ corresponds to the braneworld scenarios [84]. The correction terms coming from $f(\mathbf{T^2}) = \alpha\mathbf{T^2}$ modification are dominant over the standard GR term at high energy densities so that the model cannot explain the late time acceleration without invoking Λ or any DE source. For $\alpha < 0$ and $\Lambda > 0$, there is a maximum energy density in the early Universe, i.e. in the radiation-dominated era, which signals that there exists a bounce rather than an initial singularity at this period. It is noteworthy that the model with $\alpha < 0$ does not alter the standard cosmic evolution of the Universe after the bounce. However, if the quadratic energy density term is large enough to be effective today, then it would be the dominant term after just a few redshift from today ($z = 0$) and hence spoil the successful description of the early Universe. It is also remarkable that as the modification terms are effective at high density regimes, there is a charged blackhole solution different than the standard

Reissner-Nordström spacetime. Consequently, [106] studies the axial perturbations of charged blackholes in generalized EMSG model, i.e. with no assumption on the functional form of $f(\mathbf{T^2})$. With the same line of reasoning, [94, 95] attempt to constrain the specific EMSG model ($n = 1$) using compact astrophysical objects such as neutron stars and strange quark stars as source. They derive the hydrostatic equilibrium equations of a spherically symmetric nonrotating star which couples to curvature according to EMSG. In [94], these equations are solved via a numerical method to obtain the mass-radius relations for four different EoS representing the neutron star. The model parameter α is constrained as $-10^{-38}\text{cm}^3/\text{erg} < \alpha < 10^{-37}\text{cm}^3/\text{erg}$ and under this constraint, this EMSG modification does not alter the standard cosmological history of GR at times $t \gtrsim 10^{-4}$ s relevant to the quark-hadron phase transition but becomes influential at much earlier times. Similarly, [95] presents analytical solutions for two special cases and numerical solutions for two realistic cases: polytropic and strange quark stars. One interesting consequence is that EMSG allows the existence of pressureless stars in contrast to GR though they are not stable. It is also notable that EMSG is in agreement with the recent high mass neutron star observations for the polytropic EoS whereas GR needs a stiffer EoS to recover the same value. In addition, [104] makes a somehow similar discussion on quark stars with color flavor locked EoS.

A generalisation of the above model with $f(\mathbf{T^2}) = \alpha\mathbf{T^2}$, is Energy-Momentum Powered Gravity (EMPG), where $f(\mathbf{T^2}) = \alpha(\mathbf{T^2})^n$, as studied in [92, 93, 101, 103, 107, 108]. EMPG model sourced by dust only leads to the Hubble parameter

$$3H^2 = \Lambda + \rho_{\text{m}} + (2n-1)\,\alpha\,\rho_{\text{m}}^{2n}. \tag{2.13}$$

It can be deduced from (2.13) that this modification becomes effective at high energy densities, as in the early Universe for the cases with $n > 1/2$, and at low energy densities, as in the late Universe, when $n < 1/2$. EMPG leads to both $u(z)$ and $v(z)$ emerging dynamically and could be investigated for generating effective DE energy density passage below zero at large redshifts. Nevertheless, it is generally not

possible to obtain explicit exact solutions for $\rho_{\rm m}(z)$, and hence of $\rho_{\rm DE}(z)$, which renders EMPG inconvenient for this type of study [92, 93]. On the other hand, the model was investigated for different n values in purpose of explaining the late time accelerated expansion of the Universe without introducing Λ [92]. For instance, $n = 0$ case leads to mathematically exactly the same background dynamics as ΛCDM model despite the only physical source in the model being dust so that the fine-tuning problems of Λ value does not arise in this EMPG model. Similarly, $n \sim 0$ case behaves like a wCDM-type cosmological model without introducing any DE source. As mentioned above, EMPG model is not able to provide an explicit solution of $\rho_{\rm m}(z)$ for general power of n that is needed for the observational analysis while $z(\rho_{\rm m})$ can be obtained. However, using an approximation procedure the authors of [92] extract an expression for $\rho_{\rm m}(z)$, and on the observational ground, investigate the ranges of (α, n) parameters that yield a viable cosmological model explaining the late-time acceleration without disturbing the successes of GR related to the early Universe. Similarly, the special cases of (α, n) parameters in which the continuity equation can be integrated exactly are discussed in [93]. It should be noted that there is a richer class of de Sitter-like solutions in EMPG compared to the standard ΛCDM model. Moreover, it is possible to find an analytical solution for the general power of n in the high density limit. As discussed for $f(\mathbf{T^2}) = \alpha\mathbf{T^2}$ in [91], EMPG model with $n > 1/2$ can replace the inital singularity with an initial bounce. Here we would like to indicate that a recent study [103] argues that the initial bounce is viable in a dust-only universe for $n = 1$ case and such a viable bounce can occur during a radiation dominated era only when $n = 5/8$. Nonetheless, they further state that for $1/2 < n < 5/8$ case the initial singularity can be replaced by a nonsingular de Sitter epoch. Apart from other studies on EMSG, [93] also briefly discuss the effects of higher-order matter terms stemming from $f(\mathbf{T^2}) = \alpha(\mathbf{T^2})^n$ extension on the cosmological singularities in an anisotropic (Bianchi Type I) universe. For $n > 1/2$ case, modification terms of EMPG might avoid the domination of the shear anisotropy about the initial singularity.

The particular case $n = 1/2$, dubbed as Scale Independent EMSG [96], is another exception which provides explicit exact solution for $H(z)$ required for a detailed obser-

vational test. In this model, the new terms resulting from $f(\mathbf{T^2}) = \alpha\sqrt{\mathbf{T^2}}$ modification in the field equations enter with the same power as the usual terms in GR, yet the energy is not conserved, and this leads to $v(z) = 0$ and $u(z) = 1 - (1+z)^{3\alpha}$, which could provide the desired features in the $\alpha < 0$ case. Nevertheless, observational analysis of the model [96] suggests that α is well constrained to be so close to zero that Scale Independent EMSG is unable to resolve the issues noted in Section 1.2. In [96], the model is studied in the context of multi-fluid cosmology which separates it from other studies discussed so far. In the paper, conventional sources, i.e., baryons and photons couple to the spacetime with respect to GR while dark sector components like CDM and relativistic relics couple via Scale-Independent EMSG theory. Although CDM and relativistic relics are assumed to be minimally interacting, the continuity equations of these components come with extra terms as the conservation of EMT is violated in the model. Consequently, the density evolutions of these sources are modified by the dimensionless parameter α at both background and perturbation levels. We will make use of the same method in Chapter 4 where we consider an anisotropic multi-fluid universe in the framework of $f(\mathbf{T^2}) = \alpha\mathbf{T^2}$ model.

The paper [101] makes pure observational analysis of EMPG model using low-redshift cosmological data based on mainly Type Ia SN and Hubble parameter measurements. First, the EMPG model is assumed to be sourced by pressureless matter and a nonzero cosmological constant as a phenomenological extension of the standard ΛCDM model for three specific cases $n = \{0, 1/2, 1\}$ which provide analytical solutions for $\rho(z)$. The results constrain a very small value on the model parameter α. On the other hand, the data depicts a higher value for the preferred matter density even in $n = 0$ case which is analogous to the standard ΛCDM model. Then, the paper [101] considers the generic power case in which n is also a free parameter and also assume a general EoS parameter w. This generic case is analyzed in two approaches. In the first approach, the model is treated as an extension of the standard ΛCDM model by setting $w = 0$. The data prefers a slightly lower matter density compared to the analysis of specific n values. As a second approach, by setting $\Lambda = 0$, [101] discuss whether the EMPG model can explain the current acceleration of the Universe without

a true cosmological constant. For the matter dominated ($w = 0$) case, the data prefer a higher matter density with n being at a few percent and exhibit a positive correlation between n and the matter density. In generic w case, n cannot be constrained. The results of this case depict a critically higher matter density and slightly negative values for w but 1σ uncertainities are much larger than the ones in the rest of the analysis. It is important to note that in this generic w approach, all cases cover the canonical ΛCDM model at 2σ confidence level (CL). [101] also gives a brief comparison of wCDM and EMPG models in which dust is the only source. While wCDM model is consistent with the standard ΛCDM model at 2σ CL but prefer a slightly larger EoS parameter, EMPG model without a true cosmological constant can explain the late-time accelerated expansion of the Universe at the cost of a larger matter density. Another paper [107] studied dynamical system analysis of EMPG model by generalizing the curvature scalar term to an arbitrary power m which corresponds to the presence of the function $f(R, \mathbf{T^2}) = \beta R^m + \alpha(\mathbf{T^2})^n$ (where α, β, m, n are constants, $m \neq \{0, 1\}$ and $n \neq 0$) in the action. According to the values of the parameters m and n, the critical points of the analysis exhibits various cosmological scenarios such as an effective DE without a true cosmological constant in the presence of dust only, a super-accelerating universe or a matter dominated era with a stiff EoS parameter.

An interesting attempt is to introduce a speed of light c varying temporally (and correspondingly varying gravitational constant G) into EMSG model [102]. Varying speed of light (VSL) theories [109–113] has been proposed as an alternative route to resolve the issues related to the inflationary cosmology. For a matter dominated universe, VSL and constant speed of light theories in the framework of EMSG of the form $f(\mathbf{T^2}) = \alpha\mathbf{T^2}$ are equivalent so that time varying c does not alter the late Universe description of EMSG. VSL theory manifests itself in the presence of radiation, hence by introducing time varying c into EMSG, it is possible to construct an early universe model which is free from both the inflation and the initial big bang singularity. Additionally, a number of other studies in diverse contexts also exist such that Jeans analysis of the generalized EMSG model can be found in [114], Palatini formulation of the model in [105] and thermodynamic analysis in [108].

In the following chapter, we consider a new type of EMSG model, called Energy-Momentum Log Gravity (EMLG) constructed by the functional choice of $f(\mathbf{T^2}) = \alpha \ln(\lambda \mathbf{T^2})$, where α and $\lambda > 0$ are real constants, to the EH action with bare cosmological constant Λ (a related logarithmic modification is considered in the context of $f(R, \mathcal{T})$ gravity [66] in a recent paper [115] after our work). This form has appealing features owing to its determination of $u(z)$ and $v(z)$ in a specific way depending on α. It gives rise to new contributions that appear similar to those of a perfect fluid with constant EoS parameter on the right-hand side of the Friedmann equations, reminiscent of a source with constant inertial mass density (sum of the energy density and pressure). Furthermore, we are able to obtain an explicit exact solution of the pressureless matter energy density in terms of redshift, so that it allows us to conduct an exact theoretical investigation of the model employing the observational data without further simplifications. We search for observationally viable cosmologies, particularly, for an extension of the basic ΛCDM model. We find that the observational data, without excluding the ΛCDM limit of our model, slightly prefers $u(z) > 0$ (associated with the nonconservation of pressureless matter) and $v(z) < 0$ (associated with the new terms of the pressureless matter in the Friedmann equations), where $u(z) > 0$ emerges with the appropriate sign to produce an effective dynamical DE crossing below zero, namely a screening of Λ, at high redshifts as demanded to address the tension with the Lyman-α BAO measurements within the ΛCDM model. We also argue that the EMLG model relaxes, to a certain extent, the persistent tension that occurs between different measurements of H_0 within the standard ΛCDM model.

3. EMSG OF THE FORM $f(\mathbf{T^2}) \propto \ln(\lambda\,\mathbf{T^2})$: ENERGY-MOMENTUM LOG GRAVITY

This chapter is heavily based on the work published in [116].

In this chapter, we introduce and carry out a detailed cosmological investigation of a specific form of the EMSG model,

$$f(T_{\mu\nu}T^{\mu\nu}) = \alpha \ln(\lambda\, T_{\mu\nu}T^{\mu\nu}) \tag{3.1}$$

which is dubbed as Energy-Momentum Log Gravity (EMLG). Here λ has the dimension of inverse energy density squared which guarantees that $\lambda\, T_{\mu\nu}T^{\mu\nu}$ is dimensionless. Some particular advantageous features ensue from the choice of this model. For instance, in the cosmological application of the EMSG theory, this is the only function choice of $f(\mathbf{T^2})$ that gives rise to new contributions of the energy density of a perfect fluid on the right-hand side of the Friedmann equations yielding constant effective inertial mass density (see Section 3.1.1 for the detailed discussion). Moreover, this choice provides us with an explicit exact solution of the matter energy density, particularly in the form of $\rho_{\rm m}(z)$ which is crucial for analytical investigations. We recall that this contrasts with many EMSG-type models (see Section 2.2), in which this is usually not achievable due to the nonlinear coupling of the matter fields to gravity. As indicated previously, [92] investigated a dust-only EMPG model concerning cosmic acceleration, but the exact solution could merely be obtained in the form of $z(\rho_{\rm m})$ whereas the corresponding explicit solution of $\rho_{\rm m}(z)$ could only be attained through an approximation procedure, except for a few particular cases (see [93, 96]).

Consequently, the action (2.1) with our particular choice is

$$S = \int \left[\frac{1}{2}(R - 2\Lambda) + \alpha \ln(\lambda\, T_{\mu\nu}T^{\mu\nu}) + \mathcal{L}_{\rm m}\right] \sqrt{-g}\, \mathrm{d}^4x \tag{3.2}$$

where α is a parameter that measures the gravitational coupling strength of the EMLG modification of GR. Accordingly, the modified EFE (2.11) for this action now become,

$$G_{\mu\nu} + \Lambda g_{\mu\nu} = T_{\mu\nu} + \alpha g_{\mu\nu} \ln(\lambda\, T_{\sigma\epsilon} T^{\sigma\epsilon}) - 2\alpha \frac{\theta_{\mu\nu}}{(T_{\sigma\epsilon} T^{\sigma\epsilon})}. \tag{3.3}$$

From (3.3), the covariant divergence of the EMT reads

$$\nabla^{\mu} T_{\mu\nu} = -\alpha g_{\mu\nu} \nabla^{\mu} \ln(\lambda\, T_{\sigma\epsilon} T^{\sigma\epsilon}) + 2\alpha \nabla^{\mu} \left(\frac{\theta_{\mu\nu}}{T_{\sigma\epsilon} T^{\sigma\epsilon}} \right). \tag{3.4}$$

We note that, unless $\alpha = 0$, the right-hand side of (3.4) does not vanish in general, and thus $\nabla^{\mu} T_{\mu\nu} = 0$ is not satisfied, i.e. the EMT is not conserved.

3.1. Cosmology in EMLG

In the current study, we investigate the cosmological behaviour of the gravitational model stated above. We proceed by considering the spatially maximally symmetric spacetime, given by the RW metric,

$$\mathrm{d}s^2 = -\mathrm{d}t^2 + a^2 \left[\frac{\mathrm{d}r^2}{1 - kr^2} + r^2 (\mathrm{d}\theta^2 + \sin^2\theta \mathrm{d}\phi^2) \right] \tag{3.5}$$

where k is the spatial curvature parameter which takes values in $\{-1,\, 0,\, 1\}$ corresponding to open, flat and closed 3-spaces respectively, and the scale factor $a = a(t)$ is a function of cosmic time t only. The line element (3.5) corresponds to a diagonal metric $g_{\mu\nu} = (-1, a^2, a^2, a^2)$ for a spatially flat universe, i.e. when $k = 0$. For cosmological matter fields representing the physical component of the Universe, we consider the perfect fluid form of the EMT given by

$$T_{\mu\nu} = (\rho + p) u_{\mu} u_{\nu} + p g_{\mu\nu} \tag{3.6}$$

where $\rho > 0$ is the energy density and p is the thermodynamic pressure of the fluid satisfying the barotropic EoS as

$$\frac{p}{\rho} = w = \text{constant}, \tag{3.7}$$

and u_μ is the four-velocity satisfying the conditions

$$u_\mu u^\mu = -1 \quad , \quad \nabla_\nu u^\mu u_\mu = 0. \tag{3.8}$$

Using (3.6) and (3.8), we calculate the trace $\mathcal{T} = g^{\mu\nu}T_{\mu\nu}$ and the self-contraction of the EMT for the perfect fluid with barotropic EoS (3.7) as

$$\mathcal{T} = \rho(3w - 1), \tag{3.9}$$

$$T_{\mu\nu}T^{\mu\nu} = \rho^2(3w^2 + 1). \tag{3.10}$$

Consequently, we also calculate $\theta_{\mu\nu}$ defined in (2.10) for the perfect fluid above as follows

$$\theta_{\mu\nu} = -\rho^2(3w + 1)(w + 1)u_\mu u_\nu. \tag{3.11}$$

Next, using (3.10) and (3.11) along with the metric (3.5) in modified EFE (3.3) yields the modified Friedmann equations

$$3H^2 + \frac{3k}{a^2} = \rho + \Lambda - \alpha \ln\left[\lambda\rho^2(3w^2 + 1)\right] + 2\alpha\frac{(w + 1)(3w + 1)}{(3w^2 + 1)}, \tag{3.12}$$

$$-2\dot{H} - 3H^2 - \frac{k}{a^2} = w\rho - \Lambda + \alpha \ln\left[\lambda\rho^2(3w^2 + 1)\right] \tag{3.13}$$

where $H = \dot{a}/a$ is the Hubble parameter. Denoting the present-day values of the parameters with the subscript 0, we require the following condition for today value of

the Hubble parameter

$$3H_0^2 = \rho_0 + \alpha'\rho_0 + \Lambda \tag{3.14}$$

and accordingly, we obtain the following pair of linearly independent modified Friedmann equations, for a single fluid cosmology,

$$3H^2 + \frac{3k}{a^2} = \rho + \Lambda + \alpha'\rho_0 + \alpha'\rho_0\frac{2}{\gamma}\ln\left(\rho/\rho_0\right), \tag{3.15}$$

$$-2\dot{H} - 3H^2 - \frac{k}{a^2} = w\rho - \Lambda - \alpha'\rho_0\frac{2}{\gamma}\ln\left[\sqrt{3w^2+1}\ \left(\rho/\rho_0\right)\right] \tag{3.16}$$

where we set $\lambda = \rho_0^{-2}$. Here we note that defining $\lambda = \eta\rho_0^{-2}$, where η is a positive coefficient, we could write $\ln(\lambda\, T_{\mu\nu}T^{\mu\nu}) = \ln(\eta) + \ln(T_{\mu\nu}T^{\mu\nu}/\rho_0^2)$. The term $\alpha\ln(\eta)$ then behaves like a cosmological constant, and so simply rescales Λ in the action (3.2) and field equations (3.3). Also, λ does not have any contribution to the continuity equation (3.4) since $\nabla^\mu \ln(\lambda\, T_{\sigma\epsilon}T^{\sigma\epsilon}) = \nabla^\mu \ln(T_{\sigma\epsilon}T^{\sigma\epsilon})$. Consequently, choosing a particular value for η (e.g. $\eta = 1$ as we have done) does not lead to any loss of generality as the model already includes Λ in the action. Here, we define the parameter $\gamma = \gamma(w)$ by

$$\gamma(w) = \ln(3w^2+1) - 2\frac{(3w+1)(w+1)}{(3w^2+1)}, \tag{3.17}$$

which is negative for $-0.27 < w < 2.52$ and positive otherwise that can be seen in Figure 3.1. We also define the dimensionless constant

$$\alpha' = -\alpha\,\gamma\rho_0^{-1}. \tag{3.18}$$

We note that the model contains only a single matter source because in the action (3.2), the terms $\alpha\ln(\lambda\, T_{\mu\nu}T^{\mu\nu})$ and $\mathcal{L}_{\rm m}$ are both related to the material content of the Universe and that the EMT included in the modification term $\alpha\ln(\lambda\, T_{\mu\nu}T^{\mu\nu})$ is the one obtained from the metric variation of $\mathcal{L}_{\rm m}$. However, the terms arising from the EMLG modification couple to gravity with a different strength, α', than the normalized

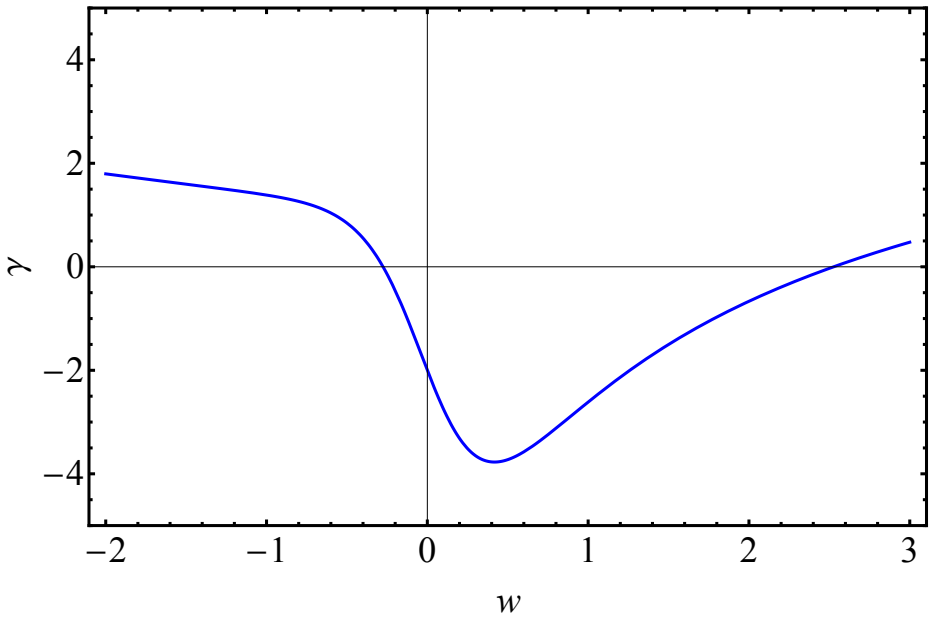

Figure 3.1. The behaviour of the parameter γ for different EoS parameters w, i.e. $\gamma(w)$. The region of most interest has $-1 < w < 1$.

gravitational coupling strength (i.e., $\kappa = 1$) of the conventional terms existing in GR. Furthermore, we notice that α' is a function of not only the true constant parameter of the EMLG modification, α, but also the current energy density, ρ_0, and the EoS parameter, w, describing the type of the perfect fluid source, so $\alpha' = \alpha'(\alpha, \rho_0, w)$. Because of the latter two dependencies implying a violation of the equivalence principle, our EMLG modification must obey constraints from solar system tests of this principle. It would also have some implications in fundamental physics. For instance, the violation of equivalence principle, which is intimately connected with some of the basic aspects of the unification of gravity with particle physics such as string theories [117] and theories of varying constants [118–120]. The consequences of this property are beyond the scope of the current study of the EMLG model, which focuses on the dynamics of a mono-fluid universe, where the only material source is pressureless matter (dust) with the purpose of extending the standard ΛCDM model by considering the new terms arising from EMLG as a correction.

3.1.1. Constant Effective Inertial Mass Density

It is worth noting here that, for a perfect fluid with barotropic EoS, both $\theta_{\mu\nu}$ and $T_{\mu\nu}T^{\mu\nu}$ are proportional to ρ^2 and therefore the last term including the ratio $\theta_{\mu\nu}/(T_{\sigma\epsilon}T^{\sigma\epsilon})$ in (3.3) is independent of the energy density scale, and instead depends only on the type of the fluid (i.e., the EoS of the matter source) and the four-velocity of the fluid. Furthermore, for usual cosmological applications, when we consider a comoving (i.e. $u^\mu = (1, 0, 0, 0)$) fluid with a constant EoS parameter w, this term becomes a constant determined by the model parameter α and the EoS under consideration. On the other hand, the second term proportional to the metric $g_{\mu\nu}$ on the right-hand side of (3.3) will always contribute equally but with opposite signs to the time and space components of this equation in Lorentzian spacetimes, that is to the energy density and pressure equations arising from the metric given in (3.5), and therefore the summation of these equations results in the modifications from the second term on the right-hand side of (3.3) cancelling each other. Consequently, the argument above produces a characteristic feature of the model: if we define the new terms that originate from the EMLG modification in the energy density equation (3.15) as an effective energy density

$$\rho' = \alpha'\rho_0 + \alpha'\rho_0\frac{2}{\gamma}\ln\left(\rho/\rho_0\right) \tag{3.19}$$

and those in the pressure equation (3.16) as an effective pressure

$$p' = -\alpha'\rho_0\frac{1}{\gamma}\ln(3w^2+1) - \alpha'\rho_0\frac{2}{\gamma}\ln\left(\rho/\rho_0\right), \tag{3.20}$$

then the "effective inertial mass density" defined as $\rho' + p'$ is always constant; namely,

$$\rho' + p' = \alpha'\rho_0[1 - \gamma^{-1}\ln(3w^2+1)] \tag{3.21}$$

for $p/\rho = w =$ constant. This feature of the model yields

$$\rho' = \alpha' \rho_0 [1 - \gamma^{-1} \ln(3w^2 + 1)] - p' \tag{3.22}$$

which means that ρ' changes sign when $p' = \alpha' \rho_0 [1 - \gamma^{-1} \ln(3w^2 + 1)]$, and manifests our model's relevance to the studies [36, 52] suggesting that a DE model achieving negative energy density values for redshifts larger than a certain value (e.g., $z \gtrsim 2$ as suggested by [33, 36, 52]) might improve the fit to observational data. It is noteworthy to indicate that the sign change of ρ' does not signal any pathologies since it is an effective energy density, not the physical energy density. For example, in the case of dust ($w = 0$), we have

$$\rho' = \alpha' \rho_{\mathrm{m}0} - p', \tag{3.23}$$

which implies that $\rho' < 0$ when $p' > \alpha' \rho_{\mathrm{m}0}$.

3.1.2. Continuity Equation

The local energy-momentum conservation equation (3.4) of EMLG model is

$$\dot{\rho} + 3H(1 + w)\rho \left[\frac{\gamma\rho(3w^2 + 1) - 2\alpha'\rho_0(3w + 1)}{\gamma\rho(3w^2 + 1) + 2\alpha'\rho_0(3w^2 + 1)} \right] = 0. \tag{3.24}$$

The expression in square brackets is the modification arising due to EMLG and is equal to unity in the case of $\alpha' = 0$, corresponding to GR. One can see that when $\alpha' \neq 0$, the covariant energy-momentum conservation $\nabla^\mu T_{\mu\nu} = 0$, which in GR would lead to $\rho \propto a^{-3(1+w)}$, does not hold for any $w \neq -1$, while the case $w = -1$, corresponding to vacuum energy (i.e. conventional DE), is unmodified by EMLG.

We shall now determine some preliminary constraints on α by considering separately two standard cosmological matter sources: radiation and dust. We commence

with rewriting (3.24) in terms of α

$$\dot{\rho} = -3(1+w)H\rho\left[\frac{\rho(3w^2+1)+2\alpha(3w+1)}{\rho(3w^2+1)-2\alpha(3w^2+1)}\right]. \tag{3.25}$$

A viable cosmological model should satisfy the following conditions

$$H > 0 \quad , \quad \dot{H} < 0 \quad , \quad \rho > 0 \quad , \quad \dot{\rho} < 0 \tag{3.26}$$

where $H > 0$ and $\dot{H} < 0$ together lead to an expanding Universe in line with observations. $\dot{\rho} < 0$ implies that the energy density is decreasing with time, and therefore $H > 0$ and $\dot{\rho} < 0$ together assure that the density is larger at early times and decreases as the Universe expands. As seen from (3.25), taking $H > 0$ and $\dot{\rho} < 0$ leads to

$$(1+w)\rho\left[\frac{\rho(3w^2+1)+2\alpha(3w+1)}{\rho(3w^2+1)-2\alpha(3w^2+1)}\right] > 0. \tag{3.27}$$

Substituting $w = 1/3$ into (3.27), we obtain

$$\frac{4}{3}\,\rho_{\rm r}\left[\frac{\rho_{\rm r}+3\alpha}{\rho_{\rm r}-2\alpha}\right] > 0, \tag{3.28}$$

which gives the interval

$$-\frac{\rho_{\rm r}}{3} < \alpha < \frac{\rho_{\rm r}}{2} \tag{3.29}$$

over which it is guaranteed that the energy density of radiation, $\rho_{\rm r}$, increases as one goes to earlier times. Next, we also substitute $w = 0$ into (3.27) and obtain the inequality

$$\rho_{\rm m}\left[\frac{\rho_{\rm m}+2\alpha}{\rho_{\rm m}-2\alpha}\right] > 0, \tag{3.30}$$

leading to the interval

$$-\frac{\rho_{\rm m}}{2} < \alpha < \frac{\rho_{\rm m}}{2} \tag{3.31}$$

over which it is assured that energy density of dust, $\rho_{\rm m}$, decreases as the Universe expands. From (3.15) and (3.16), wee see that the energy density corresponding to the spatial curvature evolves as $\rho_k = \frac{3k}{a^2}$. Recall that this is equivalent to a matter source with an EoS parameter $w = -1/3$ via $\nabla^\mu T_{\mu\nu} = 0$ in GR, but this case is not valid for our model since, unless $\alpha' = 0$, $\nabla^\mu T_{\mu\nu} \neq 0$ for a matter source with $w = -1/3$ (see (3.37) in Section 3.1.2 for the corresponding solution). Finally, in order to align with standard cosmology, we demand to avoid spatial curvature domination over dust in the early Universe. Consequently, using the continuity equation (3.25) for dust and the curvature evolution that is $\rho_k \propto a^{-2}$, we must have

$$3\left[\frac{\rho_{\rm m} + 2\alpha}{\rho_{\rm m} - 2\alpha}\right] > 2, \tag{3.32}$$

leading to the following permitted interval

$$-\frac{\rho_{\rm m}}{10} < \alpha < \frac{\rho_{\rm m}}{2} \tag{3.33}$$

which is a tighter bound than the one given in (3.31).

As stated earlier, one of the difficulties in studying EMSG-type models is that it is generally not possible to obtain the explicit exact solution of ρ in terms of redshift z (or scale factor a). We remind that [92] investigated cosmic acceleration in a dust-only universe via EMPG, and could only obtain the explicit solution of $\rho_{\rm m}(z)$ through an approximation procedure. In what follows, we shall look for the cases providing explicit solutions of $\rho(z)$ and show that EMLG model (3.1) provides us with an exact solution for the dust-only universe.

For convenience, we begin by defining a new parameter

$$\beta(w) = \frac{3w + 1}{3w^2 + 1}, \tag{3.34}$$

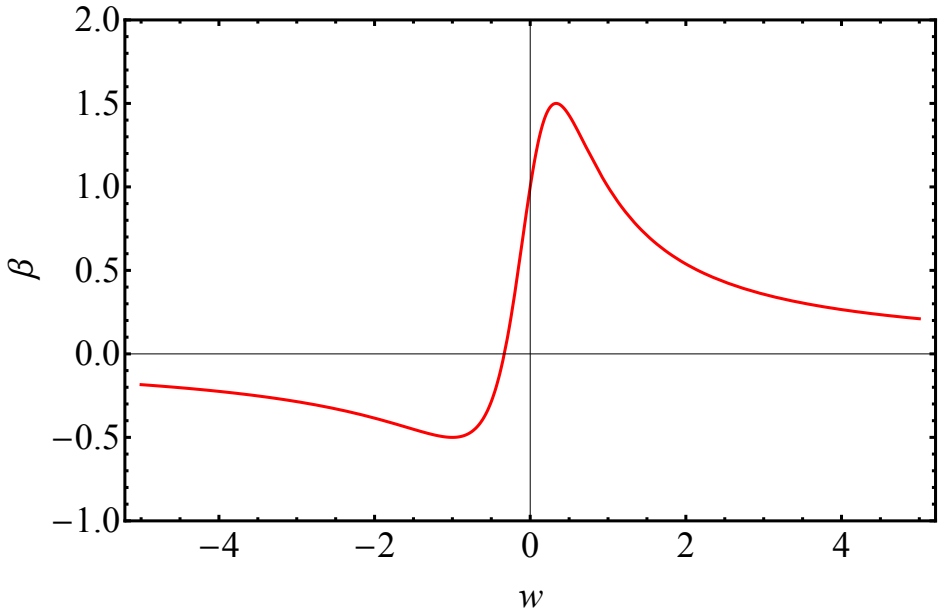

Figure 3.2. The behaviour of the parameter β for different EoS parameters w, i.e. $\beta(w)$. The region of most interest has $-1 \leq w \leq 1$.

and rewrite the continuity equation (3.25) as

$$\frac{\dot{\rho}}{\rho}\left[\frac{\rho - 2\alpha}{\rho + 2\alpha\beta}\right] = -3(1+w)\frac{\dot{a}}{a}, \tag{3.35}$$

which can be solved implicitly as

$$\rho\left(1 + \frac{2\alpha}{\rho}\beta\right)^{\frac{1}{\beta}+1} \propto a^{-3(1+w)}. \tag{3.36}$$

From Figure 3.2, we notice first that β attains a maximum value of $3/2$ at $w = 1/3$, and a minimum of $-1/2$ at $w = -1$. Due to the fact that β is not injective, there exist two values of w which provide the same right-hand side of (3.36). Nevertheless, as the left-hand side also has a w dependence, it is guaranteed that the behaviour of the perfect fluid for the two different equations of state does not coincide. We must note that at $w = -1/3$, $\beta = 0$. Accordingly, we consider the limiting behaviour of

(3.36), which takes exponential form as

$$\rho e^{\frac{2\alpha}{\rho}} \propto a^{-2}. \tag{3.37}$$

We could also recover this solution by directly integrating (3.25) for $w = -1/3$. As we have indicated before, this EoS no longer represents the density of the spatial curvature as in GR, but describes the evolution of cosmic strings. We also notice the similarities between the behaviour for $w = -1/3$ in this model and that in EMPG, as studied in [93].

The implicit solution (3.36) depends on the behaviour of the parameter β, and in general it is not expected to find explicit solutions for the energy density in terms of the scale factor (or redshift). Essentially, we are able to find explicit closed form solutions in certain physically relevant cases when the left-hand side of (3.36) reduces to a polynomial in ρ of degree at most four (Abel-Ruffini theorem [121, 122]). If the exponent is written in the form of $\frac{A}{B} = \frac{1}{\beta} + 1$ as a fraction in its lowest terms (A and $B \neq 0$ are integers), one can determine the conditions on A and B which give rise to that the resulting equation is an appropriate polynomial. Then, it is possible to further constrain the exponent by considering the values which β may take. Using the interval $-1/2 < \beta < 3/2$, we find that the only appropriate values that the exponent can take are integers in the list $\{-3, -2, -1, 2, 3, 4\}$. Two of these values are of specific interest. The $\{-1\}$ case corresponds to $w = -1$, the EoS for the conventional vacuum energy, in which case the exponent of the scale factor on the right-hand side vanishes and we find that the density of the vacuum energy, ρ_{vac}, is a constant, namely equals to its value today ρ_{vac0}, that is

$$\rho_{\text{vac}} = \rho_{\text{vac0}} \tag{3.38}$$

as in the GR case. The second value of interest is $\{2\}$ at which $\beta = 1$ and the left-hand side of (3.36) reduces to a quadratic. This arises for the physically relevant cases of dust ($w = 0$) and stiff fluid ($w = 1$). Hence, it allows us to find exact solutions for the

energy densities of these fluids. The remaining cases each result from a pair of values of w, but they are irrational and thus unlikely to be of physical importance. Typically, one of the two values lies within the $-1 < w < 1$ range, and the other outside. It is apparent that we cannot solve (3.36) for the radiation, $w = 1/3$ explicitly.

Before concluding this part, it is important to note that although we have explicit solutions for some cases, and can examine features of (3.36) for others, it is not possible to investigate the behaviour of a single cosmological model using these solutions together since they are each valid only for a mono-fluid universe. In the current study, we aim to investigate the late-time acceleration of the Universe. Hence, we shall neglect the radiation and assume that there is only dust as the matter source, for which, fortunately, EMLG provides us with the explicit solution for $\rho(z)$. Also, we shall briefly discuss possible analytical solutions of a universe including radiation in Section 3.2.5.

3.1.3. Dust-Filled Universe

Since we will discuss the EMLG model in the context of late-time acceleration of the Universe, we assume that the radiation density is negligible, and the Universe is spatially flat and filled only with dust (pressureless matter). Accordingly, substituting $w = 0$ and $k = 0$ into the modified Friedmann equations (3.15) and (3.16), they reduce to the following

$$3H^2 = \rho_{\rm m} + \Lambda + \alpha'\rho_{\rm m0} - \alpha'\rho_{\rm m0}\ln\left(\rho_{\rm m}/\rho_{\rm m0}\right), \tag{3.39}$$

$$-2\dot{H} - 3H^2 = -\Lambda + \alpha'\rho_{\rm m0}\ln\left(\rho_{\rm m}/\rho_{\rm m0}\right). \tag{3.40}$$

And for $w = 0$, the continuity equation (3.24) becomes

$$\dot{\rho}_{\rm m} + 3H\rho_{\rm m}\left(\frac{\rho_{\rm m} + \alpha'\rho_{\rm m0}}{\rho_{\rm m} - \alpha'\rho_{\rm m0}}\right) = 0, \tag{3.41}$$

and hence as mentioned above, we obtain the explicit solution

$$\rho_{\rm m} = \frac{1}{2}\rho_{\rm m0}\left\{(1+\alpha')^2(1+z)^3 - 2\alpha' + \sqrt{-4\alpha'^2 + \left[(1+\alpha')^2(1+z)^3 - 2\alpha'\right]^2}\right\} \quad (3.42)$$

provided that $-1 < \alpha' \leq 1$, and using that $a = (1+z)^{-1}$. We note that when $\alpha = 0$, our solution (3.42) reduces to $\rho_{\rm m0}(1+z)^3$, the usual pressureless matter evolution, and we recover the standard ΛCDM model along with GR. We also note that (3.39) with $\Lambda = 0$ at the present time reads $3H_0^2 = \rho_{\rm m0} + \alpha'\rho_{\rm m0}$ and consequently $\Omega_{\rm m0}(1+\alpha') = 1$. Here we remind that the present day density parameters of dust and Λ are defined respectively as

$$\Omega_{\rm m0} = \frac{\rho_{\rm m0}}{3H_0^2} \quad , \quad \Omega_{\Lambda 0} = \frac{\Lambda}{3H_0^2}. \quad (3.43)$$

Using $\Omega_{\rm m0} \approx 0.3$ from the most recent observational results, we estimate that $\alpha' \approx 2.3$. Note that our solution (3.42) is not valid for this α' value. Thus, to be able to use this solution, we must include Λ in our model, so that (3.39) implies that $\Omega_{\rm m0}(1+\alpha') + \Omega_{\Lambda 0} = 1$. We notice that the intervals we deduced in Section 3.1.2 for a viable cosmology are a subset of the interval required for the validity of solution (3.42) today. Namely, using the definition (3.18) in (3.33) obtained from curvature domination discussion leads to a narrower interval for α'. Considering that interval of α', $-0.20 < \alpha' < 1$, we attain $1 - 2\ \Omega_{\rm m0} < \Omega_{\Lambda 0} < 1 - 0.8\ \Omega_{\rm m0}$. Consequently, we estimate that our solution (3.42) is valid for

$$0.40 \lesssim \Omega_{\Lambda 0} \lesssim 0.76. \quad (3.44)$$

Furthermore, as $z \to -1$, the energy density $\rho_{\rm m} \to -\alpha'\rho_{\rm m0} = \rho_{\rm min}$. This means that the energy density would never reach to zero if the Universe were to expand forever. Instead there would be a minimum energy density limit as $\rho_{\rm min} = -\alpha'\rho_{\rm m0}$, which in turn implies that α' must be negative in an eternally expanding universe. Finally we note that the solution for EoS $w = 1$ is the same as the solution for dust ($w = 0$), with the replacement $a \to a^2$ since from (3.34), these two EoS parameters

yield the same β value (see Equation (3.36)).

3.2. Improved Om Diagnostic of EMLG

Cosmological models with accelerating expansion, via DE in GR or modified theory of gravity, can be examined with the use of null-diagnostics. One such diagnostic is the jerk parameter

$$j = \frac{\dddot{a}}{aH^3}, \tag{3.45}$$

first proposed by Harrison [123] (who denoted it by Q), which is simply equal to unity in ΛCDM model (neglecting radiation), $j_{\Lambda\mathrm{CDM}} = 1$, [124–126]. Hence, any observational evidence which predicts a deviation from unity of this parameter implies that the component responsible for the late time acceleration is not the cosmological constant in GR. The second diagnostic is $Om(z)$ which is originally introduced in [127, 128] and defined via an improved version in a recent study [52] as follows

$$Omh^2(z_i; z_j) = \frac{h^2(z_i) - h^2(z_j)}{(1+z_i)^3 - (1+z_j)^3} \tag{3.46}$$

where h denotes the dimensionless reduced Hubble parameter which is defined as $h(z) = H(z)/100\,\mathrm{km\,s^{-1}Mpc^{-1}}$. We note that Om depends only on the Hubble parameter $H(z)$, and is therefore simpler to determine from observations than the jerk parameter j. Consequently, one can easily obtain the value of Omh^2 by knowing the Hubble parameter at two or more redshifts and conclude whether or not a DE modification to GR is the cosmological constant alone. In ΛCDM model, omitting radiation, which is already negligible in the late Universe, we get

$$h^2 = h_0^2 \left[\Omega_{\mathrm{m0}}(1+z)^3 + 1 - \Omega_{\mathrm{m0}}\right], \tag{3.47}$$

which simply leads to a constant as

$$Omh^2(z_i; z_j) = h_0^2 \Omega_{\rm m0}. \tag{3.48}$$

The estimates given in [52] for the Omh^2 diagnostic are obtained considering the values of $H(z_1 = 0) = 70.6 \pm 3.3 \mathrm{km\,s^{-1}Mpc^{-1}}$ [129] based on the NGC 4258 maser distance, $H(z_2 = 0.57) = 92.4 \pm 4.5 \mathrm{km\,s^{-1}Mpc^{-1}}$ [130] based on the clustering of galaxies in the SDSS-III BOSS DR9, and $H(z_3 = 2.34) = 222 \pm 7 \mathrm{km\,s^{-1}Mpc^{-1}}$ [51] based on the BAO in the Lyman-α forest of SDSS DR11 data and read

$$\begin{aligned} Omh^2(z_1; z_2) &= 0.124 \pm 0.045, \\ Omh^2(z_1; z_3) &= 0.122 \pm 0.010, \\ Omh^2(z_2; z_3) &= 0.122 \pm 0.012. \end{aligned} \tag{3.49}$$

We realize that the model-independent values of Omh^2 above are stable at about 0.12 which is in considerable tension with the value

$$Omh^2 = \Omega_{\rm m0} h_0^2 = 0.1430 \pm 0.0011 \tag{3.50}$$

estimated for the base ΛCDM model from the Planck 2018 release [6]. It is remarkable that owing to the high-precision measurement of $H(z = 2.34)$ [52], Omh^2 is not affected significantly by $H(z = 0)$ whose accurate value is in fact subject to a great debate in the contemporary cosmology (see, e.g., [3] for a comprehensive list of references on the H_0 tension).

As we mentioned previously, it is argued in [52] that this tension can be alleviated in models in which cosmological constant Λ was dynamically screened in the past. In line with this argument, until Section 3.3, we investigate the features of the EMLG model (parametrised by α') in comparison with the basic ΛCDM model mostly by referring to [52]. Hence, we intentionally make use of the aforementioned three $H(z)$ data (rather than the latest data, which would not change our arguments in what follows)

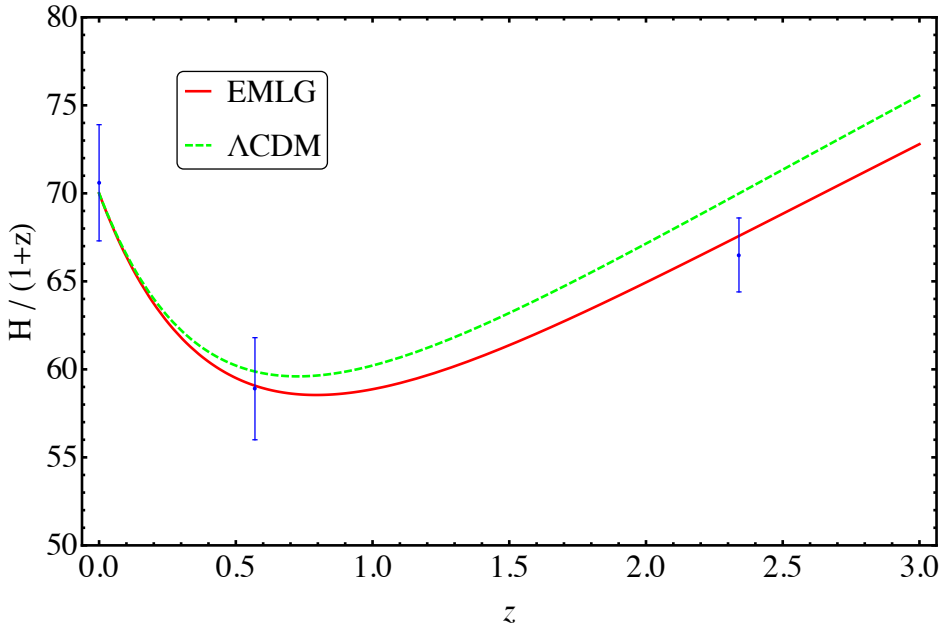

Figure 3.3. $H(z)/(1+z)$ vs. z graph of the EMLG and ΛCDM. Plotted by using $\Omega_{\mathrm{m0}} = 0.28$, $H_0 = 70\,\mathrm{km\,s^{-1}Mpc^{-1}}$ and $\alpha' = -0.04$.

as well as the Ω_{m0} and H_0 values considered in [52]. This allows us to demonstrate how the EMLG model, with a properly chosen α' value, affects Omh^2 diagnostics by a straightforward comparison with [52]. Nevertheless, in Section 3.3, we shall discuss the observational analyses of the EMLG model and compare with the ΛCDM model using the latest cosmological data.

3.2.1. EMLG Cosmology in the light of Null-Diagnostics

We now consider the Om diagnostic expression defined in (3.46) for our EMLG model. We rewrite the Equation (3.39) as

$$\frac{H^2}{H_0^2} = 1 + \Omega_{\mathrm{m0}}\left\{ (\rho_{\mathrm{m}}/\rho_{\mathrm{m0}}) - 1 - \alpha' \ln (\rho_{\mathrm{m}}/\rho_{\mathrm{m0}}) \right\} \tag{3.51}$$

using the fact that $\Omega_{\Lambda 0} = 1 - (1+\alpha')\,\Omega_{\rm m0}$. Then, substituting the matter density solution (3.42) into (3.51), we obtain

$$\begin{aligned}\frac{h^2}{h_0^2} =& 1 - \Omega_{\rm m0}\Bigg\{1 - \frac{1}{2}\Bigg[(1+\alpha')^2(1+z)^3 - 2\alpha' + \sqrt{-4\alpha'^2 + \left[(1+\alpha')^2(1+z)^3 - 2\alpha'\right]^2}\Bigg] \\ &+ \alpha' \ln\Bigg\{\frac{1}{2}\Bigg[(1+\alpha')^2(1+z)^3 - 2\alpha' + \sqrt{-4\alpha'^2 + \left[(1+\alpha')^2(1+z)^3 - 2\alpha'\right]^2}\Bigg]\Bigg\}\Bigg\}.\end{aligned} \tag{3.52}$$

Using this in the definition (3.46) leads to

$$\begin{aligned}Omh^2(z_i; z_j) =& h_0^2\Omega_{\rm m0}\Big\{\left(\alpha'+1\right)^2\left(z_i+1\right)^3 \\ &+ \sqrt{\left[\left(\alpha'+1\right)^2\left(z_i+1\right)^3 - 2\alpha'\right]^2 - 4\alpha'^2} \\ &-2\alpha' \ln\Bigg[\frac{1}{2}\Big(-2\alpha' + \left(\alpha'+1\right)^2\left(z_i+1\right)^3 \\ &+\sqrt{\left[\left(\alpha'+1\right)^2\left(z_i+1\right)^3 - 2\alpha'\right]^2 - 4\alpha'^2}\Big)\Bigg] \\ &- \left(\alpha'+1\right)^2\left(z_j+1\right)^3 \\ &-\sqrt{\left[\left(\alpha'+1\right)^2\left(z_j+1\right)^3 - 2\alpha'\right]^2 - 4\alpha'^2} \\ &+2\alpha' \ln\Bigg[\frac{1}{2}\Big(-2\alpha' + \left(\alpha'+1\right)^2\left(z_j+1\right)^3 \\ &+\sqrt{\left[\left(\alpha'+1\right)^2\left(z_j+1\right)^3 - 2\alpha'\right]^2 - 4\alpha'^2}\Big)\Bigg]\Big\} / \\ &2\left[\left(z_i+1\right)^3 - \left(z_j+1\right)^3\right].\end{aligned} \tag{3.53}$$

In Figure 3.3, following the three observational $H(z)$ values with errors given in [52], we plot $H(z)/(1+z)$ with respect to redshift using $\Omega_{\rm m0} = 0.28$ and $H_0 = 70\,{\rm km\,s^{-1}Mpc^{-1}}$ for both the ΛCDM model (green) and the EMLG model with $\alpha' = -0.04$ (red), which provides us $H(z)/(1+z)$, the proper velocity between two objects 1 comoving Mpc apart, in agreement with all data points whereas the one for ΛCDM model does not fit to the data point from $z = 2.34$. We note that the true constant of the model in the action (3.2) is, accordingly, $\alpha = -0.02\rho_{\rm m0}$. The model-independent value of the Om diagnostic estimated in [52] is quite stable at $Omh^2 \simeq 0.12$ which is in tension with the ΛCDM-based value $Omh^2(\Lambda{\rm CDM}) \simeq 0.14$. On the other hand, in the EMLG model with the use of parameters $\Omega_{\rm m0} = 0.28$, $H_0 = 70\,{\rm km\,s^{-1}Mpc^{-1}}$ and $\alpha' = -0.04$,

we find $Omh^2(z_1; z_2) = 0.129$, $Omh^2(z_1; z_3) = 0.127$ and $Omh^2(z_2; z_3) = 0.127$ where $z_1 = 0$, $z_2 = 0.57$ and $z_3 = 2.34$. It is apparent that these values are in good agreement with the estimates given in [52] that we have indicated in Equation (3.49).

3.2.2. A Comparison via General Relativistic Interpretation

In [52], it is suggested that lower values for Omh^2 can be achieved in models in which the cosmological constant Λ was screened in the past by means of a dynamically evolving counter-term $f(z)$. In accordance with this argument, $H^2(z)$ is modified, with respect to the standard ΛCDM model, as

$$H^2(z) = \frac{1}{3}\rho_{\mathrm{m}0}(1+z)^3 + \frac{\Lambda}{3} - f(z) \tag{3.54}$$

and at a redshift z_*, $\Lambda/3$ is balanced by $f(z)$ (i.e. $f(z_*) = \Lambda/3$). We point out that our expression (1.27) denoting the most general extension of $H^2(z)$ is equivalent to Equation (3.54) when $3f(z) = \rho_{\mathrm{m}0}(1+z)^3 u(z) + v(z)$. Comparing (3.54) and (3.39) yields

$$f(z) = \frac{1}{3}\Big\{\rho_{\mathrm{m}0}(1+z)^3 - \rho_{\mathrm{m}} - \alpha'\rho_{\mathrm{m}0}\big[1 - \ln(\rho_{\mathrm{m}}/\rho_{\mathrm{m}0})\big]\Big\}, \tag{3.55}$$

and along with our solution (3.42), it emerges that in dust-only EMLG model,

$$\begin{aligned} f(z) = \frac{1}{6}\rho_{\mathrm{m}0}\Bigg\{ &\left[2 - (1+\alpha')^2\right](1+z)^3 - \sqrt{-4\alpha'^2 + \left[(1+\alpha')^2(1+z)^3 - 2\alpha'\right]^2} \\ &+ 2\alpha' \ln\left\{\frac{1}{2}\left[(1+\alpha')^2(1+z)^3 - 2\alpha' + \sqrt{-4\alpha'^2 + \left[(1+\alpha')^2(1+z)^3 - 2\alpha'\right]^2}\right]\right\}\Bigg\}. \end{aligned} \tag{3.56}$$

It is not possible to calculate z_*, the redshift at which screening of Λ occurs, exactly from (3.56). Nevertheless, for $\Omega_{\mathrm{m}0} = 0.28$ and $\alpha' = -0.04$, we can numerically calculate that $z_* = 2.29$ for our model (similar to the value $z_* \simeq 2.4$ given in [52] for a specific braneworld model).

Moreover, [52] discusses that evolving DE models in which Λ, as only a part of a more complicated DE, was screened in the past exhibit a better fit to the BAO data than the ΛCDM model, as well as alleviating the tension mentioned in the preceding sections. It is also indicated that in such temporally evolving DE models, the effective EoS of the DE displays a pole at high redshifts. This pole in $w_{\rm DE}$ means that the energy density of the DE changes sign at that redshift value. This behavior of the DE is also suggested in another study [36] by the BOSS collaboration using the BAO data by including the BOSS CMASS and Lyman-α forest measurements of $H(z)$, SN and Planck data sets. In the next section, we will investigate the dust-only EMLG model from this perspective.

3.2.3. Effective Dynamical Dark Energy

In order to test our model in light of the above discussion, we reconstruct the EMLG model via the definition of an effective DE by rewriting (3.39) and (3.40) in the following form

$$3H^2 = \rho_{\rm m0}(1+z)^3 + \rho_{\rm DE}, \tag{3.57}$$

$$-2\dot{H} - 3H^2 = p_{\rm DE}. \tag{3.58}$$

Thus, the energy density and pressure of the effective DE are respectively given by

$$\rho_{\rm DE} = \rho_{\rm m} + \alpha'\rho_{\rm m0}\left[1 - \ln\left(\rho_{\rm m}/\rho_{\rm m0}\right)\right] - \rho_{\rm m0}(1+z)^3 + \Lambda, \tag{3.59}$$

$$p_{\rm DE} = \alpha'\rho_{\rm m0}\ln\left(\rho_{\rm m}/\rho_{\rm m0}\right) - \Lambda. \tag{3.60}$$

Next, using (3.42) in these equations we obtain $\rho_{\rm DE}$ and $p_{\rm DE}$ in terms of redshift z as follows

$$\rho_{\rm DE} = \Lambda + \frac{1}{2}\rho_{\rm m0}\Bigg\{ \left[(1+\alpha')^2 - 2\right](1+z)^3 + \sqrt{-4\alpha'^2 + \left[(1+\alpha')^2(1+z)^3 - 2\alpha'\right]^2} - 2\alpha' \ln\left\{\frac{1}{2}\left[(1+\alpha')^2(1+z)^3 - 2\alpha' + \sqrt{-4\alpha'^2 + \left[(1+\alpha')^2(1+z)^3 - 2\alpha'\right]^2}\right]\right\}\Bigg\}, \tag{3.61}$$

$$p_{\rm DE} = -\Lambda + \alpha'\rho_{\rm m0} \ln\left\{\frac{1}{2}\left[(1+\alpha')^2(1+z)^3 - 2\alpha' + \sqrt{-4\alpha'^2 + \left[(1+\alpha')^2(1+z)^3 - 2\alpha'\right]^2}\right]\right\}. \tag{3.62}$$

The corresponding EoS parameter of the effective DE denoted by $w_{\rm DE} = \frac{p_{\rm DE}}{\rho_{\rm DE}}$ is

$$w_{\rm DE} = -1 + \frac{\rho_{\rm m} - \rho_{\rm m0}(1+z)^3 + \alpha'\rho_{\rm m0}}{\rho_{\rm m} - \rho_{\rm m0}(1+z)^3 + \alpha'\rho_{\rm m0}\left[1 - \ln\left(\rho_{\rm m}/\rho_{\rm m0}\right)\right] + \Lambda}. \tag{3.63}$$

Defining the present-day density parameter of the effective DE as $\Omega_{\rm DE0} = \frac{\rho_{\rm DE0}}{3H_0^2}$, (3.63) along with (3.42) and (3.59) yields

$$\begin{aligned} w_{\rm DE} = &-1 + (1-\Omega_{\rm DE0})\Bigg[\left((1+\alpha')^2 - 2\right)(1+z)^3 \\ &+ \sqrt{-4\alpha'^2 + \left[(1+\alpha')^2(1+z)^3 - 2\alpha'\right]^2}\Bigg] \Bigg/ \\ &\Bigg\{(1-\Omega_{\rm DE0})\Bigg\{\left[(1+\alpha')^2 - 2\right](1+z)^3 - 2\alpha' \\ &+ \sqrt{-4\alpha'^2 + \left[(1+\alpha')^2(1+z)^3 - 2\alpha'\right]^2} \\ &- 2\alpha' \ln\left(\frac{1}{2}\Bigg[(1+\alpha')^2(1+z)^3 - 2\alpha' \right. \\ &\left. + \sqrt{-4\alpha'^2 + \left[(1+\alpha')^2(1+z)^3 - 2\alpha'\right]^2}\Bigg]\right)\Bigg\} + 2\Omega_{\rm DE0}\Bigg\}, \end{aligned} \tag{3.64}$$

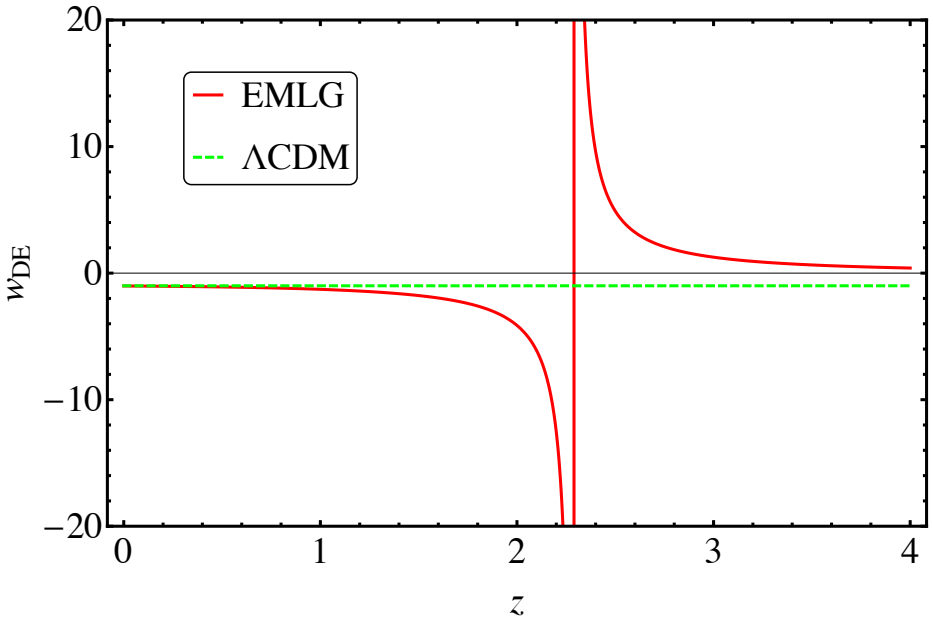

Figure 3.4. $w_{\rm DE}$ versus z graphs of the EMLG and ΛCDM. Plotted by using $\Omega_{\rm m0} = 0.28$ and $\alpha' = -0.04$. $|w_{\rm DE}| \to \infty$ at $z = 2.29$ in EMLG.

where we have used that $\Omega_{\rm m0} + \Omega_{\rm DE0} = 1$. The value of the EoS parameter of the effective DE evaluated today ($z = 0$) is

$$w_{\rm DE0} = -1 + \alpha' \frac{1 - \Omega_{\rm DE0}}{\Omega_{\rm DE0}}. \tag{3.65}$$

We note that it lies in the 'phantom' region, i.e. $w_{\rm DE0} < -1$ for $\alpha' < 0$. Specifically, for $\alpha' = -0.04$ and $\Omega_{\rm DE0} = 0.72$ (following from $\Omega_{\rm m0} = 0.28$), we have $w_{\rm DE0} = -1.0156$.

As is seen from (3.64), the model reduces to ΛCDM when $\alpha' = 0$ giving rise to $w_{\rm DE} = w_{\rm DE0} = -1$. We now plot illustrative graphs by using $\Omega_{\rm m0} = 0.28$ and $\alpha' = -0.04$. With these properly chosen values, we can extract from (3.61) that $\rho_{\rm DE} = 0$ at $z = 2.29$. In accordance with the arguments in [52], which we have mentioned previously, within the effective DE source interpretation of dust-only EMLG model, Λ is screened at the redshift $z_* = 2.29$ and the effective EoS of the DE exhibits a pole at this redshift (note the similarity with the estimate $z_* \simeq 2.4$ made in [52] for a

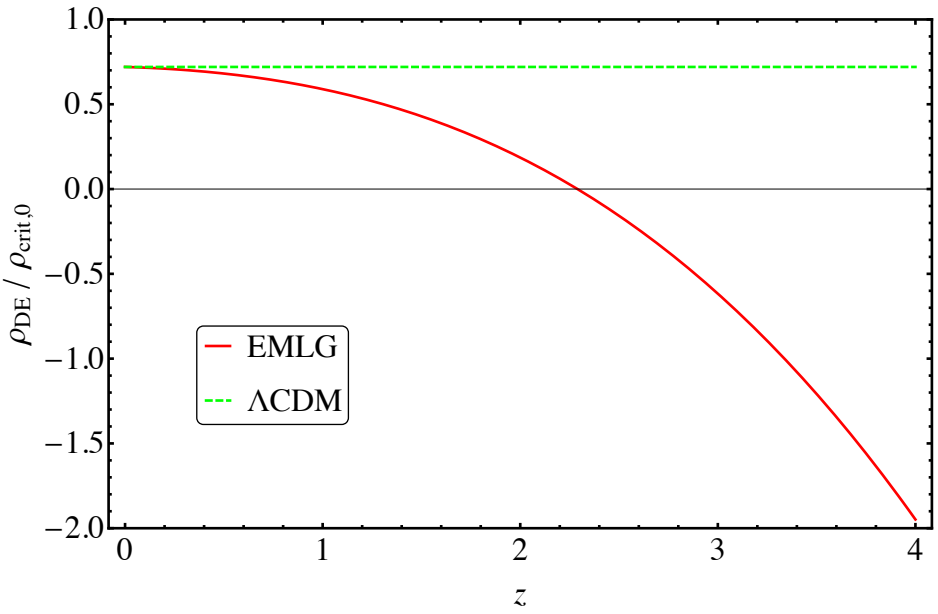

Figure 3.5. $\rho_{\rm DE}/\rho_{\rm crit0}$ versus z graphs of the EMLG and ΛCDM. Plotted by using $\Omega_{\rm m0} = 0.28$ and $\alpha' = -0.04$. $\rho_{\rm DE} = 0$ at $z = 2.29$ in EMLG.

braneworld model). We depict the pole of $w_{\rm DE}$ at $z = 2.29$ in Figure 3.4, which is due to the sign change of $\rho_{\rm DE}$ at that redshift, as can be observed from Figure 3.5. Note that Figure 3.5 shows clearly that the effective dark energy density $\rho_{\rm DE}$ changing sign at $z = 2.29$ is in agreement with Figure 11 of [36] revealing that $\rho_{\rm DE}$ crosses below zero at a redshift located in the interval $1.6 \leq z \leq 3.0$. We further display, both for the EMLG and ΛCDM models, the density parameters of dust, $\Omega_{\rm m} = \rho_{\rm m}/3H^2$, and the effective DE, $\Omega_{\rm DE} = \rho_{\rm DE}/3H^2$, which corresponds to $\Omega_\Lambda = \Lambda/3H^2$ for the ΛCDM model, up to $z = 1100$ in Figure 3.6. We notice that the density parameters are the same for $z = 0$ and do not show much difference for low redshifts. For large redshifts, in contrast, the unusual behavior of the dust-only EMLG model emerges, so that $\Omega_{\rm m}$ becomes equal to unity at $z = z_* = 2.29$ (at $z \to \infty$ for the ΛCDM model) and then, for $z > z_* = 2.29$, settles in a plateau larger than unity which results from $\rho_{\rm DE}$ becoming negative at $z = z_* = 2.29$.

Now we calculate two important kinematical parameters that are of interest in cosmology in order to make comparison between different models. First, we calculate

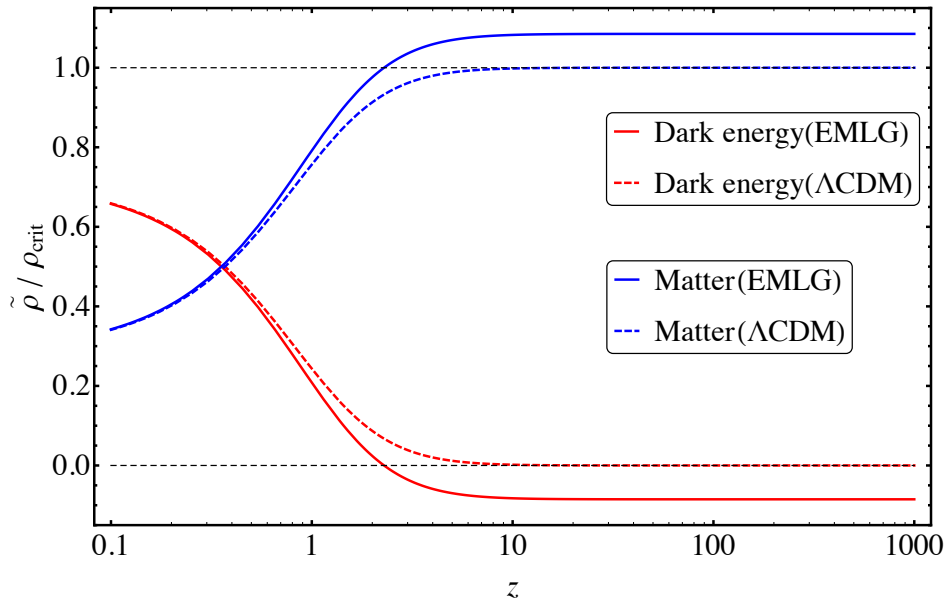

Figure 3.6. Density parameters (shown as $\tilde{\rho}/\rho_{\rm crit}$) vs. z graphs of the EMLG and ΛCDM for dust and effective DE. Here $\tilde{\rho} = \rho_{\rm m0}(1+z)^3$ for matter and $\tilde{\rho} = \rho_{\rm DE}$ for effective DE. Plotted by using $\Omega_{\rm m0} = 0.28$ and $\alpha' = -0.04$.

the deceleration parameter q defined as

$$q = -1 - \frac{\dot{H}}{H^2}, \tag{3.66}$$

accordingly, using (3.39) and (3.40) gives

$$q = -1 + \frac{3}{2}\,\frac{\Omega_{\rm m0}\left[(\rho_{\rm m}/\rho_{\rm m0}) + \alpha'\right]}{1 - \Omega_{\rm m0}\left[1 - (\rho_{\rm m}/\rho_{\rm m0}) + \alpha' \ln(\rho_{\rm m}/\rho_{m0})\right]}, \tag{3.67}$$

which can be written in terms of redshift z, by using the matter density solution (3.42),

as follows

$$q = -1 + \frac{3}{4}\Omega_{\rm m0}\left[(1+\alpha')^2(1+z)^3 + \sqrt{-4\alpha'^2 + \left[(1+\alpha')^2(1+z)^3 - 2\alpha'\right]^2}\right] \Big/ \left\{1 - \Omega_{\rm m0}\left\{1 - \frac{1}{2}\left[(1+\alpha')^2(1+z)^3 - 2\alpha' + \sqrt{-4\alpha'^2 + \left[(1+\alpha')^2(1+z)^3 - 2\alpha'\right]^2}\right]\right\} + \alpha' \ln\left\{\frac{1}{2}\left[(1+\alpha')^2(1+z)^3 - 2\alpha' + \sqrt{-4\alpha'^2 + \left[(1+\alpha')^2(1+z)^3 - 2\alpha'\right]^2}\right]\right\}\right\}. \tag{3.68}$$

Setting $\alpha' = 0$ recovers the deceleration parameter of ΛCDM model, which is expressed by

$$q_{\Lambda\rm CDM} = -1 + \frac{3}{2}\,\frac{\Omega_{\rm m0}(1+z)^3}{1 - \Omega_{\rm m0}[1-(1+z)^3]}. \tag{3.69}$$

It can be seen from (3.68) that $q \to -1$ as $z \to -1$, implying that our model asymptotically approaches ΛCDM model in the far future. For large redshifts, $z \gg 1$, in (3.68) the deceleration parameter of the matter dominated era in ΛCDM model, $q = 1/2$, is recovered. Calculating the current value of the deceleration parameter of our model, we find

$$q_0 = -1 + \frac{3}{2}\Omega_{\rm m0}(1+\alpha'). \tag{3.70}$$

As is seen in the top panel of Figure 3.7, the accelerated expansion begins at the transition redshift $z_{\rm tr} \approx 0.79$ and the present-day value of the deceleration parameter is $q_0 = -0.60$, whereas these are $z_{\rm tr} \approx 0.73$ and $q_0 = -0.58$ in ΛCDM model. Second, we calculate the jerk parameter $j = \frac{\dddot{a}}{aH^3}$, which was briefly discussed in Section 3.2 and, as mentioned there, is simply equal to unity for ΛCDM model (ommiting radiation).

On the contrary, in EMLG j is dynamical and is given by

$$
\begin{aligned}
j =& \Big\{ \alpha' \rho_0 \Omega_0 (1+z)^2 \rho_z^2 - \alpha' \rho_0 \Omega_0 (1+z) \rho \big[(1+z)\rho_{zz} - 2\rho_z \big] \\
& + \rho^2 \big[\Omega_0 (1+z) \big((1+z)\rho_{zz} - 2\rho_z \big) - 2\rho_0 \big(\alpha' \Omega_0 \ln(\rho/\rho_0) + \Omega_0 - 1 \big) \big] + 2\Omega_0 \rho^3 \Big\} \Big/ \\
& \Big\{ 2\rho^2 \big[\Omega_0 \rho - \rho_0 \big(\alpha' \Omega_0 \ln(\rho/\rho_0) + \Omega_0 - 1 \big) \big] \Big\},
\end{aligned}
\tag{3.71}
$$

where we have used, specific to this equation, a different notation that is $\rho = \rho_{\rm m}(z)$, $\Omega_0 = \Omega_{\rm m0}$, and a subscript of z denotes differentiation with respect to redshift. The explicit expression in terms of redshift can be attained by substituting $\rho_{\rm m}(z)$ from (3.42) but, for reasons of brevity, we do not provide its explicit form here. To illustrate the dynamical nature of the jerk parameter in EMLG, we depict $j(z)$ in the lower panel of Figure 3.7. We see that it deviates from unity at $z \sim 0$ but we have $j \to 1$ in both limits as either $z \to \infty$ or $z \to -1$ implying that EMLG recovers the kinematics of ΛCDM model both at early times and in the far future.

3.2.4. Screening of Λ by the Nonconservation of Dust

In Section 3.2.3, we rearranged the original field equations of the EMLG model, (3.39) and (3.40), in order to compare with the evolving DE model first described in [52]. To be able to make this comparison, we assumed that the energy density of the dust behaves exactly as in GR, i.e., $\rho_{\rm m} \propto (1+z)^3$, and then compensated it as a part of the effective DE (see (3.57)). In other words, we assumed that all of the terms with α', including those coming from the true dust energy density (3.42) of EMLG, contribute to the energy density of the effective DE (3.61). Through this comparison, we have determined the dimensionless parameter of our model, α', with which EMLG is able to relax the issues of the ΛCDM model stated in [52].

We now examine the actual behavior of dust in EMLG. The true energy density of dust in EMLG is given by (3.42) and includes terms with the EMLG modification parameter α' (corresponding to $u(z)$ in (1.27)). Furthermore, we have new terms with

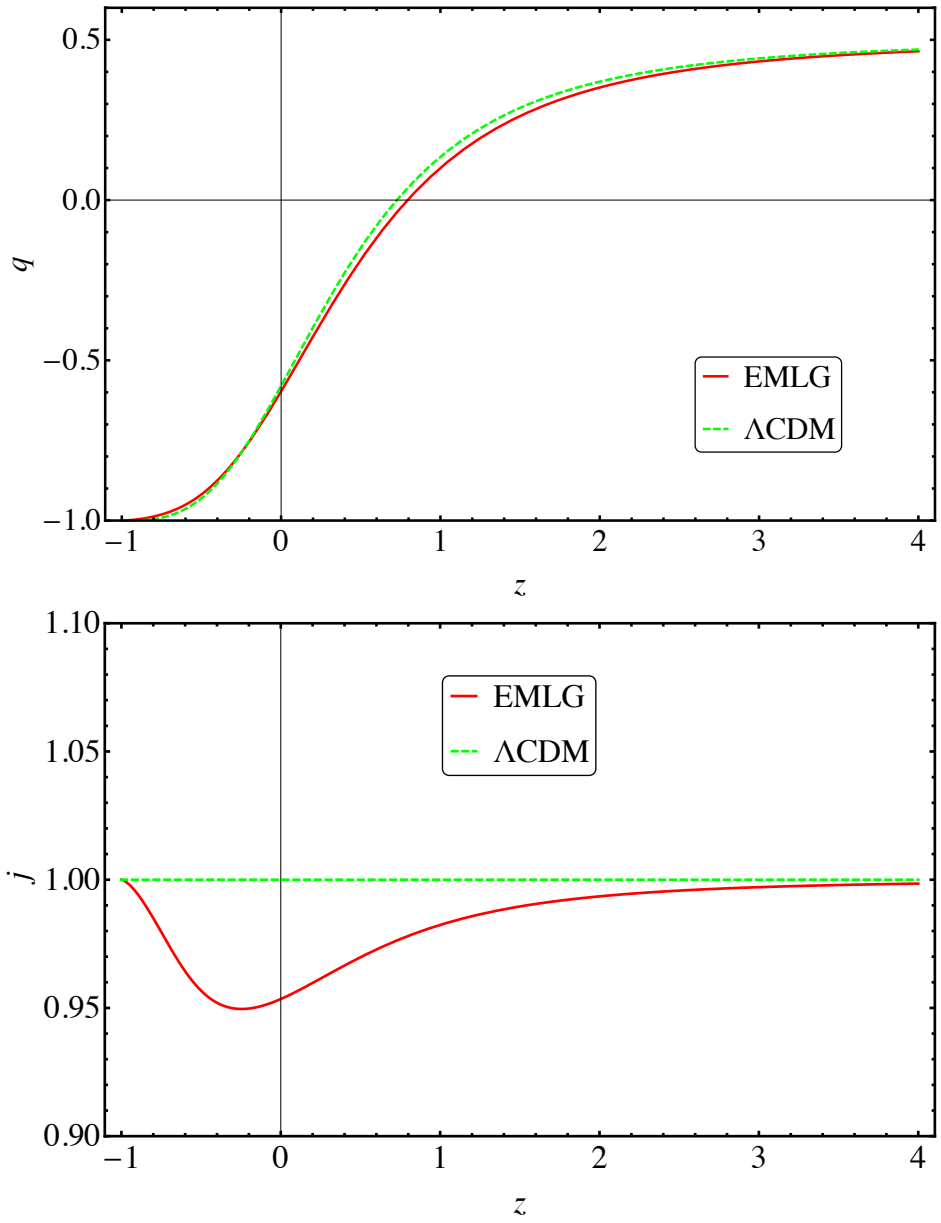

Figure 3.7. $q(z)$ vs. z (upper panel) and $j(z)$ vs. z (lower panel) graphs of the EMLG and ΛCDM. Plotted by using $\Omega_{\mathrm{m0}} = 0.28$, $H_0 = 70\,\mathrm{km\,s^{-1}Mpc^{-1}}$ and $\alpha' = -0.04$.

α' (corresponding to $v(z)$ in (1.27)) in our original field equations, (3.39) and (3.40), arising due to the EMLG modification to standard GR. As a result, both the energy density of dust and the forms of the energy density and pressure equations of our EMLG model differ from those of GR. Consequently, we find it useful to display, in Figure 3.8, the redshift dependency of the each density parameter corresponding to

the components of the energy density equation (3.39). To do so, we define $\Omega_{\rm m} = \rho_{\rm m}/3H^2$ (red) for dust, $\Omega_\Lambda = \Lambda/3H^2$ (yellow) for cosmological constant and $\Omega_{\rm x} = [\alpha'\rho_{\rm m0} - \alpha'\rho_{\rm m0}\ln(\rho_{\rm m}/\rho_{\rm m0})]/3H^2$ (green) for the new terms which represent the EMLG modification to the standard form of Friedmann equation. We use $\Omega_{\rm m0} = 0.28$, $H_0 = 70\,{\rm km\,s^{-1}Mpc^{-1}}$ and $\alpha' = -0.04$, the same values used in the preceding sections. We especially note the small and nonmonotonic contribution from $\Omega_{\rm x}$ in Equation (3.39).

For a better view, we display the behavior of $\Omega_{\rm x}(z)$ separately in Figure 3.9. This figure is of particular interest since it reveals a critical point about the model under consideration; that the contribution from $\Omega_{\rm x}$ is negative at low redshifts, positive at $z \sim 1$ and then, while remaining positive, asymptotically approaches zero at larger redshifts. This implies that $\Omega_{\rm x}$, due to the EMLG modification, screens Λ only at low redshifts in contrast to the arguments in [52]. On the other hand, within the effective DE source interpretation of our model in line with [36, 52], we have already shown that $\rho_{\rm DE} > 0$ at low redshifts and crosses below zero at $z = 2.29$ exactly as suggested in [36, 52]. This means that, in the EMLG model, the feature of screening Λ does not arise due to the new type of contributions of $\rho_{\rm m}$ on the right-hand side of (3.39) which appear as an effective source with constant inertial mass density as $\rho' + p' = \alpha'\rho_{\rm m0}$ (see Section 3.1.1 for details), but instead due to the altered redshift dependency of the true energy density of dust, $\rho_{\rm m}$, arising from the nonconservation of the EMT in the EMLG model.

3.2.5. Inclusion of Radiation

In order to be able to investigate the implications of our model for the early Universe while preserving its agreement with the current data for the late Universe, we need to search for solutions in the case that radiation is the second source besides dust. Including both radiation and dust as sources in our model gives rise to complicated field equations which include the cross terms of $\rho_{\rm r}$ and $\rho_{\rm m}$ which render exact solutions impossible. Furthermore, if we make use of the same $\alpha' = -0.04$ value, which corresponds to $\alpha = -0.02\rho_{\rm m0}$, for radiation, it remains outside today's viability interval

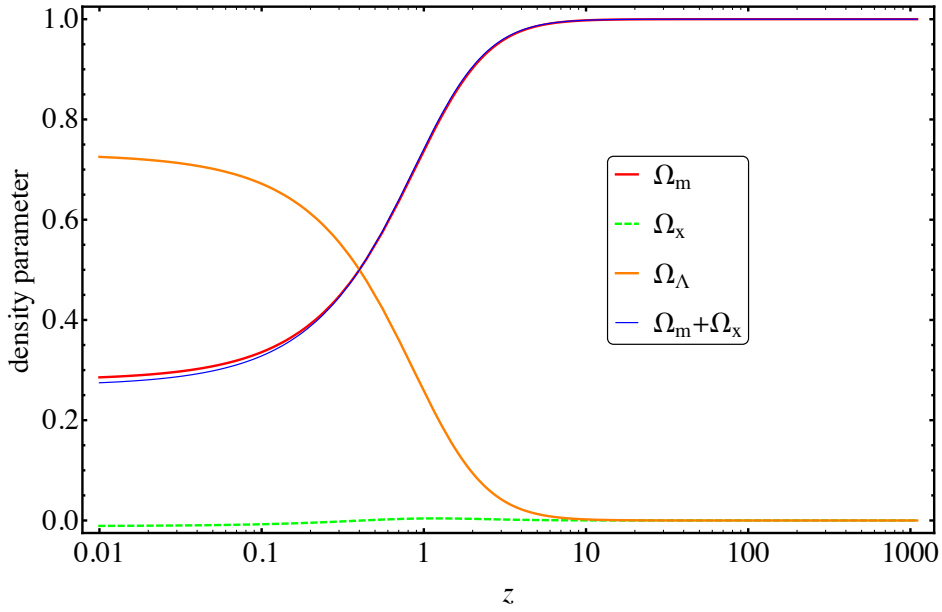

Figure 3.8. Ω vs. z graphs of the EMLG for matter ($\Omega_{\rm m}$), modification terms ($\Omega_{\rm x}$), cosmological constant (Ω_Λ) and matter+modification ($\Omega_{\rm m}+\Omega_{\rm x}$). Plotted by using $\Omega_{\rm m0}=0.28$, $H_0=70\,{\rm km\,s^{-1}Mpc^{-1}}$ and $\alpha'=-0.04$.

(3.29) as we know from the latest observations that $\rho_{\rm m0}/\rho_{\rm r0}\sim 10^3$. This stems from the fact that the interval (3.29) is valid only for a mono-fluid universe. We would need to decrease the absolute value $|\alpha|$ to obtain viable cosmological solutions when our model contains radiation as well. However, this would result in compromising the goodness of fit of our model with the latest data compared to that of ΛCDM model for the late-time accelerated cosmic expansion. Thus, we conclude that it does not seem possible to extend our model by both adding radiation and preserving the features we have been discussing so far when there is only one α parameter involving in both fluids.

As mentioned briefly in Section 2.2, a recent study [96] demonstrates that different sources can couple to gravity in different ways for a particular model of $f(\mathbf{T^2})$ modification. One can follow the same idea for EMLG model. Namely, the multi-fluid model can be constructed with the use of different α parameters for different types of sources which means that different gravitational couplings occur for each source. To

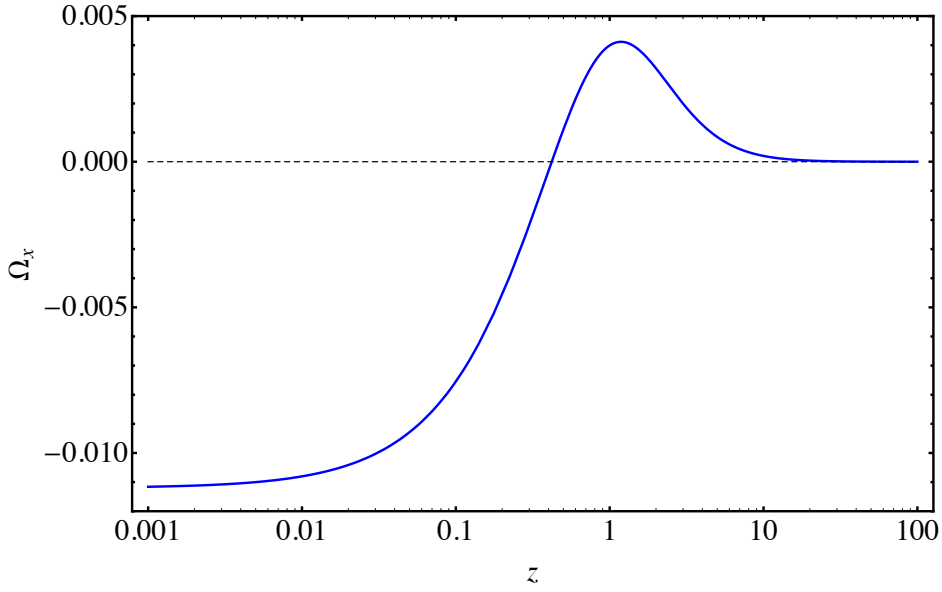

Figure 3.9. The density parameter of modification terms ($\Omega_{\rm x}$) vs. z graph of the EMLG. Plotted by using $\Omega_{\rm m0} = 0.28$, $H_0 = 70\,{\rm km\,s^{-1}Mpc^{-1}}$ and $\alpha' = -0.04$.

do so, one can commence with a modification term as follows

$$f(T_{\mu\nu}T^{\mu\nu}) = \sum_i \alpha_i \ln(\lambda_i\, T^{(i)}_{\mu\nu} T^{\mu\nu}_{(i)}), \tag{3.72}$$

where α_i (the gravitational coupling parameter) and λ_i are the constants for ith fluid, and the sum over i evades the issue of cross terms occurring in the case of more than one fluid. However, it brings along the increase in the number of free parameters. In order to relax this issue, fluids can be separated as conventional sources, such as radiation (r) or baryons (b), and dark sector/unknown sources like CDM (c). Then, it can be assumed that known sources couple to gravity according to the standard GR, that is the corresponding α_i's are zero, while dark sector/unknown sources couple in accordance with the modified gravity theory [96]. Through this idea, the modified

Friedmann equations in EMLG read

$$3H^2 = \rho_{\rm r} + \rho_{\rm b} + \rho_{\rm c} + \alpha'\rho_{\rm c0}\left[1 - \ln\left(\frac{\rho_{\rm c}}{\rho_{\rm c0}}\right)\right] + \Lambda, \tag{3.73}$$

$$-2\dot{H} - 3H^2 = \frac{\rho_{\rm r}}{3} + \alpha'\rho_{\rm c0}\ln\left(\frac{\rho_{\rm c}}{\rho_{\rm c0}}\right) - \Lambda. \tag{3.74}$$

Here $\rho_{\rm r} \propto (1+z)^4$, $\rho_{\rm b} \propto (1+z)^3$ as in GR and $\rho_{\rm c}$ obeys the modified continuity equation (3.24) evaluated for $w = 0$, which gives the energy density solution in (3.42). Using these energy density evolutions, (3.73) can be rewritten as

$$\frac{H^2}{H_0^2} = \Omega_{\rm r0}(1+z)^4 + \Omega_{\rm b0}(1+z)^3 + \Omega_{\rm c0}\left\{\frac{\rho_{\rm c}}{\rho_{\rm c0}} + \alpha'\left[1 + \ln\left(\frac{\rho_{\rm c}}{\rho_{\rm c0}}\right)\right]\right\} + \Omega_{\Lambda 0} \tag{3.75}$$

where $\Omega_{\rm i0} = \frac{\rho_{\rm i0}}{3H_0^2}$ is the present-day density parameter for the ith fluid. We reserve such an investigation for the EMLG model to our future works.

3.3. Constraints from Latest Cosmological Data

In the preceding sections, we have investigated the EMLG model theoretically, particularly in comparison with the papers [36, 52]. For convenience, we assumed the values of the Hubble constant and density parameter of dust as used in [52] and chose a value of the coupling parameter of the EMLG modification so as to produce results similar to those given in [52]. In this section, we shall analyze the constraints on the parameters of the EMLG model from the latest observational data and discuss the model further. In order to explore the parameter space, we use a modified version of a simple and fast Markov Chain Monte Carlo (MCMC) code, named SimpleMC [36, 131], that computes distances and expansion rates using the Friedmann equation. The code uses a compressed version of a recent reanalysis of Type Ia SN data, and high-precision BAO measurements at different redshifts with $z < 2.36$ [36]. We also include a collection of currently available $H(z)$ measurements from cosmic chronometers (CC), see [132] and references therein. For an extended review of cosmological parameter inference, we refer the reader to [133]. Table 3.1 displays the parameters used throughout the current

study along with the corresponding flat priors. Note that we do not consider CMB data in our analysis, because the current EMLG model does not contain radiation (see Section 3.2.5 for the relevant discussion) and therefore we omit radiation in the ΛCDM model in order to be able to compare these two models under the same conditions.

We use the dimensionless Hubble parameter $h = H/100\,\mathrm{km\,s^{-1}Mpc^{-1}}$ [15], the physical baryon density $\Omega_{\mathrm{b}}h^2$ and the pressureless matter density (including CDM) Ω_{m}. Throughout the analysis we assume flat priors over our sampling parameters: $\Omega_{\mathrm{m0}} = [0.05, 1.5]$ for the pressureless matter density parameter today, $\Omega_{\mathrm{b0}}h_0^2 = [0.02, 0.025]$ for the baryon density parameter today and $h_0 = [0.4, 1.0]$ for the reduced Hubble constant. For the EMLG parameter we assume $\alpha' = [-1, 1]$, which is also the validity interval of our solution (see Equation (3.42)).

For simplicity, and noticing the near-gaussianity of the posterior distributions (Figure 3.10), to perform a model selection we include the Akaike Information Criterion (AIC) [134] which is defined as

$$\mathrm{AIC} = -2\ln L_{\max} + 2K \tag{3.76}$$

where the first term incorporates the goodness-of-fit through the likelihood L, and the second term is interpreted as the penalisation factor given by two times the number of parameters K of the model. The preferred model is then the one that minimises AIC. A rule of thumb used in the literature is that if the AIC value of a model relative to that of the preferred model $\Delta\mathrm{AIC} \leq 2$, it has substantial support; if $4 \leq \Delta\mathrm{AIC} \leq 7$, it has considerably less support, with respect to the preferred model. A Bayesian model selection applied to the EoS of DE is performed by [30, 33, 34].

Table 3.1 summarizes the observational constraints on the free parameters, as well as the derived parameters labelled by $*$, of the EMLG model using the combined dataset BAO+SN+CC. In order to be able to make comparison, we also include parameters describing the ΛCDM model. We notice the EMLG model fits the data slightly better,

Table 3.1. Constraints on the EMLG parameters using the combined datasets BAO+SN+CC. For one-tailed distributions the upper limit 95% CL is given. For two-tailed the 68% is shown.

Parameter	EMLG	ΛCDM	Priors
$\Omega_{\rm m0}$	0.2983 ± 0.0185	0.2861 ± 0.0102	[0.05,1.5]
$\Omega_{\rm b0}h_0^2$	0.02196 ± 0.00045	0.02205 ± 0.00045	[0.02, 0.025]
h_0	0.682 ± 0.021	0.668 ± 0.009	[0.4, 1.0]
α'	-0.032 ± 0.043	[0]	[-1, 1]
${}^*w_{\rm DE0}$	-1.015 ± 0.019	[-1]	
${}^*z_*$	2.23 ± 0.81	-	
$-\ln L_{\rm max}$	34.22	34.49	–
AIC	76.44	74.98	–

however EMLG is penalized by the inclusion of the extra parameter α, viz., with $\Delta\text{AIC} = 1.46$, and hence it has evidence to be a good model with respect to the ΛCDM model, but the ΛCDM model is slightly preferred over it. Figure 3.10 displays the 1D and 2D marginalized posterior distributions of the parameters used to describe the EMLG model (blue) and the ΛCDM model (red). The inner ellipses show the 68% confidence region, and the outer edges the 95% region. Scatter points indicate values of α' labelled by the colour bar, and the vertical line corresponds to the ΛCDM case ($\alpha' = 0$).

The data constrains the parameter of the EMLG model as $\alpha' = -0.032 \pm 0.043$ at 68% CL, which well covers $\alpha' = 0$ (ΛCDM), but prefers slightly negative values. In comparison with the ΛCDM model, the preference of the EMLG model for slightly negative values of α' leads to a widening of the 1D posterior distributions of $\Omega_{\rm m0}$ and h_0 towards larger values, which in turn shifts the peak values of both parameters to larger values as well. Indeed, we can see in Table 3.1 that, in comparison with the ΛCDM model, the EMLG model predicts larger $\Omega_{\rm m0}$ and h_0 values along with larger errors against the data. The strong anti-correlations on the parameters $\Omega_{\rm m0}$ and α' and also on the h_0 and α' observed in 2D marginalised posterior distributions for the EMLG are an interesting point to note. These two anti-correlations lead to a correlation on the

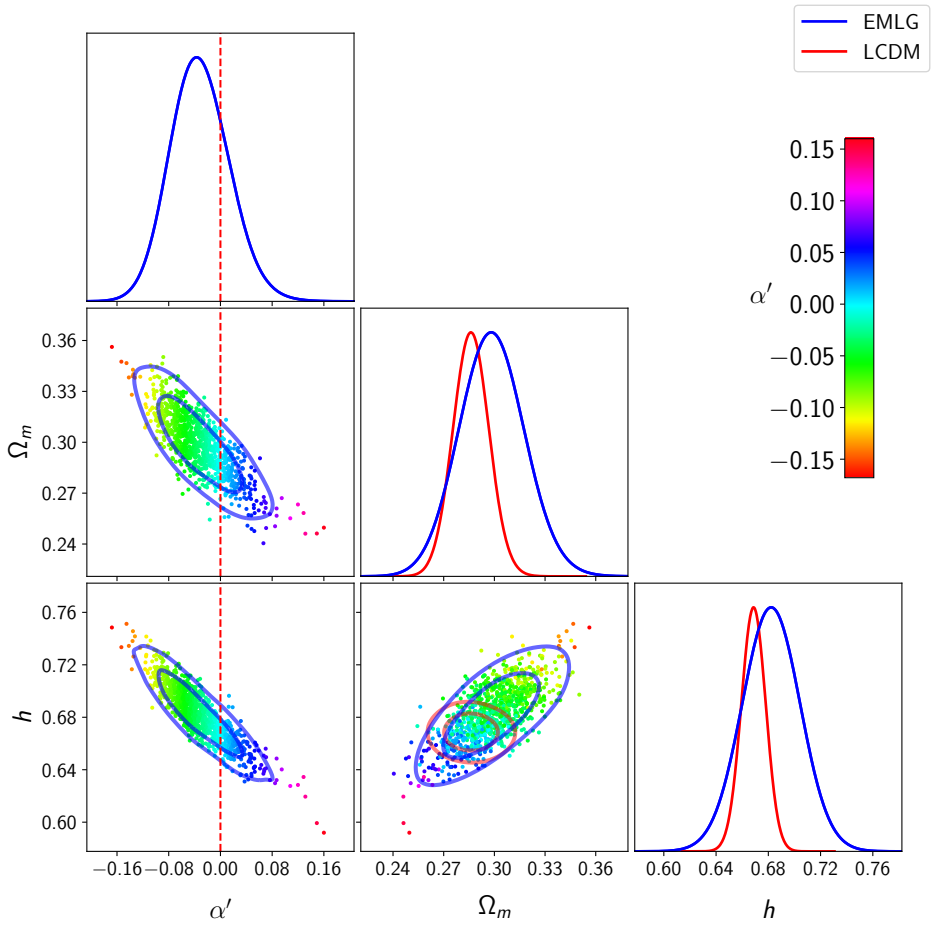

Figure 3.10. 1D and 2D marginalized posterior distributions of the parameters used to describe the EMLG model (blue) and the ΛCDM model (red).

parameters $\Omega_{\rm m0}$ and h_0, so that the larger negative values of α' lead to larger values of both of them. In contrast, in the ΛCDM model there is no noticeable correlation on the parameters $\Omega_{\rm m0}$ and h_0. These can be observed directly in the $\{\Omega_{\rm m0}, h_0\}$ panel of the 3D scatter color plots in Figure 3.10. For the EMLG model, 2D $\{\Omega_{\rm m0}, h_0\}$ contours exhibit a tilt of about 45 degrees and the more reddish (implying larger negative values of α') corresponds to larger $\Omega_{\rm m0}$ and h_0 values.

We study the constraints on the $Omh^2(z_i; z_j)$ diagnostic values of the EMLG model using Equation (3.53) for $\{z_1, z_2, z_3\} = \{0, 0.57, 2.34\}$, where the latter two redshift values are chosen in accordance with the BOSS CMASS and Lyman-α forest

measurements of $H(z)$, and obtain

$$\begin{aligned} Omh^2(z_1;z_2) &= 0.132 \pm 0.008, \\ Omh^2(z_1;z_3) &= 0.130 \pm 0.006, \quad \text{(EMLG)} \\ Omh^2(z_2;z_3) &= 0.130 \pm 0.006. \end{aligned} \tag{3.77}$$

Using the $\Omega_{\rm m0}$ and h_0 obtained for the EMLG model in $Omh^2(z_i;z_j) = \Omega_{\rm m0}h_0^2$ of the ΛCDM model (assuming $\alpha' = 0$) we find a larger value as $Omh^2(z_i;z_j) = 0.139 \pm 0.012$, which clearly shows the reducing effect of $\alpha' < 0$ on the $Omh^2(z_i;z_j)$. On the other hand, for the ΛCDM model, in our analysis the data predicts a slightly lower value, with respect to those in the EMLG model, as

$$Omh^2(z_i;z_j) = 0.128 \pm 0.006, \quad (\Lambda\text{CDM}) \tag{3.78}$$

which results from $h_0 = 0.668 \pm 0.009$ and $\Omega_{\rm m0} = 0.2861 \pm 0.0102$. Note that this low value for the ΛCDM model is very much consistent with $Omh^2 \approx 0.122 \pm 0.010$ from BOSS CMASS and Lyman-α forest measurements of $H(z)$, which is obtained since we do not consider CMB data in our analysis. Indeed, the Planck 2018 [6] release gives $\Omega_{\rm m0}h_0^2 = 0.1430 \pm 0.0011$ from $h_0 = 0.674 \pm 0.005$ and $\Omega_{\rm m0} = 0.315 \pm 0.007$. This shows that reducing the value of Omh^2 in ΛCDM model comes at the cost of reducing $\Omega_{\rm m0}$ to values in tension with the Planck result, and also of reducing h_0 to values which, while consistent with Planck results, exacerbate the persistent tension in the measurement of H_0 between the Planck ΛCDM model and direct measurements from astrophysical data (see, e.g., [3] for a comprehensive list of references on the H_0 tension).

In Figure 3.11 we depict 3D scatter color plots describing the EMLG model marginalised posterior distributions for the parameter α' in the $\{\alpha', Omh^2(z_i;z_j), h_0\}$ subspace for $\{z_1, z_2\}$, $\{z_1, z_3\}$ and $\{z_2, z_3\}$. The color code indicates the value of α' labeled by the colour bar. Red lines display 2D marginalised posterior distributions for the ΛCDM model. In this figure, we see that the 2D marginalised posterior distributions of $\{Omh^2(z_i;z_j), h_0\}$ for the EMLG model (blue contours) are more tilted

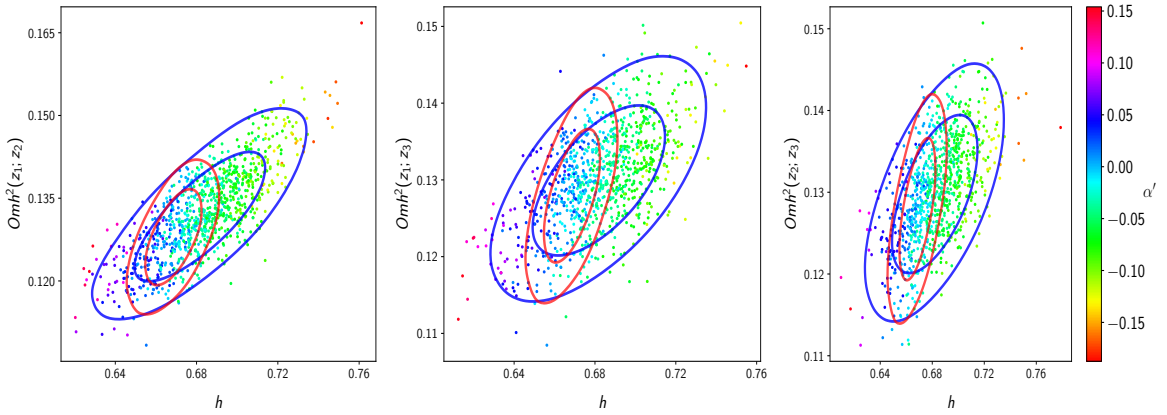

Figure 3.11. Blue lines and 3D scatter color plots describing the EMLG model marginalised posterior distributions for EMLG parameter α' in the $\{\alpha', Omh^2(z_i; z_j), h_0\}$ subspace for $\{z_1, z_2\}$, $\{z_1, z_3\}$ and $\{z_2, z_3\}$.

than the ones for the ΛCDM model (red contours), implying that a certain increment in h_0 would lead to a lesser increment in $Omh^2(z_i; z_j)$ in the EMLG model compared to the ΛCDM model, and that larger h_0 values are allowed for a given Omh^2 value provided that α' takes a correspondingly larger negative value, as can be seen from the color gradient indicating α'. This implies that the EMLG model compensates for the larger values of h_0 by lowering the value of α' and keeps $Omh^2(z_i; z_j)$ at lower values. Whereas, in the ΛCDM model, lowering the value of Omh^2 would lead to low h_0 values (see Table 3.1) which would exacerbate the tension between the Planck ΛCDM model and direct H_0 measurements. Similarly, increasing the value of h_0 would lead to higher Omh^2 values but with the difference that a small increment in h_0 would lead to relatively larger increments in Omh^2 since the red contours for the ΛCDM model are almost vertical. Indeed, for the ΛCDM model, in this analysis we obtain $Omh^2 \approx 0.128$ along with $h_0 \approx 0.668$, whereas the recent Planck release gives $Omh^2 \approx 0.143$ along with $h_0 \approx 0.674$. Note that the about 1% larger value of h_0 is accompanied by a roughly 10% larger value of Omh^2.

The data predicts the following constraints on the Hubble constant along with their errors at the 68% and 95% CL for the EMLG and the ΛCDM models:

$$H_0 = 68.20 \pm 2.13 \pm 4.15 \text{ km s}^{-1} \text{Mpc}^{-1}, \text{ (EMLG)} \tag{3.79}$$

$$H_0 = 66.86 \pm 0.90 \pm 1.74 \text{ km s}^{-1} \text{Mpc}^{-1}. \text{ (ΛCDM)} \tag{3.80}$$

In comparison, the most recent distance-ladder estimates of H_0 from the SHOES (SN, H_0, for the EoS of DE) project give $H_0 = 73.24 \pm 1.74 \text{km s}^{-1}\text{Mpc}^{-1}$ [50], $H_0 = 73.48 \pm 1.66 \text{km s}^{-1}\text{Mpc}^{-1}$ [135] and $H_0 = 73.52 \pm 1.62 \text{km s}^{-1}\text{Mpc}^{-1}$, using Gaia parallaxes [136]. We note that, at 68% CL, H_0 values both from the EMLG model and the ΛCDM model are in tension with these, yet it is worse in the ΛCDM model. Indeed we see that, at 95% CL, the H_0 of the EMLG model becomes consistent with these results, while the H_0 of the ΛCDM model remains in tension.

We depict $H(z)/(1+z)$ (upper panel) and $\rho_{\text{DE}}/\rho_{\text{crit0}}$ (lower panel) plots of the EMLG. For both panels, these show the posterior probability $\Pr(g|z)$: the probability of g as normalized in each slice of constant z, with color scale in confidence interval values. The 1σ and 2σ confidence intervals are plotted as black lines. The upper panel of Figure 3.12 displays a subset of the BAO measurements (blue bars) from $z = 0$, $z = 0.57$ and $z = 2.34$ (see [36]) with scalings that illustrate their physical content along with the distance-ladder estimate of H_0, the direct observational value (red bar) given in [135], and the plot of the posterior probability of $H(z)/(1+z)$, which is the proper velocity between two objects with a constant comoving separation of 1 Mpc, for the EMLG model. We note that the strip (yellow) of $H(z)/(1+z)$ for the EMLG model is consistent with all three BAO data at 1σ CL (though, marginally with the data from $z = 0.57$), whereas it is in tension with the distance-ladder estimate of H_0 at 1σ but marginally consistent with it at 2σ CL. These indeed are considerable improvement with respect to the ΛCDM model (green lines displaying the best-fit value with dotted line and 1σ contour levels in the same figure) which is inconsistent with both the BAO data from $z = 0.57$ and the distance-ladder estimate of H_0 even at 2σ CL. We would like to note that in our case the ΛCDM model is in tension with

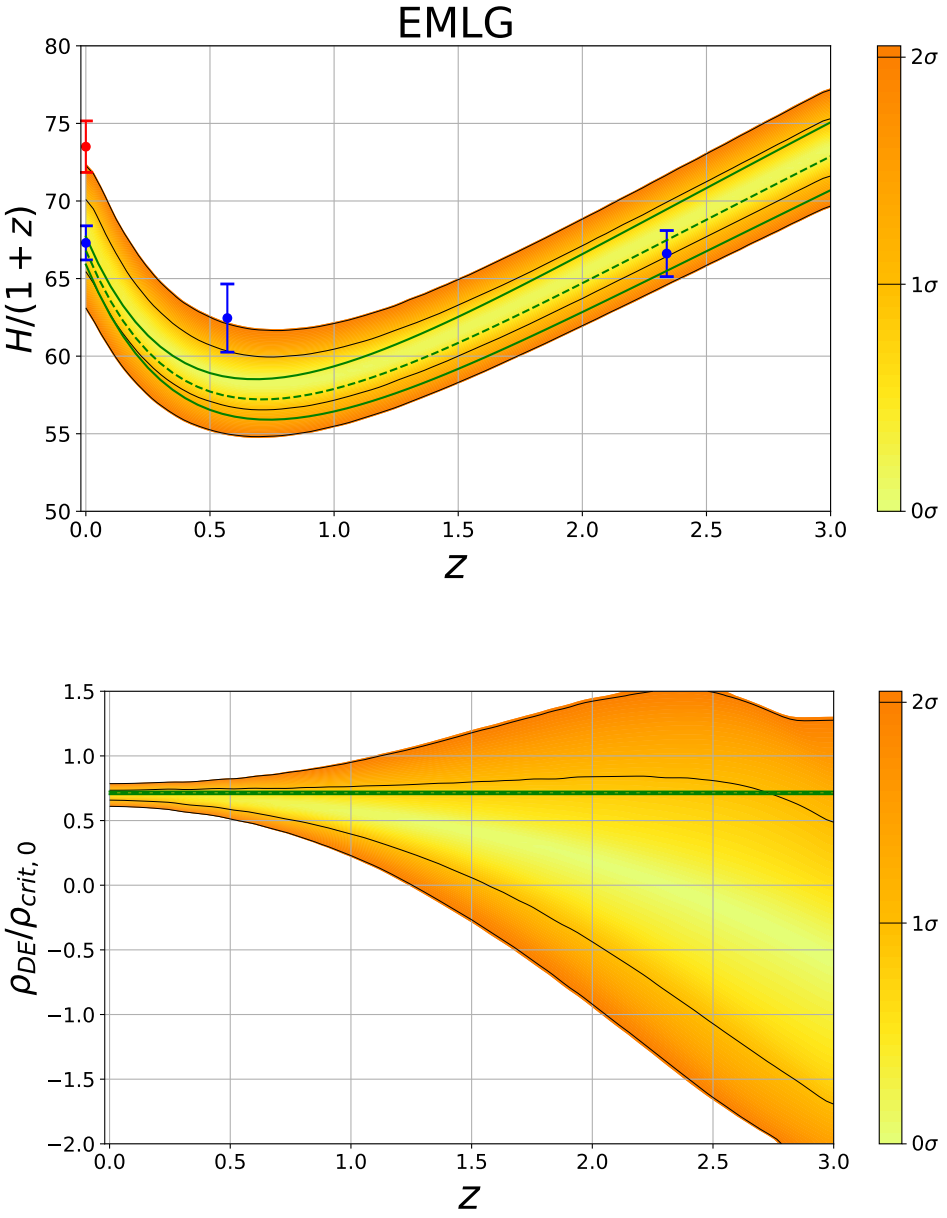

Figure 3.12. (Top panel) $H(z)/(1+z)$ vs. z graph of the EMLG. (Bottom panel) $\rho_{\rm DE}/\rho_{\rm crit0}$ vs. z graph of the EMLG. The 1σ and 2σ confidence intervals are plotted as black lines.

the BAO data from $z = 0.57$ whereas it is consistent with the one from $z = 2.34$ in BOSS [36] and Planck [6]. The reason being that in our analysis we did not consider the data from CMB since we omitted radiation in our models.

The lower panel of Figure 3.12 shows the probability distribution (yellow tones) of the redshift dependency of the energy density of the effective DE scaled to the critical energy density of the present time Universe, i.e. $\rho_{\rm DE}/\rho_{\rm crit0}$, within 1σ and 2σ CL for the EMLG model. Whereas the thin green strip in the panel is for the ΛCDM model at 1σ CL. We see that the effective DE achieves negative values after few redshifts, namely, we obtain $\rho_{\rm DE} = 0$ at $z_* = 2.23 \pm 0.81$ at 1σ CL. It is noteworthy that this value is in line with that in the BOSS collaboration paper [36] estimating DE with a negative energy density for $z > 1.6$ and paper [52] suggesting that cosmological models providing effective DE yielding sign change at $z \sim 2.4$ to obtain, from the model, Omh^2 values consistent with the model-independent estimations.

3.4. Summary and Discussion

In this chapter, we have studied a new model of EMSG, which we call Energy-Momentum Log Gravity (EMLG) described by the function choice of $f(\mathbf{T^2}) = \alpha \ln(\lambda \mathbf{T^2})$. We have studied the cosmological solutions of the spatially homogeneous and isotropic RW metric that satisfies the field equations of this theory of gravitation. Using these solutions, we then conducted an investigation into the ways in which the EMLG extension to ΛCDM model addresses the tensions between existing data sets that beset the standard ΛCDM model. Among the tensions of various degrees of significance reported in the literature, we have particularly focused on the ones discussed in [36, 52], which stem from the Lyman-α forest measurement of BAO at the redshift $z \sim 2.3$ by the BOSS collaboration [51]. It has been argued that this tension can be alleviated in a physically motivated way through a modified gravity theory, rather than as a pure physical DE source within the framework of GR [52], since it necessitates a DE yielding negative energy density values at high redshifts [36, 52].

EMLG allows us to find an explicit exact solution for the pressureless matter density, $\rho_{\rm m}(z)$, and thus of Hubble parameter $H(z)$ and effective DE density $\rho_{\rm DE}(z)$, which has provided us with the opportunity to conduct a detailed theoretical and observational investigation of the model without employing further simplifications.

Following this, upon setting $h_0 = 0.70$ and $\Omega_{\rm m0} = 0.28$ for both models, we have demonstrated analytically that EMLG with $\alpha' = -0.04$ leads to effective DE behaving as suggested in [36, 52] and estimates Omh^2 diagnostic values consistent with the model-independent value from observations [52], whereas the value predicted by the ΛCDM model exhibits a considerable tension with the same model-independent value. We have constrained both models against the latest observational data from the combined dataset BAO+SN+CC and then discussed the improvements due to the EMLG modification. It emerges that the data does not rule out the ΛCDM model limit of the model ($\alpha' = 0$), but prefers slightly negative values of the EMLG model parameter ($\alpha' = -0.032 \pm 0.043$), which produces an effective DE indistinguishable from positive Λ at low redshifts but results in negative energy density values (i.e., screening of Λ) at redshifts larger than $z \sim 2.2$, in line with the arguments developed in [36, 52] for alleviating the tensions relevant to Lyman-α BAO data. We concluded that this feature of the effective DE from the EMLG modification to the ΛCDM model arises from the altered redshift dependency of $\rho_{\rm m}$ due to its nonconservation in this model, not from the new type of contributions of it on the right-hand side of the Friedmann equation (3.39), which yields an effective EoS of a fluid with constant inertial mass density. We observe further that the EMLG model achieves this without lowering the values of H_0 and $\Omega_{\rm m0}$ compared to the results from Planck [6, 16], and moreover relieves, at some level, the persistent tension with the measurements of H_0 within the standard ΛCDM model. On the other hand, as we did not consider CMB data in our observational analyses, in the case of the ΛCDM model, we observed that Omh^2 reduces to values consistent with the model independent value but it happens at the cost of reducing $\Omega_{\rm m0}$ to values in tension with the Planck result, and also of reducing H_0 to values exacerbating the persistent tension in the measurement of H_0.

We see that although our findings are promising in favor of alleviating the tensions considered in the current study, they are not yet conclusive. The reason for this is that we have studied only single fluid cosmology, that is we have considered only pressureless matter as the material source and excluded the presence of radiation in our model, and equally in the ΛCDM model in order to be able to conduct a fair comparison between

two models. In order to confirm these initial results, this study must be extended by the inclusion of radiation together with pressureless matter, and then can also be constrained by considering the CMB data along with the other data sets. We have discussed the difficulties of including radiation, either by itself or as the second source, in our model and suggested a possible method of achieving this, which we reserve for our future works. It is important to note that the study in this chapter demonstrates that, through our particular model, EMLG, EMSG-type extensions to the standard ΛCDM model are capable of addressing some of the prominent tensions which beset ΛCDM model and merit further investigation.

We would like to conclude our discussion on the EMLG model with the following remarks. Our initial motivation for considering $f(\mathbf{T^2}) \propto \ln(\lambda\,\mathbf{T^2})$ was phenomenological, as gives rise to new contributions by pressureless matter on the right-hand side of the EFE which mimic a fluid with constant inertial mass density. The corresponding energy density could then change sign at high redshifts as has been suggested for addressing the tension relevant to the Lyman-α measurements within the standard ΛCDM model, although it emerged that our model was able to do so because of the modified redshift dependency of pressureless matter due to the nonconservation of EMT. Our model is also expedient as it provides us with the opportunity to obtain an explicit exact solution. On the other hand, one might question the microphysical motivation for such a term; in particular, whether there is a way of realizing such a term in the action within a particular field theoretical model that leads to the EMT. For instance, naively substituting $T_{\mu\nu}$ with the energy momentum tensor of a scalar field would lead to a quite nonstandard (and probably nonanalytic) action, which in turn would raise questions about a consistent quantization procedure, the consistency of the corresponding effective field theory, and so on. However, the primary aim of the study in this chapter is to highlight the EMLG model's cosmological signatures, and in that sense, the work presented here can be understood as a phenomenological contribution to exploring the scope of possibilities. It would be interesting to look for a potential origin of this modification in a theory of fundamental physics and see whether some relationship as between the EMSG of the form $f(\mathbf{T^2}) \propto \mathbf{T^2}$ [91, 93–95]

and loop quantum gravity [81, 82] as well as braneworld scenarios [84], all of which add quadratic contributions of the matter stresses' energy density to the Friedmann equation, could be found.

4. EMSG OF THE FORM $f(\mathbf{T^2}) \propto \mathbf{T^2}$ IN AN ANISOTROPIC UNIVERSE

This chapter is heavily based on the work published in [137].

With an increasing consensus, the standard ΛCDM model has begun to be seen as an approximation to a more realistic cosmological model that still needs to be fully understood [138]. Its extensions to date, as we briefly discussed in Section 1.2.1, mostly focus on replacing either Λ with a dynamical DE or the GR with a modified theory of gravity [58, 60–62, 64]. There is, actually, another option that has not been much emphasized so far, that is replacing the spatially maximally symmetric and flat RW metric assumption of the ΛCDM model with a more generic metric, e.g., with a spatially homogeneous but anisotropic metric, which typically gives rise to a dynamical geometrical modification, likewise the spatial curvature (k) term evolving with a^{-2}, in the usual Friedmann equation (1.21) of the standard ΛCDM model, the *shear scalar*, which is a measure of the anisotropic expansion.

4.1. Anisotropic Expansion

The spatially flat RW background assumption has conventionally been justified via the standard inflationary models, which employ canonical scalar fields [9–12], wherein the space dynamically flattens and very efficiently isotropizes (see [139, 140] for cosmic no-hair theorem). While retaining isotropic spatial curvature, allowing anisotropic expansion leads to a generalized form of Friedmann equation bringing in average Hubble parameter along with a shear scalar [141–144] mimicking the stiff fluid [145,146] described by an EoS of the form $p = \rho$ (or $w = 1$) which implies $\rho_{\rm s} \propto a^{-6}$ (see Equation (1.16)), and hence diluting faster than any other fluid for which $p = \rho$ is the causality limit [144] as the Universe expands. This stiff fluid-like shear scalar is very typical for general relativistic anisotropic universes with isotropic spatial curvature sourced by only isotropic perfect fluids having no peculiar velocities [144]. Hence,

one does not expect there to be an anisotropic expansion at detectable levels in the observable Universe. Nonetheless, the interest in anisotropic cosmologies has never been ceased, as, for instance, deviations from the stiff fluid-like behavior of shear scalar might suggest the replacement of Λ with anisotropic stresses that excludes even the most common DE models such as the minimally coupled scalar fields. We refer the reader to [147] for a list of well known anisotropic stresses (e.g. vector fields and spatial curvature anisotropies), and their effects on the shear scalar/expansion anisotropy. Some new observations, e.g. unexpected features in the CMB data from the WMAP and Planck missions and in other types of independent cosmological data (see [148–153] and references therein), has frequently reinforced this interest in anisotropic cosmologies. Also, References [154–163] argue that the lack of quadrupole moment in the CMB temperature angular power spectrum [148–151] can be alleviated by anisotropic expansion driven, by anisotropic DE, well after the matter-radiation decoupling (see also [164–170], and, for constraints on such models, [171–174]). Seeking possible significant deviations from isotropic cosmic expansion occupies a crucial place in the upcoming projects such as the Euclid mission [175], as it can shed light on the nature of DE, namely, modified gravity theories generically induce nonzero anisotropic stresses that give rise to characteristic modifications on the stiff fluid-like dynamics of the shear scalar (see [77, 176–178]). All these works essentially focus on the idea of relaxing the limits upon the anisotropic expansion by rendering the shear scalar less stiff, by replacing either Λ with an anisotropic DE or GR by a modified gravity theory that can induce an anisotropic DE component. Through such setups, one can considerably weaken the limits obtained from BBN with respect to the ones imposed by the CMB [147]. However, in such models, the generalized Friedmann equation, accordingly, $H(z)$ usually deviates from that of the ΛCDM model because of both the replacement of Λ with an anisotropic stress and the modified dynamics of shear scalar led by it.

4.1.1. Screening Mechanism

In this chapter, relying on EMSG theory, we search for a new possibility of that the stiff fluid-like behavior of shear scalar is retained (i.e., no anisotropic fluids em-

ployed) but its contribution to $H(z)$ is compensated by CDM, so that, for instance, the CMB quadrupole temperature fluctuation can be manipulated without giving rise to any deviation, on average, from either the standard ΛCDM model or the standard BBN. As we have discussed in Section 2.2, EMSG of the form $f(\mathbf{T^2}) \propto \mathbf{T^2}$ is unique in that the pressureless matter in this case satisfies the conservation of the EMT and yet its linear (usual GR) contribution, $\rho_{\rm m}$, to the $H(z)$ is accompanied by its quadratic (new EMSG) contribution, $\alpha\rho_{\rm m}^2$ (see Equation (2.12)), which mimics stiff fluid behavior as exactly like the shear scalar does too.

The observational upper limits on the present-day density parameter of a stiff fluid-like term, i.e., the term evolving as a^{-6}, included in the standard Friedmann equation of the standard ΛCDM model can be adopted from [179]; it is $\sim 10^{-15}$ from the latest joint CMB and BAO data, and $\sim 10^{-23}$ from BBN. Consequently, in both extensions of the basic ΛCDM model, i.e., in either its anisotropic extension or its extension via the CDM coupling to gravity in accordance with the EMSG model of the form $f(\mathbf{T^2}) = \alpha\mathbf{T^2}$, the stiff fluid-like term included in the Friedmann equation should today be extremely small, in fact, the corresponding present-day density parameter should be less than 10^{-23} not to spoil the successful description of the Universe all the way to the BBN era. This argument might give the impression that such extensions to the standard ΛCDM model are permitted to be relevant only to the dynamics of the early Universe well before the BBN. In what follows in this chapter, we shall discuss and show that this is not the case, in particular, when these two extensions are considered simultaneously. We begin with constructing a generalization of the standard ΛCDM model, wherein we concurrently replace the spatially flat RW metric with its simplest anisotropic generalization, locally rotationally symmetric (LRS) Bianchi I metric, and couple the CDM to the gravity in accordance with the EMSG of the form $f(\mathbf{T^2}) \propto \mathbf{T^2}$, while all other sources existing in the Standard Model of particle physics couple as usual in accordance with GR. Then, we shall demonstrate that these two modifications can mutually cancel out owing to the possibility of α being negative (for which the new contribution of the CDM resembles a stiff fluid with negative energy density), namely, the shear scalar can be completely screened by CDM and recovers mathematically

exactly the same Friedmann equation of the standard ΛCDM model. This feature of the model allows us to get around the BBN limits on the anisotropic expansion, and thereby provides us with an opportunity to manipulate the CMB quadrupole temperature fluctuation at the desired amount through a slightly anisotropic expansion in the late Universe. We further investigate the consequences of this model on both the very early times and far future of the Universe, and finally briefly discuss that such constructions might even be considered in the context of a major issue of the current cosmology, the so-called H_0 problem [3].

4.2. Multi-fluid EMSG Model

In order to be able to investigate a multi-fluid universe in the context of EMSG, folowing the same line of reasoning in [96] (see Section 2.2), we generalize the action (2.1) by the replacement

$$f\left(T_{\mu\nu}T^{\mu\nu}\right)+\mathcal{L}_{\mathrm{m}}\longrightarrow f\left(T_{\mu\nu}T^{\mu\nu},\mathcal{L}_{\mathrm{m}}\right), \tag{4.1}$$

and arrive at

$$S=\int \mathrm{d}^4x\sqrt{-g}\,\left[\frac{1}{2}\left(R-2\Lambda\right)+f\left(T_{\mu\nu}T^{\mu\nu},\mathcal{L}_{\mathrm{m}}\right)\right]. \tag{4.2}$$

We carry out the same steps as in Section 2.1, and vary the action (4.2) with respect to the inverse metric $g^{\mu\nu}$ as

$$\begin{aligned}\delta S=\int \mathrm{d}^4x\sqrt{-g}\Bigg[&\frac{1}{2}\delta R+\frac{\partial f}{\partial(T_{\alpha\beta}T^{\alpha\beta})}\frac{\delta(T_{\sigma\epsilon}T^{\sigma\epsilon})}{\delta g^{\mu\nu}}\delta g^{\mu\nu}+\frac{\partial f}{\partial\mathcal{L}_{\mathrm{m}}}\frac{\delta\mathcal{L}_{\mathrm{m}}}{\delta g^{\mu\nu}}\delta g^{\mu\nu}\\&-\frac{1}{2}g_{\mu\nu}\delta g^{\mu\nu}\left\{\frac{1}{2}\left(R-2\Lambda\right)+f\left(T_{\sigma\epsilon}T^{\sigma\epsilon},\mathcal{L}_{\mathrm{m}}\right)\right\}\Bigg],\end{aligned} \tag{4.3}$$

and the EMT of the matter field $T_{\mu\nu}$ is defined in the usual fashion (see (2.3)).

We proceed with the most straightforward model of the EMSG, which considers the linear contribution of the new scalar $\mathbf{T^2} = T_{\mu\nu}T^{\mu\nu}$ in the action (4.2), expressed by

$$f(T_{\mu\nu}T^{\mu\nu}, \mathcal{L}_{\rm m}) = \sum_i \left(\alpha_i T^{(i)}_{\mu\nu} T^{\mu\nu}_{(i)} + \mathcal{L}^{(i)}_{\rm m}\right). \tag{4.4}$$

Here i denotes the ith matter field (fluid), and the summation over index i is used for the sake of simplicity so that it avoids the cross-terms involving the product of the energy densities of different fluids in the modified Friedmann equation, and α_i's are constants that measure the coupling strength of the EMSG modifications to gravity for the ith fluid [96]. Thus, we make use of the action specified as follows

$$S = \int \mathrm{d}^4x\sqrt{-g}\left[\frac{R}{2} - \Lambda + \sum_i \left(\alpha_i T^{(i)}_{\mu\nu} T^{\mu\nu}_{(i)} + \mathcal{L}^{(i)}_{\rm m}\right)\right], \tag{4.5}$$

from which the modified EFE read

$$G_{\mu\nu} + \Lambda g_{\mu\nu} = \sum_i T^{(i)}_{\mu\nu} + \sum_i \alpha_i \big(T^{(i)}_{\sigma\epsilon} T^{\sigma\epsilon}_{(i)} g_{\mu\nu} - 2\,\Xi^{(i)}_{\mu\nu}\big). \tag{4.6}$$

Here the new tensor analogous to (2.10) for the multi-fluid Universe is defined as

$$\Xi^{(i)}_{\mu\nu} = -2\mathcal{L}^{(i)}_{\rm m}\left(T^{(i)}_{\mu\nu} - \frac{1}{2}g_{\mu\nu}\mathcal{T}^{(i)}\right) - \mathcal{T}^{(i)}T^{(i)}_{\mu\nu} + 2T^{\gamma(i)}_{\mu} T^{(i)}_{\nu\gamma} - 4T^{\sigma\epsilon}_{(i)}\frac{\partial^2\mathcal{L}^{(i)}_{\rm m}}{\partial g^{\mu\nu}\partial g^{\sigma\epsilon}}, \tag{4.7}$$

where $\mathcal{T}^{(i)}$ is the trace of the EMT of the ith fluid, and the last term vanishes as $T^{(i)}_{\mu\nu}$ does not include the second metric variation of $\mathcal{L}^{(i)}_{\rm m}$, which can be extracted from (2.3). From (4.6), we see that the covariant divergence of the total EMT reads

$$\nabla^\mu \sum_i T^{(i)}_{\mu\nu} = -\nabla^\mu \sum_i \alpha_i \big(T^{(i)}_{\sigma\epsilon} T^{\sigma\epsilon}_{(i)} g_{\mu\nu} - 2\,\Xi^{(i)}_{\mu\nu}\big), \tag{4.8}$$

which means that the total EMT is not conserved in general unless $\alpha_i = 0$ (GR).

4.2.1. Anisotropic Cosmology in EMSG

We now investigate this model in the context of anisotropic cosmology. We consider $\mathcal{L}_{\rm m}^{(i)} = p_i$ for the definition of the matter Lagrangian density that leads to the isotropic perfect fluid EMT of the form [180, 181]

$$T_{\mu\nu}^{(i)} = (\rho_i + p_i)u_\mu u_\nu + p_i g_{\mu\nu} \tag{4.9}$$

where ρ_i and p_i are the energy density and the thermodynamic pressure of the ith fluid respectively and u_μ is the four-velocity satisfying the conditions $u_\mu u^\mu = -1$ and $\nabla_\nu u^\mu u_\mu = 0$. Using (4.9) along with barotropic equation of states defined as

$$w_i = \frac{p_i}{\rho_i} = \text{constant}, \tag{4.10}$$

we calculate

$$\mathcal{T} = \rho_i(3w_i - 1), \tag{4.11}$$

$$T_{\mu\nu}^{(i)} T_{(i)}^{\mu\nu} = \rho_i^2(3w_i^2 + 1), \tag{4.12}$$

and accordingly, (4.7) leads to

$$\Xi_{\mu\nu}^{(i)} = -\rho_i^2(3w_i + 1)(w_i + 1)u_\mu u_\nu. \tag{4.13}$$

Hence, the covariant divergence of the total EMT given in (4.8) reads

$$\sum_i [\dot{\rho}_i + \Theta(1 + w_i)\rho_i] = \sum_i \alpha_i \frac{2\Theta w_i(1 + w_i)(5 + 3w_i)\rho_i^2}{1 + 2\alpha_i(1 + 8w_i + 3w_i^2)\rho_i}, \tag{4.14}$$

where a dot denotes derivative with respect to the comoving proper time t. Also, $\Theta = \mathrm{D}^\mu u_\mu$ is the volume expansion rate in which the derivative operator D_μ is defined through $\mathrm{D}_\mu u_\nu = \nabla_\mu u_\nu + u_\mu \dot{u}_\nu$ [143] and simply reduces to standard covariant derivative for a comoving fluid. Note that, unless $\alpha_i = 0$ (GR), we can recover the local

conservation of the total EMT only for $w_i = \{-5/3, -1, 0\}$.

As we briefly mentioned before, in the current study, we consider the simplest anisotropic extension of the spatially flat RW metric (the LRS Bianchi I) in which we allow for a different expansion factor in only one orthogonal direction while retaining spatial homogeneity and flatness. Thus, the LRS Bianchi I spacetime metric is represented by

$$\mathrm{d}s^2 = -\mathrm{d}t^2 + a^2(t)\,\mathrm{d}x^2 + b^2(t)\,(\mathrm{d}y^2 + \mathrm{d}z^2) \tag{4.15}$$

where $\{a(t), b(t), b(t)\}$ are the directional scale factors along the principal axes $\{x, y, z\}$ [142–144]. Accordingly, the directional Hubble parameters along the x- and y- (or z-) axes are

$$H_a = \frac{\dot{a}}{a} \quad , \quad H_b = \frac{\dot{b}}{b}. \tag{4.16}$$

The corresponding average expansion scale factor, s, reads

$$s(t) = (ab^2)^{1/3}, \tag{4.17}$$

and from which the average Hubble parameter, $H = \Theta/3$, becomes

$$H \equiv \frac{\dot{s}}{s} = \frac{1}{3}(H_a + 2H_b). \tag{4.18}$$

And, we consider the usual cosmological fluids: radiation (photon γ and neutrinos ν) (r) described by the EoS parameter $w_{\mathrm{r}} = \frac{1}{3}$, and baryons (b) and CDM (c) described by $w_{\mathrm{b}} = w_{\mathrm{c}} = 0$. However, we assume the particles present in the Standard Model of particle physics (b, γ, and three types of ν) couple to gravity in the same way as in the GR (i.e., for these $\alpha_{\mathrm{r}} = \alpha_{\mathrm{b}} = 0$) whereas the CDM arbitrarily couples to gravity in accordance with the EMSG implying that α_{c} is not necessarily null. Consequently, we calculate the relevant terms given in (4.12) and (4.13), and using (4.6), reach the

following set of equations

$$2H_aH_b + H_b^2 - \Lambda = \rho_{\rm r} + \rho_{\rm b} + \rho_{\rm c} + \alpha_{\rm c}\,\rho_{\rm c}^2, \tag{4.19}$$

$$-2\dot{H}_b - 3H_b^2 + \Lambda = \frac{\rho_{\rm r}}{3} + \alpha_{\rm c}\,\rho_{\rm c}^2, \tag{4.20}$$

$$-\dot{H}_a - \dot{H}_b - H_a^2 - H_b^2 - H_aH_b + \Lambda = \frac{\rho_{\rm r}}{3} + \alpha_{\rm c}\,\rho_{\rm c}^2. \tag{4.21}$$

These equations can be rewritten in terms of the average expansion rate H and the shear scalar σ^2, which quantifies the anisotropic expansion, defined as

$$\sigma^2 = \frac{1}{2}\sigma_{\alpha\beta}\sigma^{\alpha\beta}, \tag{4.22}$$

where the shear tensor $\sigma_{\alpha\beta}$ is given by

$$\sigma_{\alpha\beta} = \frac{1}{2}(u_{\mu;\nu} + u_{\nu;\mu})h^{\mu}_{\alpha}h^{\nu}_{\beta} - \frac{1}{3}u^{\mu}_{;\mu}h_{\alpha\beta} \tag{4.23}$$

with $h_{\mu\nu} = g_{\mu\nu} + u_\mu u_\nu$ being the projection tensor [143]. Accordingly, for the LRS Bianchi I metric (4.15), we have

$$\sigma^2 = \frac{1}{3}\left(H_a - H_b\right)^2 \tag{4.24}$$

which, along with (4.18), lead to

$$3H^2 - \sigma^2 - \Lambda = \rho_{\rm r} + \rho_{\rm b} + \rho_{\rm c} + \alpha_{\rm c}\,\rho_{\rm c}^2, \tag{4.25}$$

$$-2\dot{H} - 3H^2 - \sigma^2 + \Lambda = \frac{\rho_{\rm r}}{3} + \alpha_{\rm c}\,\rho_{\rm c}^2, \tag{4.26}$$

$$\dot{\sigma} + 3H\sigma = 0, \tag{4.27}$$

which are, respectively, the energy density (4.25), average pressure (4.26) and shear propagation (4.27) equations. It seems reasonable to suppose that, on cosmological scales, these fluids are interacting only gravitationally, which gives rise to the separation of Equation (4.14) into different pieces for each one. Despite the fact that the energy

density of CDM appears in the field equations in a modified way, as we have discussed previously, it satisfies $\nabla^{\mu}T_{\mu\nu} = 0$ (i.e., right-hand side of (4.14) vanishes) and scales as usual as $\rho_{\rm c} = \rho_{\rm c0}s^{-3}$. Since the baryons and radiation couple to gravity as in the GR, these also scale as usual as $\rho_{\rm b} = \rho_{\rm b0}s^{-3}$ and $\rho_{\rm r} = \rho_{\rm r0}s^{-4}$. Additionally, the shear propagation equation (4.27) dictates that the shear scalar scales as $\sigma^2 = \sigma_0^2 s^{-6}$ (like a stiff fluid). We remind that here, throughout the thesis as well, a subscript 0 attached to any quantity denotes its present-day ($s = 1$ in this case) value. Consequently, we arrive at the following modified Friedmann equation of our model:

$$\frac{H^2}{H_0^2} = \Omega_{\Lambda 0} + \Omega_{\rm b0}s^{-3} + \Omega_{\rm r0}s^{-4} + \Omega_{\rm c0}\left(s^{-3} + \alpha_{\rm c}' s^{-6}\right) + \Omega_{\sigma 0}s^{-6} \tag{4.28}$$

with $\alpha_{\rm c}' = \alpha_{\rm c}\,\rho_{\rm c0}$ being the dimensionless parameter of the model. Here $\Omega_{i0} = \frac{\rho_{i0}}{3H_0^2}$ are the present-day density parameters of the ith matter field, while $\Omega_{\Lambda 0} = \frac{\Lambda}{3H_0^2}$ and $\Omega_{\sigma 0} = \frac{\sigma_0^2}{3H_0^2}$ are those corresponding to Λ and σ^2. Evaluated at $s = 1$ (today), Equation (4.28) implies the following condition

$$\Omega_{\Lambda 0} + \Omega_{\rm b0} + \Omega_{\rm r0} + \Omega_{\rm c0}\,(1 + \alpha_{\rm c}') + \Omega_{\sigma 0} = 1 \tag{4.29}$$

on the present-day density parameters of this model.

4.3. ΛCDM with Hidden Anisotropic Expansion

Our model provides a mechanism for screening the shear scalar, which can even recover the standard Friedmann equation of ΛCDM model in spite of the presence of anisotropic expansion. In other words, collecting the like terms in (4.28) together yields

$$\frac{H^2}{H_0^2} = \Omega_{\Lambda 0} + (\Omega_{\rm b0} + \Omega_{\rm c0})s^{-3} + \Omega_{\rm r0}s^{-4} + (\Omega_{\sigma 0} + \alpha_{\rm c}'\,\Omega_{\rm c0})\,s^{-6} \tag{4.30}$$

wherein $\alpha_{\rm c}'\,\Omega_{\rm c0}s^{-6}$ (the quadratic contribution of the CDM due to the EMSG) for $\alpha_{\rm c}' < 0$ perpetually screens $\Omega_{\sigma 0}s^{-6}$ (the stiff fluid-like contribution of the shear scalar), and the

particular setting as

$$\alpha_{\rm c}' = -\frac{\Omega_{\sigma 0}}{\Omega_{\rm c0}}, \tag{4.31}$$

even hides it and leads to the equation

$$\frac{H^2}{H_0^2} = (\Omega_{\rm b0} + \Omega_{\rm c0})s^{-3} + \Omega_{\rm r0}s^{-4} + \Omega_{\Lambda 0}, \tag{4.32}$$

which is mathematically exactly the same with the Friedmann equation of the standard ΛCDM model. On the other hand, physically, the $H(s)$ here is the average expansion rate, and the expansion rates along the principal axes, H_a and H_b, need not necessarily be equal. As the CDM production is typically expected to occur much earlier than the BBN takes place, it can be supposed that this screening mechanism is working since then the times much before the BBN. For instance, if CDM could be described by WIMPs, starting from the energy scale $\sim 0.1\,\mathrm{TeV}$ corresponding to the time (redshift) scale $\sim 10^{-10}\,\mathrm{s}$ ($z \sim 10^{15}$), whereas the corresponding values are $\sim 0.1\,\mathrm{MeV}$ and $\sim 100\,\mathrm{s}$ ($z \sim 10^9$) for the standard BBN [182].

The model-independent upper limits on the present-day anisotropic expansion in terms of $\Omega_{\sigma 0}$ is of the order of $\mathcal{O}(10^{-3})$, e.g., from Type Ia SN [183, 184] (see also [185–188]). This, within the simplest anisotropic (Bianchi I) generalization of the standard ΛCDM model (i.e. $\alpha_{\rm c}' = 0$), implies the domination of the shear scalar at $z \sim 10$ and hence the spoilt of the successful description of the earlier ($z \gtrsim 10$) Universe. Indeed, while the constraint on a stiff fluid-like term ($\rho_{\rm s} = \rho_{\rm s0}s^{-6}$, likewise the shear scalar) on top of the standard ΛCDM model is $\Omega_{\rm s0} \lesssim 10^{-3}$ from the combined $H(z)$ and Pantheon data set (relevant to $z \lesssim 2.4$), it is tightened to $\Omega_{\rm s0} \lesssim 10^{-15}$ when the combined BAO and CMB (relevant to $z \sim 1100$) data set also is included, and $\Omega_{\rm s0} \lesssim 10^{-23}$ upon demanding no significant deviation from the standard BBN (relevant to $z \sim 10^9$) [179]. All these can straightforwardly be adopted to our model

upon redefining the terms evolving with s^{-6} as

$$\Omega_{\rm s0} = \Omega_{\sigma 0} + \alpha_{\rm c}' \, \Omega_{\rm c0} \tag{4.33}$$

in Equation (4.30). And our model, thus, can concurrently accommodate the constraints $\Omega_{\rm s0} \lesssim 10^{-23}$ (even $\Omega_{\rm s0} = 0$) and $\Omega_{\sigma 0} \lesssim 10^{-3}$, by means of the screening term $\alpha_{\rm c}' \, \Omega_{\rm c0}$ for properly chosen values of $\alpha_{\rm c}'$. However, as the shear scalar still scales as $\sigma^2 \propto s^{-6}$, the typical upper limit $\Omega_{\sigma 0} \sim 10^{-20}$ derived from the observed CMB quadrupole temperature fluctuation, that is $\Delta T/T \sim 10^{-5}$, setting an upper limit at the same order of magnitude on the anisotropy at the recombination era ($\sqrt{\Omega_\sigma^{\rm rec}} \sim 10^{-5}$ at $z_{\rm rec} \sim 10^3$) still applies [189–192]. Accordingly, one can attempt to manipulate the CMB quadrupole temperature via anisotropic expansion consistent with $\Omega_{\sigma 0} \sim 10^{-20}$ while retaining exactly the same expansion history for the comoving volume element of the Universe as that of the standard ΛCDM model all the way to the time (redshift) scale of $\sim 10^{-10}\,$s ($z \sim 10^{15}$), which can be promising, for instance, to address the so-called "quadrupole temperature problem" [148–151]. We shall now investigate this aspect of our model.

4.3.1. Manipulating CMB Quadrupole Temperature Fluctuation

Since anisotropic cosmic expansion gives rise to different evolution of the temperature of the free streaming photons through the different expansion factors in three orthogonal axes, it can enable us to manipulate the quadrupole (multipole moment $\ell = 2$ corresponding to the angular scale $\theta = \pi/2$) power spectrum of temperature fluctuations in the CMB, ΔT, with no alteration on the higher multipole moments. The evolution of the photon temperature along the x-axis and y-axis (or z-axis) is given by

$$T_x = T_0 \frac{a_0}{a} = T_0 e^{-\int H_a \mathrm{d}t}, \tag{4.34}$$

$$T_y = T_0 \frac{b_0}{b} = T_0 e^{-\int H_b \mathrm{d}t} \tag{4.35}$$

where $T_0 = 2.7255 \pm 0.0006\,\mathrm{K}$ [4] is the present-day CMB monopole temperature [147, 193]. Correspondingly, the difference between the photon temperatures, due to the anisotropic expansion, along the y- and x-axes since the time of recombination ($z = z_{\rm rec}$) to the present time ($z = 0$) , $\Delta T_\sigma \equiv T_y - T_x$, reads

$$\begin{aligned}\Delta T_\sigma &= T_0 \int_{t_{\rm rec}}^{t_0} (H_a - H_b)\mathrm{d}t \\ &= T_0 \int_{t_{\rm rec}}^{t_0} \sqrt{3}\sigma \mathrm{d}t \\ &= 3T_0\sqrt{\Omega_{\sigma 0}} \int_0^{z_{\rm rec}} \frac{H_0(1+z)^2}{H}\mathrm{d}z\end{aligned} \tag{4.36}$$

for small anisotropies, which imply

$$e^{-\int H_a \mathrm{d}t} \simeq 1 - \int H_a \mathrm{d}t, \tag{4.37}$$

$$e^{-\int H_b \mathrm{d}t} \simeq 1 - \int H_b \mathrm{d}t. \tag{4.38}$$

In (4.36), we make use of the relation $\mathrm{d}t = -\frac{\mathrm{d}z}{H(1+z)}$ with $z = \frac{1}{s} - 1$ denoting the average redshift defined from the average expansion scale factor, also, assume the CMB was last scattered at the recombination epoch (redshift) $t_{\rm rec}$ ($z_{\rm rec}$). Thus, under the condition (4.31) ensuring exactly the same expansion history for the comoving volume element with that of the standard ΛCDM model, it is possible to have change in ΔT up to

$$\Delta T_\sigma = 3T_0\sqrt{-\alpha'_{\rm c}\,\Omega_{\rm c0}} \int_0^{z_{\rm rec}} \frac{H_0(1+z)^2}{H}\mathrm{d}z \tag{4.39}$$

on top of the best-fit standard ΛCDM predicted value $\Delta T_{\rm std} \approx 34\,\mu K$ ($\Delta T_{\rm std+var} \approx 28\,\mu K$ if the cosmic variance is included) [1, 155], and bring it to the observed value $\Delta T_{\rm PLK} \approx 14\,\mu K$ by the Planck satellite [149]. Accordingly, we can make use of the observational best-fit values from the recent Planck release [6], $\Omega_{\rm b0} = 0.049$ and $\Omega_{\rm c0} = 0.264$, along with the recombination redshift $z_{\rm rec} \sim z_{\rm dec}$ (where $z_{\rm dec} \approx 1090$) and the present-day density parameter of radiation $\Omega_{\rm r0} \approx 10^{-4}$. Then, if we set $\Omega_{\sigma 0} = 4 \times 10^{-21}$

which corresponds to $\alpha'_{\rm c} = -1.52{\times}10^{-20}$ ($\alpha_{\rm c} = -1.8{\times}10^{-11}{\rm cm}^3/{\rm erg}$) from the screening condition (4.31), we reach $\Omega_\sigma^{\rm rec} = 1.23 \times 10^{-11}$ along with that $\Delta T_\sigma = 20.5\ \mu$K which is able to reduce ΔT from the value $\Delta T_{\rm std} \approx 34\mu$K predicted within the standard ΛCDM model to the observed value $\Delta T_{\rm PLK} \approx 14\,\mu K$ provided that the orientation of the expansion anisotropy is set suitably.

For the radiation dominated era (namely, for $z > z_{\rm eq}$, where $z_{\rm eq} = -1 + (\rho_{\rm c0} + \rho_{\rm b0})/\rho_{\rm r0}$ is the redshift of matter-radiation equality) during which the shear scalar and the new quadratic contribution of the CDM energy density are subdominant while Λ and the usual linear contributions of the baryon and CDM energy densities are negligible, the Equation (4.25) can be recast as

$$3H^2 = \rho_{\rm r} + \rho_{\rm s}, \tag{4.40}$$

where $\rho_{\rm r}$ and $\rho_{\rm s}$ are defined as follows

$$\rho_{\rm r} = \frac{\pi^2}{30} g_* T^4 \qquad , \qquad \rho_{\rm s} = \alpha_{\rm c}\, \rho_{\rm c}^2 + \sigma^2, \tag{4.41}$$

or can be expressed, in a more useful way, as

$$3H^2 = \frac{\pi^2}{30} \tilde{g}_* T^4 \tag{4.42}$$

with $\tilde{g}_* = (1-\Omega_{\rm s})^{-1} g_*$ being the modified effective number of degrees of freedom where $\Omega_{\rm s} = \Omega_\sigma \left(1 + \alpha'_{\rm c} \frac{\Omega_{\rm c0}}{\Omega_{\sigma 0}}\right)$ from (4.33). The usual effective number of degrees of freedom g_*, which counts the number of relativistic species determining the radiation energy density, expressed as [194, 195]

$$g_* = \sum_{\rm bosons} g_i + \frac{7}{8} \sum_{\rm fermions} g_i. \tag{4.43}$$

In the Standard Model of particle physics at $T = 1\,\mathrm{MeV}$,

$$g_* = 2 + \frac{7}{8}(2 + 2 + N_\nu + N_\nu) \tag{4.44}$$

$$= 5.5 + \frac{7}{4}N_\nu, \tag{4.45}$$

where $g_i = 2$ for photons, electrons and positrons, and $N_\nu = 3$ ($N_\nu = 3.045$ when small corrections for nonequilibrium neutrino heating are included in the thermal evolution) is the effective number of (nearly) massless neutrino flavors as well as of their anti-neutrinos ($g_i = 1$ for each) [1]. $\tilde{g}_*$ is conventionally parametrized by $\Delta N_\nu = N_\nu - 3$, which denotes the deviation of N_ν from the Standard Model value $N_\nu = 3$, as

$$\tilde{g}_* = (1 + \frac{7}{43}\Delta N_\nu) g_*. \tag{4.46}$$

Consequently, at the time of neutrino freeze-out, i.e., when the rate of the weak-interaction that interconverts protons and neutrons falls behind the Hubble expansion rate at $T_{\mathrm{fr}} \sim 1\,\mathrm{MeV}$, two relations given above for $\tilde{g}_*$ imply that the stiff fluid-like term ρ_{s} in our model can be interpreted as a change in the total number of effectively massless degrees of freedom as

$$\Omega_{\mathrm{s}}^{\mathrm{fr}} = \frac{7}{43}\Delta N_\nu \tag{4.47}$$

for small $\Omega_{\mathrm{s}}^{\mathrm{fr}}$ values, namely $(1 - \Omega_{\mathrm{s}}^{\mathrm{fr}})^{-1} \simeq 1 + \Omega_{\mathrm{s}}^{\mathrm{fr}}$. This can then be translated into the density parameter of the stiff fluid-like term at the recombination through the following relation [147]

$$\Omega_{\mathrm{s}}^{\mathrm{rec}} = \Omega_{\mathrm{s}}^{\mathrm{fr}}(1 + z_{\mathrm{fr}})^{-2}(1 + z_{\mathrm{eq}})^{-1}(1 + z_{\mathrm{rec}})^3. \tag{4.48}$$

For the freeze-out redshift $z_{\mathrm{fr}} \sim 10^9$, consistent with the standard BBN, along with $z_{\mathrm{eq}} = 3390$ and $z_{\mathrm{rec}} = 1090$ from the best-fit values of the standard ΛCDM model in the most recent Planck release [6], it turns out that $\Omega_{\mathrm{s}}^{\mathrm{rec}} = 6.23 \times 10^{-14}\Delta N_\nu$ (or $\Omega_{\mathrm{s}}^{\mathrm{rec}} = 3.83 \times 10^{-13}\Omega_{\mathrm{s}}^{\mathrm{fr}}$). Next, using $\Omega_{\mathrm{b0}} = 0.049$, $\Omega_{\mathrm{c0}} = 0.264$, and $\Omega_{\mathrm{r0}} \approx 10^{-4}$

as well, we find $\Omega_{s0} = 3.24 \times 10^{-10}\Omega_s^{rec}$ implying $\Omega_{s0} = 2.02 \times 10^{-23}\Delta N_\nu$. All these relations, eventually, lead to $\Omega_s^{fr} = 0.163$, $\Omega_s^{rec} = 6.23 \times 10^{-14}$ and $\Omega_{s0} = 2.02 \times 10^{-23}$ for $\Delta N_\nu = 1$, and $\Omega_s^{fr} = 0.05$, $\Omega_s^{rec} = 1.87 \times 10^{-14}$ and $\Omega_{s0} = 6.06 \times 10^{-24}$ for the upper limit of $\Delta N_\nu = 0.30$ from the recent Planck release [6].

In the case of the straightforward Bianchi I extension of the standard ΛCDM model ($\alpha_c' = 0$), these limits on the stiff fluid-like term simply correspond to the limits on the shear scalar and hence, through (4.36), on ΔT_σ as well. In other words, now, we have $\Omega_\sigma^{fr} = 0.05$, $\Omega_\sigma^{rec} = 1.87 \times 10^{-14}$, and $\Omega_{\sigma 0} = 6.06 \times 10^{-24}$ leading to $\Delta T_\sigma = 0.82\ \mu$K. Thus, in this case, the BBN restricts the possible manipulation upon the CMB quadrupole temperature fluctuation via the anisotropic expansion to insignificant values (viz., $\Delta T_\sigma \lesssim 1\mu$K). On the other hand, in our model, the limit $\Omega_{s0} \lesssim 10^{-23}$ required by the BBN does not necessarily lead to $\Delta T_\sigma \lesssim 1\mu$K. Provided that the gravitational coupling of the CDM is augmented by the EMSG with the dimensionless coupling strength $\alpha_c' \sim -10^{-20}$, this limit can still be satisfied when $\Omega_{\sigma 0} \sim 10^{-21}$ (or $\Omega_\sigma^{rec} \sim 10^{-11}$) which leads to an amount of manipulation upon the CMB quadrupole temperature fluctuation on the same order of magnitude with its observed value. Moreover, under the screening condition (4.31), in addition to this opportunity of manipulating the CMB quadrupole temperature fluctuation at desired values, we reproduce exactly the same expansion history with that of the standard ΛCDM cosmology all the way to BBN era. Thus, our model provides us with possibility to fine tune the CMB quadrupole temperature fluctuation (e.g., for addressing the so-called "quadrupole temperature problem") without leading to any other detectable alteration in the standard ΛCDM model.

4.3.2. Early and Late Dynamics

By eliminating the terms scaling as s^{-6} in (4.30) via the screening condition $\Omega_{s0} = 0$ given in (4.31), we have reached exactly the same mathematical expression with the Friedmann equation in the standard ΛCDM model, where however physically, cosmic expansion is anisotropic and $H(z)$ represents the average expansion rate. This

relies on the cooperation between the anisotropic expansion and the CDM coupled to gravity in accordance with the EMSG of the form $f(\mathbf{T^2}) \propto \mathbf{T^2}$, and hence will be valid all the way to the CDM generation redshift, $z_{\rm c}$, which is typically considered to be much larger than the BBN redshift ($z_{\rm BBN} \sim z_{\rm fr}$). Therefore, even if it is ensured that the average expansion rate of the Universe during BBN equals the one in the standard BBN (in spite of that $\Omega_{\sigma 0} = 4 \times 10^{-21}$, which leads to $\Delta T_\sigma \approx 20.5\ \mu$K manipulation in the CMB quadrupole temperature fluctuation), for the times $z > z_{\rm c}$ (i.e., when CDM did not exist yet) the Universe is described by the general relativistic LRS Bianchi I cosmological model [143,144] in the presence of radiation, which approximates the LRS Kasner vacuum solution with the increasing redshift. The LRS Kasner metric [196] is an exact solution of GR in vacuum and represented by the line element

$$\mathrm{d}s^2 = -\mathrm{d}t^2 + t^{2p_1}\,\mathrm{d}x^2 + t^{2p_2}\,(\mathrm{d}y^2 + \mathrm{d}z^2) \tag{4.49}$$

where p_1 and p_2 are constants that satisfy the conditions $p_1 + 2p_2 = p_1^2 + 2p_2^2 = 1$ giving rise to two different solutions $\{p_1 = 1, p_2 = 0\}$ and $\{p_1 = -1/3, p_2 = 2/3\}$. On the other hand, the opportunity of letting safely to $\Delta T_\sigma \approx 20.5\ \mu$K manipulation is in fact not subject to the screening condition $\Omega_{\rm s0} = 0$ evading BBN limits, but to the condition of $\left|\Omega_{\rm s0}\right| \lesssim 10^{-23}$ (corresponding to $\left|\Delta N_\nu\right| \lesssim 0.30$ in line with the limits given in the most recent Planck release [6]). Consideration of this slightly relaxed condition brings along several other possibilities for the dynamics of the early Universe for $z > z_{\rm BBN}$:

(i) In the case of $0 < \Omega_{\rm s0} \lesssim 10^{-23}$, as z increases, domination of the stiff fluid-like term over radiation can develop at a redshift either smaller or larger than $z_{\rm c}$. And, for $z > z_{\rm c}$, the Universe is described by the general relativistic LRS Bianchi I cosmological model in the presence of radiation.

(ii) In the case of $-10^{-23} \lesssim \Omega_{\rm s0} < 0$, the stiff fluid-like term, which yields negative energy density due to $\alpha_{\rm c}'\Omega_{\rm c0} < -\Omega_{\sigma 0} < 0$ in this case, gives rise to the following three different scenarios:

- As z increases, the stiff fluid-like term slows down the increment of $H(z)$ in redshift, but $z = z_{\rm c}$ is reached before it starts to decrease $H(z)$ itself. And,

for $z > z_c$, the Universe is described by the general relativistic LRS Bianchi I cosmological model in the presence of radiation.

- As z increases, the stiff fluid-like term slows down the increment of $H(z)$ in redshift and then it starts to decrease $H(z)$ itself, but $z = z_c$ is reached before $H(z)$ vanishes. And, for $z > z_c$, the Universe is described by the general relativistic LRS Bianchi I cosmological model in the presence of radiation so that $H(z)$ starts to increase with redshift once again.
- As z increases, the stiff fluid-like term slows down the increment of $H(z)$ in redshift and it eventually decreases $H(z)$ until it vanishes completely before $z = z_c$ is reached. This is the most interesting one among the possible scenarios, as it implies that the CDM was never generated but was always there, and that the Universe started to expand from a nonzero volume.

As the Universe continues to expand in the future (when $-1 \leq z < 0$), both the deviation from GR (i.e., the quadratic contribution of the CDM energy density due to the EMSG) and the expansion anisotropy (i.e., the shear scalar) keep on diluting faster than all the other terms that constitute the standard ΛCDM part in (4.30). In other words, the EMSG approaches the GR and the Universe isotropizes so that our model will asymptotically approach the usual standard ΛCDM model and the de Sitter solution in the arbitrarily far future.

In this section, we have contented ourselves with solely commenting on the very early ($z > z_{\rm BBN}$) and future ($z < 0$) dynamics of the Universe, rather than presenting a comprehensive analysis. Yet, one may find it quite enlightening to see Reference [197] which examines the cosmological model which includes stiff fluid source on top of the standard ΛCDM model, regarding particularly the evolution of the average expansion scale factor in our model, and Reference [146] which presents an investigation of anisotropic cosmologies in the presence of stiff fluid with a positive energy density (reminiscent of our model for $\alpha_c > 0$).

4.4. Generic Anisotropic Spacetimes

The simplest anisotropic extension of the standard ΛCDM model that is replacing the spatially flat RW metric with the Bianchi I leads to a generalized Friedmann equation containing the average Hubble parameter $H(z)$ along with a shear scalar of the form $\sigma^2 = \sigma_0^2(1+z)^6$ which mimics stiff fluid with a positive energy density [179]. Our model given in (4.28) then just adds into it another stiff fluid-like term, $\alpha_{\rm c}\rho_{\rm c}^2 = \alpha'_{\rm c}\rho_{\rm c0}(1+z)^6$, the quadratic contribution of the CDM energy density scaled by the dimensionless constant $\alpha'_{\rm c}$, which is not necessarily positive while representing the gravitational coupling strength of CDM in accordance with the EMSG of the form $f(\mathbf{T^2}) \propto \mathbf{T^2}$. However, the Bianchi I metric described by the line element [142–144]

$$\mathrm{d}s^2 = -\mathrm{d}t^2 + a^2(t)\,\mathrm{d}x^2 + b^2(t)\,\mathrm{d}y^2 + c^2(t)\,\mathrm{d}z^2 \tag{4.50}$$

with $\{a(t), b(t), c(t)\}$ being the directional scale factors, is atypical in that it brings in no restoring forcelike term in the shear propagation equation (see (4.27) in which we considered LRS case, $b = c$, without loss of generality) whereas, in more complicated anisotropic metrics, one set of such terms arise from anisotropic spatial curvature of the metric itself [143,144,147]. This means that the stiff fluid-like behavior of the shear scalar is not generic, even for the general relativistic cosmologies allowing anisotropic expansion in the presence of usual cosmological fluids (isotropic perfect fluids with no peculiar velocities) only. For instance, the Bianchi VII_0 metric [143, 144], the most general spatially homogeneous and flat anisotropic metric, with the line element [142]

$$\mathrm{d}s^2 = -\mathrm{d}t^2 + a^2(t)\,\mathrm{d}x^2 + b^2(t)\left(\cos x\,\mathrm{d}y - \sin x\,\mathrm{d}z\right)^2 + c^2(t)\left(\sin x\,\mathrm{d}y + \cos x\,\mathrm{d}z\right)^2 \tag{4.51}$$

yields an anisotropic spatial curvature that resembles a traceless anisotropic fluid [147] in addition to the simple expansion-rate anisotropies present in the Bianchi I. In the general relativistic universes close to isotropy, this causes the shear scalar to scale as $\sigma^2 \propto (1+z)^5$ during the dust era and as $\sigma^2 \propto \ln(z/z_{\rm fr})^{-2}(1+z)^4$ during the radiation era, hence causing the limit on its present-day density parameter from BBN to be weaker

than that from CMB in contrast to the situation in the Bianchi I, and both of the limits to be weaker than the ones derived through the Bianchi I metric consideration [147,194]. It is conceivable that, if we switch to the Bianchi VII_0 metric in EMSG as well, it will result in the same shear scalar dynamics in our model. This aspect of our model arises from the fact that the EMSG does not induce nonzero anisotropic stresses [93] contrarily to the modified gravity theories (e.g., the scalar-tensor theories of gravity [77,176–178]) in general and therefore gives rise to the same shear propagation equations with the usual ones derived in GR. Consequently, as the shear scalar in Bianchi VII_0 case will grow slower than the stiff fluid-like contribution of CDM, it is no longer possible to achieve the mutual cancellation of these two terms perpetually and write the Equation (4.32). Thus, if we reconsider our model by switching to the Bianchi VII_0 metric, we expect the strongest limits upon the shear scalar to come from CMB, and the ones on the stiff fluid-like contribution of CDM to come from BBN. In other words, in this case, since we can write the stiff fluid-like term as $\Omega_{\mathrm{s}0} = \alpha_{\mathrm{c}}' \, \Omega_{\mathrm{c}0}$, it will be necessary to satisfy $|\alpha_{\mathrm{c}}' \, \Omega_{\mathrm{c}0}| \lesssim 10^{-23}$, which implies $|\alpha_{\mathrm{c}}'| \lesssim 10^{-22}$ for $\Omega_{\mathrm{c}0} \sim 0.25$, corresponding to $\left|\Delta N_\nu\right| \lesssim 0.30$ in line with the limits given in the most recent Planck release [6].

The discussion above also shows that, to create a measurable change in the CMB quadrupole temperature fluctuation without spoiling the successes of the standard BBN, it is no longer needed in the Bianchi VII_0 case to apply the mechanism of screening the shear scalar by the stiff fluid-like contribution of CDM. Indeed, it is well known that the strong limits upon the shear scalar/anisotropic expansion are usually model-dependent and can be vastly weakened by promoting its simplest stiff fluid-like evolution to a more complex one by means of a nontrivial anisotropic spatial curvature existing in more generic anisotropic metrics such as the Bianchi VII_0 [147] and/or an anisotropic fluid either as an actual source or an effective source arising from a modified theory of gravity. We note that our work distinguishes from such works as it investigates a possibility of an alternative mechanism weakening the limits upon shear scalar through screening its contribution to $H(z)$ instead of modifying its dynamics. In other words, by counterbalancing the shear scalar term $\Omega_{\sigma 0}(1+z)^6$ via the new term $\alpha_{\mathrm{c}}' \, \Omega_{\mathrm{c}0}(1+z)^6$ arising from the gravitational coupling of CDM in accordance with

the EMSG of the form $f(\mathbf{T^2}) \propto \mathbf{T^2}$, we have evaded the limits upon the anisotropic expansion coming from the enhancing influence of the shear scalar on $H(z)$ (e.g., the limits from BBN), but kept on using the ones coming directly from the anisotropy in the expansion itself (e.g., the limits from the CMB quadrupole temperature fluctuations). If it turns out that there is one additional neutrino species beyond the three estimated by the Standard Model of particle physics (as, e.g., suggested for alleviating the tension in the H_0 value [198]), this feature of our model would be more significant because one extra species amounts to $\Omega_\sigma \sim 0.16$ during BBN and so leaves less room for the anisotropic expansion (see Section 4.3.1) whereas in our model, there can still be anisotropic expansion large enough to have a measurable effect in the CMB radiation, since we can still evade the BBN limits by compensating the contributions both from the shear scalar and additional neutrino species.

4.5. Summary and Discussion

In this chapter, as a second study, we have considered the previously introduced EMSG model described by the simplest linear contribution of the new scalar $\mathbf{T^2} = T_{\mu\nu}T^{\mu\nu}$ in the context of anisotropic cosmology. In the current study, we have focused on the aspect of the model that the matter field coupled to the gravity in accordance with the EMSG of the form $f(\mathbf{T^2}) \propto \mathbf{T^2}$ [91, 93] can compensate for the enhancing influence of anisotropy on the average expansion rate of the Universe. Yet, through this model, we have learned also lessons on some other aspects of the cosmological models that employ EMSG. It would be useful to briefly mention the some that may give insight into the possible prospective works. In the literature to date, the EMSG of this form, as well as its power-law generalization $f(\mathbf{T^2}) \propto (\mathbf{T^2})^n$ with $n > \frac{1}{2}$ (called as EMPG), has been mostly studied in the context of the early Universe dynamics and used, particularly, to replace the initial big bang singularity with a nonsingular beginning/bounce [91–94,103,105,107]. For, the new contributions of the matter field to the Friedmann equation in these studies scale faster than the usual linear contributions; therefore, the earlier times the more effective these new contributions are. However, we notice that all these studies consider spatially homogeneous and isotropic RW metric

and then the inclusion of anisotropy can prevent such scenarios from happening. In other words, it is possible that, as we move backward in time, the shear scalar grows fast enough to dominate over the new contributions of the matter field before these could give rise to a nonsingular beginning/bounce and then the very early Universe will be best described by the usual anisotropic spacetime vacuum solutions of GR (e.g., the Kasner vacuum solution). In a realistic description of the Universe one can suppose the observable Universe is almost-exactly isotropic but not exactly isotropic. Therefore, it is important to pick, among these scenarios developed under the RW metric assumption, the ones that can survive when anisotropy is included. One another lesson is that, the EMSG models that add, into the Friedmann equation, the new contributions of the matter fields scaling faster than the usual linear contributions do have consequences on not only the early Universe but also the late Universe. The particular model we have studied in this chapter presents a good example of this, as it evades the BBN limits on the present-day expansion anisotropy of the Universe and provides us with the opportunity to address the quadrupole temperature problem. And a closer look reveals that, beyond the limited framework we have drawn in the current study, it may have consequences on a major problem relevant to the present-day Universe, the so-called H_0 problem. The stiff fluid-like term for $\alpha_{\rm c} > 0$ in our model can be regarded as an increment in the total number of effectively massless degrees of freedom (see Equation (4.47)), which has been considered as one of the possible solutions for the H_0 problem [3]. Finally, the study we have carried out in this chapter can be extended to more complicated constructions by considering more generic anisotropic metrics and/or functions of $f(\mathbf{T^2})$, albeit, most likely, one will need to compromise both the energy-momentum conservation law and simplicity we have had in this particular setup here.

5. CONCLUSION

In this thesis, we have investigated two specific forms of a new-type of modified gravity called Energy-Momentum Squared Gravity (EMSG) in the context of cosmology. In contrast to General Relativity (GR), the EMSG gives rise to nonminimal coupling of the spacetime to the source through some arbitrary function of a new scalar $\mathbf{T^2} = T_{\mu\nu}T^{\mu\nu}$ constructed from the self-contraction of the EMT. The EMSG theory is described by the addition of the term $f(\mathbf{T^2})$, envisaged as correction, to the standard EH action with bare cosmological constant Λ. EMSG is the modification of GR in the presence of material sources only.

As a first study in the framework of EMSG, we have introduced a new model characterized by the functional choice of $f(\mathbf{T^2}) = \alpha \ln(\lambda \mathbf{T^2})$, and accordingly, named this model as Energy-Momentum Log Gravity (EMLG). The choice of this modification is distinguished from other EMSG models in the literature owing to that it both generates new terms on the right-hand side of the Einstein field equations (EFE) which are reminiscent of a fluid with constant effective inertial mass density and, more importantly provides us with the opportunity to obtain an explicit exact solution for the pressureless matter energy density in terms of redshift. The model has been studied on both theoretical and observational grounds in point of its cosmological applications, mainly as an extension of the standard ΛCDM model within the context of Robertson-Walker (RW) spacetime. The new terms arising from both the nonconservation of the energy density of pressureless matter and EMLG modification to the field equations of GR constitute an effective dynamical dark energy whose equation of state displays a pole at large redshifts. This feature of our EMLG model, in accordance with suggestions for alleviating some tensions between observational data sets within the standard ΛCDM model, induces a mechanism for screening (compensating) the cosmological constant Λ in the past. We have presented the theoretical investigation of the single-fluid (pressureless matter) cosmological model in detail, and furthermore compared the model with the standard ΛCDM model via observational analysis. We

have constrained the free parameter α', a normalization of α employing the latest observational data (a compressed version of a recent reanalysis of Type Ia SN data, and high-precision BAO measurements at different redshifts with $z < 2.36$, and a collection of currently available $H(z)$ measurements from Cosmic Chronometers (CC)). The data do not exclude the ΛCDM limit of the EMLG model ($\alpha' = 0$), but prefers slightly negative values of the model parameter ($\alpha' = -0.032 \pm 0.043$), which provides the screening of Λ. We have also discussed how EMLG relaxes the persistent tension that exists in the measurements of H_0 within the standard ΛCDM model.

In the second study, as a generalization of the standard ΛCDM model, we have constructed a cosmological model wherein we allowed only cold dark matter (CDM) to couple to the gravity via EMSG of the form $f(\mathbf{T^2}) = \alpha\mathbf{T^2}$ while all other standard fluids coupled in accordance with GR, and concurrently replaced the spatially maximally symmetric and flat RW metric with its simplest anisotropic generalization, locally rotationally symmetric (LRS) Bianchi I metric. These two modifications add two new stiff fluid-like terms of different nature into the Friedmann equation which can mutually cancel out each other. In other words, new quadratic contribution of CDM is able to compensate (screen) the shear scalar completely. This screening mechanism provides us with the opportunity of recovering mathematically exactly the same Friedmann equation of the standard ΛCDM model. This feature of the model leads to evading the BBN limits on the present-day expansion anisotropy, and accordingly allows us to be able to manipulate the cosmic microwave background (CMB) quadrupole temperature fluctuation at the desired amount. We also have briefly discussed the consequences of the model on the very early times and far future of the Universe under the slightly relaxed screening condition. We have further indicated possible effects of more generic/complicated anisotropic metrics on our cosmological model due to the alteration of shear scalar dynamics. Contrary to the studies to date, this study presents an example of that the EMSG of the form $f(\mathbf{T^2}) \propto \mathbf{T^2}$, as well as similar type other models, is not necessarily relevant only to early Universe but may even be considered in the context of a major problem of the current cosmology related to the present-day Universe, the so-called H_0 problem.

REFERENCES

1. Dodelson, S. and F. Schmidt, *Modern Cosmology*, Elsevier Science, 2020.

2. Hubble, E., "A relation between distance and radial velocity among extra-galactic nebulae", *Proceedings of the National Academy of Sciences*, Vol. 15, pp. 168–173, 1929.

3. Di Valentino, E. *et al.*, "Cosmology Intertwined II: The Hubble Constant Tension", *arXiv:2008.11284*, 2020.

4. Fixsen, D., "The Temperature of the Cosmic Microwave Background", *The Astrophysical Journal*, Vol. 707, pp. 916–920, 2009.

5. Smoot, G. F. *et al.*, "Structure in the COBE differential microwave radiometer first year maps", *The Astrophysical Journal Letters*, Vol. 396, pp. L1–L5, 1992.

6. Aghanim, N. *et al.*, "Planck 2018 results. VI. Cosmological parameters", *Astronomy & Astrophysics*, Vol. 641, p. A6, 2020.

7. Perlmutter, S. *et al.*, "Measurements of Ω and Λ from 42 high redshift supernovae", *The Astrophysical Journal*, Vol. 517, pp. 565–586, 1999.

8. Riess, A. G. *et al.*, "Observational evidence from supernovae for an accelerating universe and a cosmological constant", *The Astronomical Journal*, Vol. 116, pp. 1009–1038, 1998.

9. Starobinsky, A. A., "A New Type of Isotropic Cosmological Models Without Singularity", *Advanced Series in Astrophysics and Cosmology*, Vol. 3, pp. 130–133, 1987.

10. Guth, A. H., "The Inflationary Universe: A Possible Solution to the Horizon and

Flatness Problems", *Advanced Series in Astrophysics and Cosmology*, Vol. 3, pp. 139–148, 1987.

11. Linde, A. D., "A New Inflationary Universe Scenario: A Possible Solution of the Horizon, Flatness, Homogeneity, Isotropy and Primordial Monopole Problems", *Advanced Series in Astrophysics and Cosmology*, Vol. 3, pp. 149–153, 1987.

12. Albrecht, A. and P. J. Steinhardt, "Cosmology for Grand Unified Theories with Radiatively Induced Symmetry Breaking", *Advanced Series in Astrophysics and Cosmology*, Vol. 3, pp. 158–161, 1987.

13. Alam, S. *et al.*, "The clustering of galaxies in the completed SDSS-III Baryon Oscillation Spectroscopic Survey: cosmological analysis of the DR12 galaxy sample", *Monthly Notices of the Royal Astronomical Society*, Vol. 470, No. 3, pp. 2617–2652, 2017.

14. Abbott, T. *et al.*, "Dark Energy Survey year 1 results: Cosmological constraints from galaxy clustering and weak lensing", *Physical Review D*, Vol. 98, No. 4, p. 043526, 2018.

15. Komatsu, E. *et al.*, "Seven-Year Wilkinson Microwave Anisotropy Probe (WMAP) Observations: Cosmological Interpretation", *Astrophysical Journal Supplements*, Vol. 192, p. 18, 2011.

16. Ade, P. *et al.*, "Planck 2015 results. XIII. Cosmological parameters", *Astronomy & Astrophysics*, Vol. 594, p. A13, 2016.

17. Weinberg, S., "The Cosmological Constant Problem", *Reviews of Modern Physics*, Vol. 61, pp. 1–23, 1989.

18. Peebles, P. and B. Ratra, "The Cosmological Constant and Dark Energy", *Reviews of Modern Physics*, Vol. 75, pp. 559–606, 2003.

19. Padmanabhan, T., "Cosmological constant: The Weight of the vacuum", *Physics Reports*, Vol. 380, pp. 235–320, 2003.

20. Sahni, V. and A. A. Starobinsky, "The Case for a positive cosmological Lambda term", *International Journal of Modern Physics D*, Vol. 9, pp. 373–444, 2000.

21. Sahni, V., "Dark matter and dark energy", *Lecture Notes in Physics*, Vol. 653, pp. 141–180, 2004.

22. Obied, G., H. Ooguri, L. Spodyneiko and C. Vafa, "De Sitter Space and the Swampland", *arXiv:1806.08362*, 2018.

23. Agrawal, P., G. Obied, P. J. Steinhardt and C. Vafa, "On the Cosmological Implications of the String Swampland", *Physics Letters B*, Vol. 784, pp. 271–276, 2018.

24. Ó Colgáin, E., M. H. van Putten and H. Yavartanoo, "de Sitter Swampland, H_0 tension & observation", *Physics Letters B*, Vol. 793, pp. 126–129, 2019.

25. Heisenberg, L., M. Bartelmann, R. Brandenberger and A. Refregier, "Dark Energy in the Swampland", *Physical Review D*, Vol. 98, No. 12, p. 123502, 2018.

26. Akrami, Y., R. Kallosh, A. Linde and V. Vardanyan, "The Landscape, the Swampland and the Era of Precision Cosmology", *Fortschritte der Physik*, Vol. 67, No. 1-2, p. 1800075, 2019.

27. Raveri, M., W. Hu and S. Sethi, "Swampland Conjectures and Late-Time Cosmology", *Physical Review D*, Vol. 99, No. 8, p. 083518, 2019.

28. Cicoli, M., S. De Alwis, A. Maharana, F. Muia and F. Quevedo, "De Sitter vs Quintessence in String Theory", *Fortschritte der Physik*, Vol. 67, No. 1-2, p. 1800079, 2019.

29. Colgáin, E. O. and H. Yavartanoo, "Testing the Swampland: H_0 tension", *Physics Letters B*, Vol. 797, p. 134907, 2019.

30. Alberto Vazquez, J., M. Bridges, M. Hobson and A. Lasenby, "Reconstruction of the Dark Energy equation of state", *Journal of Cosmology and Astroparticle Physics*, Vol. 09, p. 020, 2012.

31. Bhattacharyya, A., U. Alam, K. L. Pandey, S. Das and S. Pal, "Are H_0 and σ_8 tensions generic to present cosmological data?", *The Astrophysical Journal*, Vol. 876, No. 2, p. 143, 2019.

32. Raveri, M. and W. Hu, "Concordance and Discordance in Cosmology", *Physical Review D*, Vol. 99, No. 4, p. 043506, 2019.

33. Tamayo, D. and J. A. Vazquez, "Fourier-series expansion of the dark-energy equation of state", *Monthly Notices of the Royal Astronomical Society*, Vol. 487, No. 1, pp. 729–736, 2019.

34. Hee, S., J. Vázquez, W. Handley, M. Hobson and A. Lasenby, "Constraining the dark energy equation of state using Bayes theorem and the Kullback–Leibler divergence", *Monthly Notices of the Royal Astronomical Society*, Vol. 466, No. 1, pp. 369–377, 2017.

35. Di Valentino, E., "Crack in the cosmological paradigm", *Nature Astronomy*, Vol. 1, No. 9, pp. 569–570, 2017.

36. Aubourg, E. *et al.*, "Cosmological implications of baryon acoustic oscillation measurements", *Physical Review D*, Vol. 92, No. 12, p. 123516, 2015.

37. Zhao, G.-B. *et al.*, "Dynamical dark energy in light of the latest observations", *Nature Astronomy*, Vol. 1, No. 9, pp. 627–632, 2017.

38. Bullock, J. S. and M. Boylan-Kolchin, "Small-Scale Challenges to the ΛCDM

Paradigm", *Annual Review of Astronomy and Astrophysics*, Vol. 55, pp. 343–387, 2017.

39. Freedman, W. L., "Cosmology at a Crossroads", *Nature Astronomy*, Vol. 1, p. 0121, 2017.

40. Verde, L., T. Treu and A. Riess, "Tensions between the Early and the Late Universe", *Nature Astronomy*, Vol. 3, p. 891, 7 2019.

41. Riess, A. G., S. Casertano, W. Yuan, L. M. Macri and D. Scolnic, "Large Magellanic Cloud Cepheid Standards Provide a 1% Foundation for the Determination of the Hubble Constant and Stronger Evidence for Physics beyond ΛCDM", *The Astrophysical Journal*, Vol. 876, No. 1, p. 85, 2019.

42. Freedman, W. L. *et al.*, "The Carnegie-Chicago Hubble Program. VIII. An Independent Determination of the Hubble Constant Based on the Tip of the Red Giant Branch", *The Astrophysical Journal*, Vol. 882, No. 1, p. 34, 2019.

43. Mörtsell, E. and S. Dhawan, "Does the Hubble constant tension call for new physics?", *Journal of Cosmology and Astroparticle Physics*, Vol. 09, p. 025, 2018.

44. Dutta, K., Ruchika, A. Roy, A. A. Sen and M. Sheikh-Jabbari, "Beyond ΛCDM with low and high redshift data: implications for dark energy", *General Relativity and Gravitation*, Vol. 52, No. 2, p. 15, 2020.

45. Vagnozzi, S., "New physics in light of the H_0 tension: An alternative view", *Physical Review D*, Vol. 102, No. 2, p. 023518, 2020.

46. Handley, W., "Curvature tension: evidence for a closed universe", *Physical Review D*, Vol. 103, No. 4, p. L041301, 2021.

47. Di Valentino, E., A. Melchiorri and J. Silk, "Planck evidence for a closed Universe and a possible crisis for cosmology", *Nature Astronomy*, Vol. 4, No. 2, pp. 196–

203, 2019.

48. Akarsu, O., J. D. Barrow, L. A. Escamilla and J. A. Vazquez, "Graduated dark energy: Observational hints of a spontaneous sign switch in the cosmological constant", *Physical Review D*, Vol. 101, No. 6, p. 063528, 2020.

49. Di Valentino, E., A. Melchiorri and J. Silk, "Investigating Cosmic Discordance", *Astrophysical Journal Letters*, Vol. 908, No. 1, p. L9, 2021.

50. Riess, A. G. *et al.*, "A 2.4% Determination of the Local Value of the Hubble Constant", *The Astrophysical Journal*, Vol. 826, No. 1, p. 56, 2016.

51. Delubac, T. *et al.*, "Baryon acoustic oscillations in the Lyα forest of BOSS DR11 quasars", *Astronomy & Astrophysics*, Vol. 574, p. A59, 2015.

52. Sahni, V., A. Shafieloo and A. A. Starobinsky, "Model independent evidence for dark energy evolution from Baryon Acoustic Oscillations", *The Astrophysical Journal Letters*, Vol. 793, No. 2, p. L40, 2014.

53. Barrow, J. D., "Graduated Inflationary Universes", *Physics Letters B*, Vol. 235, pp. 40–43, 1990.

54. Nojiri, S. and S. D. Odintsov, "Inhomogeneous equation of state of the universe: Phantom era, future singularity and crossing the phantom barrier", *Physical Review D*, Vol. 72, p. 023003, 2005.

55. Barrow, J. D., "String-Driven Inflationary and Deflationary Cosmological Models", *Nuclear Physics B*, Vol. 310, pp. 743–763, 1988.

56. Ratra, B. and P. J. E. Peebles, "Cosmological Consequences of a Rolling Homogeneous Scalar Field", *Physical Review D*, Vol. 37, p. 3406, 1988.

57. Caldwell, R. R., R. Dave and P. J. Steinhardt, "Cosmological imprint of an energy

component with general equation of state", *Physical Review Letters*, Vol. 80, pp. 1582–1585, 1998.

58. Copeland, E. J., M. Sami and S. Tsujikawa, "Dynamics of dark energy", *International Journal of Modern Physics D*, Vol. 15, pp. 1753–1936, 2006.

59. Caldwell, R. R. and M. Kamionkowski, "The Physics of Cosmic Acceleration", *Annual Review of Nuclear and Particle Science*, Vol. 59, pp. 397–429, 2009.

60. Clifton, T., P. G. Ferreira, A. Padilla and C. Skordis, "Modified Gravity and Cosmology", *Physics Reports*, Vol. 513, pp. 1–189, 2012.

61. De Felice, A. and S. Tsujikawa, "f(R) theories", *Living Reviews in Relativity*, Vol. 13, p. 3, 2010.

62. Capozziello, S. and M. De Laurentis, "Extended Theories of Gravity", *Physics Reports*, Vol. 509, pp. 167–321, 2011.

63. Nojiri, S., S. Odintsov and V. Oikonomou, "Modified Gravity Theories on a Nutshell: Inflation, Bounce and Late-time Evolution", *Physics Reports*, Vol. 692, pp. 1–104, 2017.

64. Nojiri, S. and S. D. Odintsov, "Unified cosmic history in modified gravity: from F(R) theory to Lorentz non-invariant models", *Physics Reports*, Vol. 505, pp. 59–144, 2011.

65. Poplawski, N. J., "A Lagrangian description of interacting dark energy", *arXiv:gr-qc/0608031*, 2006.

66. Harko, T., F. S. Lobo, S. Nojiri and S. D. Odintsov, "$f(R,T)$ gravity", *Physical Review D*, Vol. 84, p. 024020, 2011.

67. Moraes, P. and J. Santos, "A complete cosmological scenario from $f(R,T^{\phi})$ grav-

ity theory", *The European Physical Journal C*, Vol. 76, p. 60, 2016.

68. Harko, T. and F. S. Lobo, "$f(R, L_m)$ gravity", *The European Physical Journal C*, Vol. 70, pp. 373–379, 2010.

69. Odintsov, S. D. and D. Sáez-Gómez, "$f(R, T, R_{\mu\nu}T^{\mu\nu})$ gravity phenomenology and ΛCDM universe", *Physics Letters B*, Vol. 725, pp. 437–444, 2013.

70. Haghani, Z., T. Harko, F. S. N. Lobo, H. R. Sepangi and S. Shahidi, "Further matters in space-time geometry: $f(R, T, R_{\mu\nu}T^{\mu\nu})$ gravity", *Physical Review D*, Vol. 88, No. 4, p. 044023, 2013.

71. Haghani, Z., T. Harko, H. R. Sepangi and S. Shahidi, "Matter may matter", *International Journal of Modern Physics D*, Vol. 23, No. 12, p. 1442016, 2014.

72. Harko, T., F. S. N. Lobo, G. Otalora and E. N. Saridakis, "$f(T, \mathcal{T})$ gravity and cosmology", *Journal of Cosmology and Astroparticle Physics*, Vol. 12, p. 021, 2014.

73. Brans, C. and R. Dicke, "Mach's principle and a relativistic theory of gravitation", *Physical Review*, Vol. 124, pp. 925–935, 1961.

74. Faraoni, V., E. Gunzig and P. Nardone, "Conformal transformations in classical gravitational theories and in cosmology", *Fundamentals of Cosmic Physics*, Vol. 20, p. 121, 1999.

75. Boisseau, B., G. Esposito-Farese, D. Polarski and A. A. Starobinsky, "Reconstruction of a scalar tensor theory of gravity in an accelerating universe", *Physical Review Letters*, Vol. 85, p. 2236, 2000.

76. Sahni, V. and A. Starobinsky, "Reconstructing Dark Energy", *International Journal of Modern Physics D*, Vol. 15, pp. 2105–2132, 2006.

77. Akarsu, O., N. Katırcı, N. Özdemir and J. A. Vázquez, "Anisotropic massive Brans-Dicke gravity extension of the standard ΛCDM model", *The European Physical Journal C*, Vol. 80, No. 1, p. 32, 2020.

78. Zhou, S.-Y., E. J. Copeland and P. M. Saffin, "Cosmological Constraints on $f(G)$ Dark Energy Models", *Journal of Cosmology and Astroparticle Physics*, Vol. 07, p. 009, 2009.

79. Dolgov, A., "Field model with a dynamic cancellation of the cosmological constant", *Journal of Experimental and Theoretical Physics Letters*, Vol. 41, pp. 345–347, 1985.

80. Bauer, F., J. Sola and H. Stefancic, "Dynamically avoiding fine-tuning the cosmological constant: The 'Relaxed Universe'", *Journal of Cosmology and Astroparticle Physics*, Vol. 12, p. 029, 2010.

81. Ashtekar, A., T. Pawlowski and P. Singh, "Quantum Nature of the Big Bang: Improved dynamics", *Physical Review D*, Vol. 74, p. 084003, 2006.

82. Ashtekar, A. and P. Singh, "Loop Quantum Cosmology: A Status Report", *Classical and Quantum Gravity*, Vol. 28, p. 213001, 2011.

83. Sahni, V. and Y. Shtanov, "Brane world models of dark energy", *Journal of Cosmology and Astroparticle Physics*, Vol. 11, p. 014, 2003.

84. Brax, P. and C. van de Bruck, "Cosmology and brane worlds: A Review", *Classical and Quantum Gravity*, Vol. 20, pp. R201–R232, 2003.

85. Chodos, A. and S. L. Detweiler, "Where Has the Fifth-Dimension Gone?", *Physical Review D*, Vol. 21, p. 2167, 1980.

86. Dereli, T. and R. Tucker, "Dynamical Reduction of Internal Dimensions in the Early Universe", *Physics Letters B*, Vol. 125, pp. 133–135, 1983.

87. Akarsu, O. and T. Dereli, "The Dynamical Evolution of 3-Space in a Higher Dimensional Steady State Universe", *General Relativity and Gravitation*, Vol. 45, pp. 959–986, 2013.

88. Akarsu, O. and T. Dereli, "Late Time Acceleration of the 3-Space in a Higher Dimensional Steady State Universe in Dilaton Gravity", *Journal of Cosmology and Astroparticle Physics*, Vol. 02, p. 050, 2013.

89. Russo, J. and P. Townsend, "Late-time Cosmic Acceleration from Compactification", *Classical and Quantum Gravity*, Vol. 36, No. 9, p. 095008, 2019.

90. Katırcı, N. and M. Kavuk, "$f(R, T_{\mu\nu}T^{\mu\nu})$ gravity and Cardassian-like expansion as one of its consequences", *The European Physical Journal Plus*, Vol. 129, p. 163, 2014.

91. Roshan, M. and F. Shojai, "Energy-Momentum Squared Gravity", *Physical Review D*, Vol. 94, No. 4, p. 044002, 2016.

92. Akarsu, O., N. Katırcı and S. Kumar, "Cosmic acceleration in a dust only universe via energy-momentum powered gravity", *Physical Review D*, Vol. 97, No. 2, p. 024011, 2018.

93. Board, C. V. R. and J. D. Barrow, "Cosmological Models in Energy-Momentum-Squared Gravity", *Physical Review D*, Vol. 96, No. 12, p. 123517, 2017.

94. Akarsu, O., J. D. Barrow, S. Çıkıntoğlu, K. Y. Ekşi and N. Katırcı, "Constraint on energy-momentum squared gravity from neutron stars and its cosmological implications", *Physical Review D*, Vol. 97, No. 12, p. 124017, 2018.

95. Nari, N. and M. Roshan, "Compact stars in Energy-Momentum Squared Gravity", *Physical Review D*, Vol. 98, No. 2, p. 024031, 2018.

96. Akarsu, O., N. Katirci, S. Kumar, R. C. Nunes and M. Sami, "Cosmological im-

plications of scale-independent energy-momentum squared gravity: Pseudo non-minimal interactions in dark matter and relativistic relics", *Physical Review D*, Vol. 98, No. 6, p. 063522, 2018.

97. Lovelock, D., "The Einstein tensor and its generalizations", *Journal of Mathematical Physics*, Vol. 12, pp. 498–501, 1971.

98. Lovelock, D., "The four-dimensionality of space and the einstein tensor", *Journal of Mathematical Physics*, Vol. 13, pp. 874–876, 1972.

99. Bull, P. *et al.*, "Beyond ΛCDM: Problems, solutions, and the road ahead", *Physics of the Dark Universe*, Vol. 12, pp. 56–99, 2016.

100. Straumann, N., *General Relativity: With Applications to Astrophysics*, Theoretical and Mathematical Physics, Springer Berlin Heidelberg, 2004.

101. Faria, M., C. Martins, F. Chiti and B. Silva, "Low redshift constraints on energy-momentum-powered gravity models", *Astronomy & Astrophysics*, Vol. 625, p. A127, 2019.

102. Bhattacharjee, S. and P. K. Sahoo, "Temporally varying universal gravitational "constant" and speed of light in energy momentum squared gravity", *The European Physical Journal Plus*, Vol. 135, No. 1, p. 86, 2020.

103. Barbar, A. H., A. M. Awad and M. T. AlFiky, "Viability of bouncing cosmology in energy-momentum-squared gravity", *Physical Review D*, Vol. 101, No. 4, p. 044058, 2020.

104. Singh, K. N., A. Banerjee, S. K. Maurya, F. Rahaman and A. Pradhan, "Color-flavor locked quark stars in energy-momentum squared gravity", *Physics of the Dark Universe*, Vol. 31, p. 100774, 2021.

105. Nazari, E., F. Sarvi and M. Roshan, "Generalized Energy-Momentum-Squared

Gravity in the Palatini Formalism", *Physical Review D*, Vol. 102, No. 6, p. 064016, 2020.

106. Chen, C.-Y. and P. Chen, "Eikonal black hole ringings in generalized energy-momentum squared gravity", *Physical Review D*, Vol. 101, No. 6, p. 064021, 2020.

107. Bahamonde, S., M. Marciu and P. Rudra, "Dynamical system analysis of generalized energy-momentum-squared gravity", *Physical Review D*, Vol. 100, No. 8, p. 083511, 2019.

108. Rudra, P. and B. Pourhassan, "Thermodynamics in generalized energy-momentum squared gravity", *arXiv:2008.11034*, 2020.

109. Petit, J. P., "An Interpretation of Cosmological Model With Variable Light Velocity", *Modern Physics Letters A*, Vol. 3, pp. 1527–1532, 1988.

110. Moffat, J. W., "Superluminary universe: A Possible solution to the initial value problem in cosmology", *International Journal of Modern Physics D*, Vol. 2, pp. 351–366, 1993.

111. Barrow, J. D., "Cosmologies with varying light speed", *Physical Review D*, Vol. 59, p. 043515, 1999.

112. Albrecht, A. and J. Magueijo, "A Time varying speed of light as a solution to cosmological puzzles", *Physical Review D*, Vol. 59, p. 043516, 1999.

113. Magueijo, J., "Covariant and locally Lorentz invariant varying speed of light theories", *Physical Review D*, Vol. 62, p. 103521, 2000.

114. Kazemi, A., M. Roshan, I. De Martino and M. De Laurentis, "Jeans analysis in energy–momentum-squared gravity", *The European Physical Journal C*, Vol. 80, No. 2, p. 150, 2020.

115. Elizalde, E., N. Godani and G. C. Samanta, "Cosmological dynamics in R^2 gravity with logarithmic trace term", *Physics of the Dark Universe*, Vol. 30, p. 100618, 2020.

116. Akarsu, O., J. D. Barrow, C. V. R. Board, N. M. Uzun and J. A. Vazquez, "Screening Λ in a new modified gravity model", *The European Physical Journal C*, Vol. 79, No. 10, p. 846, 2019.

117. Uzan, J.-P., "Varying Constants, Gravitation and Cosmology", *Living Reviews in Relativity*, Vol. 14, p. 2, 2011.

118. Sandvik, H. B., J. D. Barrow and J. Magueijo, "A simple cosmology with a varying fine structure constant", *Physical Review Letters*, Vol. 88, p. 031302, 2002.

119. Magueijo, J., J. D. Barrow and H. B. Sandvik, "Is it e or is it c? Experimental tests of varying alpha", *Physics Letters B*, Vol. 549, pp. 284–289, 2002.

120. Barrow, J. D. and J. Magueijo, "Cosmological constraints on a dynamical electron mass", *Physical Review D*, Vol. 72, p. 043521, 2005.

121. Ayoub, R., "Paolo Ruffini's contributions to the quintic", *Archive for History of Exact Sciences*, Vol. 23, pp. 253–277, 1980.

122. Rosen, M., "Niels Hendrik Abel and Equations of the Fifth Degree", *American Mathematical Monthly*, Vol. 102, pp. 495–505, 1995.

123. Harrison, E. R., "Observational tests in cosmology", *Nature*, Vol. 260, pp. 591–592, 1976.

124. Sahni, V., T. D. Saini, A. A. Starobinsky and U. Alam, "Statefinder: A New geometrical diagnostic of dark energy", *Journal of Experimental and Theoretical Physics Letters*, Vol. 77, pp. 201–206, 2003.

125. Visser, M., "Jerk and the cosmological equation of state", *Classical and Quantum Gravity*, Vol. 21, pp. 2603–2616, 2004.

126. Dunajski, M. and G. Gibbons, "Cosmic Jerk, Snap and Beyond", *Classical and Quantum Gravity*, Vol. 25, p. 235012, 2008.

127. Sahni, V., A. Shafieloo and A. A. Starobinsky, "Two new diagnostics of dark energy", *Physical Review D*, Vol. 78, p. 103502, 2008.

128. Zunckel, C. and C. Clarkson, "Consistency Tests for the Cosmological Constant", *Physical Review Letters*, Vol. 101, p. 181301, 2008.

129. Efstathiou, G., "H_0 Revisited", *Monthly Notices of the Royal Astronomical Society*, Vol. 440, No. 2, pp. 1138–1152, 2014.

130. Reid, B. A. *et al.*, "The clustering of galaxies in the SDSS-III Baryon Oscillation Spectroscopic Survey: measurements of the growth of structure and expansion rate at z=0.57 from anisotropic clustering", *Monthly Notices of the Royal Astronomical Society*, Vol. 426, p. 2719, 2012.

131. Slosar, A. and J. Vazquez, *A simple MCMC code for cosmological parameter estimation where only expansion history matters*, 2014, `https://github.com/slosar/april`, accessed in May 2019.

132. Gómez-Valent, A. and L. Amendola, "H_0 from cosmic chronometers and Type Ia supernovae, with Gaussian Processes and the novel Weighted Polynomial Regression method", *Journal of Cosmology and Astroparticle Physics*, Vol. 04, p. 051, 2018.

133. Padilla, L. E., L. O. Tellez, L. A. Escamilla and J. A. Vazquez, "Cosmological parameter inference with Bayesian statistics", *arXiv:1903.11127*, 2019.

134. Akaike, H., "A new look at the statistical model identification", *IEEE Transac-*

tions on Automatic Control, Vol. 19, pp. 716–723, 1974.

135. Riess, A. G. *et al.*, "New Parallaxes of Galactic Cepheids from Spatially Scanning the Hubble Space Telescope: Implications for the Hubble Constant", *The Astrophysical Journal*, Vol. 855, No. 2, p. 136, 2018.

136. Riess, A. G. *et al.*, "Milky Way Cepheid Standards for Measuring Cosmic Distances and Application to Gaia DR2: Implications for the Hubble Constant", *The Astrophysical Journal*, Vol. 861, No. 2, p. 126, 2018.

137. Akarsu, O., J. D. Barrow and N. M. Uzun, "Screening anisotropy via energy-momentum squared gravity: ΛCDM model with hidden anisotropy", *Physical Review D*, Vol. 102, No. 12, p. 124059, 2020.

138. Di Valentino, E. *et al.*, "Cosmology Intertwined I: Perspectives for the Next Decade", *arXiv:2008.11283*, 2020.

139. Wald, R. M., "Asymptotic behavior of homogeneous cosmological models in the presence of a positive cosmological constant", *Physical Review D*, Vol. 28, pp. 2118–2120, 1983.

140. Starobinsky, A. A., "Isotropization of arbitrary cosmological expansion given an effective cosmological constant", *Journal of Experimental and Theoretical Physics Letters*, Vol. 37, pp. 66–69, 1983.

141. Collins, C. B. and S. W. Hawking, "The rotation and distortion of the Universe", *Monthly Notices of the Royal Astronomical Society*, Vol. 162, pp. 307–320, 1973.

142. Collins, C. and S. Hawking, "Why is the Universe isotropic?", *The Astrophysical Journal*, Vol. 180, pp. 317–334, 1973.

143. Ellis, G. F. and H. van Elst, "Cosmological models: Cargese lectures 1998", *NATO Science Series C*, Vol. 541, pp. 1–116, 1999.

144. Ellis, G. F. R., R. Maartens and M. A. H. MacCallum, *Relativistic Cosmology*, Cambridge University Press, 2012.

145. Zel'dovich, Y., "The equation of state at ultrahigh densities and its relativistic limitations", *Soviet Physics Journal of Experimental and Theoretical Physics*, Vol. 14, pp. 1143–1147, 1962.

146. Barrow, J., "Quiescent cosmology", *Nature*, Vol. 272, pp. 211–215, 1978.

147. Barrow, J. D., "Cosmological limits on slightly skew stresses", *Physical Review D*, Vol. 55, pp. 7451–7460, 1997.

148. Bennett, C. *et al.*, "Seven-Year Wilkinson Microwave Anisotropy Probe (WMAP) Observations: Are There Cosmic Microwave Background Anomalies?", *Astrophysical Journal Supplements*, Vol. 192, p. 17, 2011.

149. Ade, P. *et al.*, "Planck 2013 results. XV. CMB power spectra and likelihood", *Astronomy & Astrophysics*, Vol. 571, p. A15, 2014.

150. Schwarz, D. J., C. J. Copi, D. Huterer and G. D. Starkman, "CMB Anomalies after Planck", *Classical and Quantum Gravity*, Vol. 33, No. 18, p. 184001, 2016.

151. Akrami, Y. *et al.*, "Planck 2018 results. VII. Isotropy and Statistics of the CMB", *Astronomy & Astrophysics*, Vol. 641, p. A7, 2020.

152. Wilczynska, M. R. *et al.*, "Four direct measurements of the fine-structure constant 13 billion years ago", *Science Advances*, Vol. 6, No. 17, p. eaay9672, 2020.

153. Migkas, K., G. Schellenberger, T. Reiprich, F. Pacaud, M. Ramos-Ceja and L. Lovisari, "Probing cosmic isotropy with a new X-ray galaxy cluster sample through the $L_{\rm X} - T$ scaling relation", *Astronomy & Astrophysics*, Vol. 636, p. A15, 2020.

154. Koivisto, T. and D. F. Mota, "Dark energy anisotropic stress and large scale

structure formation", *Physical Review D*, Vol. 73, p. 083502, 2006.

155. Campanelli, L., P. Cea and L. Tedesco, "Ellipsoidal Universe Can Solve The CMB Quadrupole Problem", *Physical Review Letters*, Vol. 97, p. 131302, 2006.

156. Koivisto, T. and D. F. Mota, "Accelerating Cosmologies with an Anisotropic Equation of State", *The Astrophysical Journal*, Vol. 679, pp. 1–5, 2008.

157. Rodrigues, D. C., "Anisotropic Cosmological Constant and the CMB Quadrupole Anomaly", *Physical Review D*, Vol. 77, p. 023534, 2008.

158. Koivisto, T. and D. F. Mota, "Vector Field Models of Inflation and Dark Energy", *Journal of Cosmology and Astroparticle Physics*, Vol. 08, p. 021, 2008.

159. Campanelli, L., P. Cea and L. Tedesco, "Cosmic Microwave Background Quadrupole and Ellipsoidal Universe", *Physical Review D*, Vol. 76, p. 063007, 2007.

160. Campanelli, L., P. Cea, G. Fogli and L. Tedesco, "Anisotropic dark energy and ellipsoidal universe", *International Journal of Modern Physics D*, Vol. 20, pp. 1153–1166, 2011.

161. Campanelli, L., "A Model of Universe Anisotropization", *Physical Review D*, Vol. 80, p. 063006, 2009.

162. Cea, P., "Confronting the Ellipsoidal Universe to the Planck 2018 Data", *The European Physical Journal Plus*, Vol. 135, No. 2, p. 150, 2020.

163. Akarsu, O., N. Katirci, A. A. Sen and J. A. Vazquez, "Scalar field emulator via anisotropically deformed vacuum energy: Application to dark energy", *arXiv:2004.14863*, 2020.

164. Battye, R. A. and A. Moss, "Anisotropic perturbations due to dark energy",

Physical Review D, Vol. 74, p. 041301, 2006.

165. Koivisto, T. and D. F. Mota, "Anisotropic Dark Energy: Dynamics of Background and Perturbations", *Journal of Cosmology and Astroparticle Physics*, Vol. 06, p. 018, 2008.

166. Cooray, A. R., D. E. Holz and R. Caldwell, "Measuring dark energy spatial inhomogeneity with supernova data", *Journal of Cosmology and Astroparticle Physics*, Vol. 11, p. 015, 2010.

167. Akarsu, O., T. Dereli and N. Oflaz, "Accelerating anisotropic cosmologies in Brans–Dicke gravity coupled to a mass-varying vector field", *Classical and Quantum Gravity*, Vol. 31, p. 045020, 2014.

168. Koivisto, T. S. and F. R. Urban, "Disformal vectors and anisotropies on a warped brane\protect Hulluilla on Halvat Huvit", *Journal of Cosmology and Astroparticle Physics*, Vol. 03, p. 003, 2015.

169. Heisenberg, L., R. Kase and S. Tsujikawa, "Anisotropic cosmological solutions in massive vector theories", *Journal of Cosmology and Astroparticle Physics*, Vol. 11, p. 008, 2016.

170. Yang, W., S. Pan, L. Xu and D. F. Mota, "Effects of anisotropic stress in interacting dark matter – dark energy scenarios", *Monthly Notices of the Royal Astronomical Society*, Vol. 482, No. 2, pp. 1858–1871, 2019.

171. Mota, D., J. Kristiansen, T. Koivisto and N. Groeneboom, "Constraining Dark Energy Anisotropic Stress", *Monthly Notices of the Royal Astronomical Society*, Vol. 382, pp. 793–800, 2007.

172. Appleby, S., R. Battye and A. Moss, "Constraints on the anisotropy of dark energy", *Physical Review D*, Vol. 81, p. 081301, 2010.

173. Appleby, S. A. and E. V. Linder, "Probing dark energy anisotropy", *Physical Review D*, Vol. 87, No. 2, p. 023532, 2013.

174. Amendola, L., S. Fogli, A. Guarnizo, M. Kunz and A. Vollmer, "Model-independent constraints on the cosmological anisotropic stress", *Physical Review D*, Vol. 89, No. 6, p. 063538, 2014.

175. Amendola, L. *et al.*, "Cosmology and fundamental physics with the Euclid satellite", *Living Reviews in Relativity*, Vol. 21, No. 1, p. 2, 2018.

176. Pimentel, L., "Energy Momentum Tensor in the General Scalar - Tensor Theory", *Classical and Quantum Gravity*, Vol. 6, pp. L263–L265, 1989.

177. Madsen, M., "Scalar Fields in Curved Space-times", *Classical and Quantum Gravity*, Vol. 5, pp. 627–639, 1988.

178. Faraoni, V. and J. Coté, "Imperfect fluid description of modified gravities", *Physical Review D*, Vol. 98, No. 8, p. 084019, 2018.

179. Akarsu, O., S. Kumar, S. Sharma and L. Tedesco, "Constraints on a Bianchi type I spacetime extension of the standard ΛCDM model", *Physical Review D*, Vol. 100, No. 2, p. 023532, 2019.

180. Bertolami, O., F. S. Lobo and J. Paramos, "Non-minimum coupling of perfect fluids to curvature", *Physical Review D*, Vol. 78, p. 064036, 2008.

181. Faraoni, V., "The Lagrangian description of perfect fluids and modified gravity with an extra force", *Physical Review D*, Vol. 80, p. 124040, 2009.

182. Mukhanov, V., *Physical Foundations of Cosmology*, Cambridge University Press, 2005.

183. Campanelli, L., P. Cea, G. Fogli and A. Marrone, "Testing the Isotropy of the

Universe with Type Ia Supernovae", *Physical Review D*, Vol. 83, p. 103503, 2011.

184. Wang, Y. and F. Wang, "Testing the isotropy of the Universe with type Ia supernovae in a model-independent way", *Monthly Notices of the Royal Astronomical Society*, Vol. 474, No. 3, pp. 3516–3522, 2018.

185. Beltran Jimenez, J., V. Salzano and R. Lazkoz, "Anisotropic expansion and SNIa: an open issue", *Physics Letters B*, Vol. 741, pp. 168–177, 2015.

186. Soltis, J., A. Farahi, D. Huterer and C. M. Liberato, "Percent-Level Test of Isotropic Expansion Using Type Ia Supernovae", *Physical Review Letters*, Vol. 122, No. 9, p. 091301, 2019.

187. Zhao, D., Y. Zhou and Z. Chang, "Anisotropy of the Universe via the Pantheon supernovae sample revisited", *Monthly Notices of the Royal Astronomical Society*, Vol. 486, No. 4, pp. 5679–5689, 2019.

188. Hu, J., Y. Wang and F. Wang, "Testing cosmic anisotropy with Pantheon sample and quasars at high redshifts", *Astronomy & Astrophysics*, Vol. 643, p. A93, 2020.

189. Martinez-Gonzalez, E. and J. L. Sanz, "$\Delta T/T$ and the isotropy of the universe", *Astronomy & Astrophysics*, Vol. 300, p. 346, 1995.

190. Bunn, E. F., P. Ferreira and J. Silk, "How anisotropic is our universe?", *Physical Review Letters*, Vol. 77, pp. 2883–2886, 1996.

191. Kogut, A., G. Hinshaw and A. Banday, "Limits to global rotation and shear from the COBE DMR four year sky maps", *Physical Review D*, Vol. 55, pp. 1901–1905, 1997.

192. Saadeh, D., S. M. Feeney, A. Pontzen, H. V. Peiris and J. D. McEwen, "How isotropic is the Universe?", *Physical Review Letters*, Vol. 117, No. 13, p. 131302, 2016.

193. Barrow, J. D., R. Juszkiewicz and D. H. Sonoda, "Universal rotation - How large can it be?", *Monthly Notices of the Royal Astronomical Society*, Vol. 213, pp. 917–943, 1985.

194. Barrow, J., "Light elements and the isotropy of the Universe", *Monthly Notices of the Royal Astronomical Society*, Vol. 175, pp. 359–370, 1976.

195. Campanelli, L., "Helium-4 Synthesis in an Anisotropic Universe", *Physical Review D*, Vol. 84, p. 123521, 2011.

196. Stephani, H., D. Kramer, M. MacCallum, C. Hoenselaers and E. Herlt, *Exact Solutions of Einstein's Field Equations*, Cambridge Monographs on Mathematical Physics, Cambridge University Press, 2003.

197. Chavanis, P.-H., "Cosmology with a stiff matter era", *Physical Review D*, Vol. 92, No. 10, p. 103004, 2015.

198. Carneiro, S., P. de Holanda, C. Pigozzo and F. Sobreira, "Is the H_0 tension suggesting a fourth neutrino generation?", *Physical Review D*, Vol. 100, No. 2, p. 023505, 2019.